SYNTHESIS, CHARACTERISATION AND HIRSHFELD SURFACE ANALYSIS OF PHOSPHANECOPPER(I) ACYLTHIOUREA COMPLEXES

MOHAMAD ZARIF BIN MOHD ZUBIR

FACULTY OF SCIENCE
UNIVERSITY OF MALAYA
KUALA LUMPUR

2019

SYNTHESIS, CHARACTERISATION AND HIRSHFELD SURFACE ANALYSIS OF PHOSPHANECOPPER(I) ACYLTHIOUREA COMPLEXES

MOHAMAD ZARIF BIN MOHD ZUBIR

DISSERTATION SUBMITTED IN FULFILMENT OF THE REQUIREMENTS FOR THE DEGREE OF MASTER OF SCIENCE

DEPARTMENT OF CHEMISTRY
FACULTY OF SCIENCE
UNIVERSITY OF MALAYA
KUALA LUMPUR

2019

UNIVERSITY OF MALAYA
ORIGINAL LITERARY WORK DECLARATION

Name of Candidate: **Mohamad Zarif Bin Mohd Zubir**

Matric No: **SMA170026**

Name of Degree: **Master**

Title of Project Paper/Research Report/Dissertation/Thesis ("this Work"):

Synthesis, Characterisation and Hirshfeld Surface Analysis of Phosphanecopper(I) Acylthiourea Complexes

Field of Study: **Inorganic Chemistry**

I do solemnly and sincerely declare that:

(1) I am the sole author/writer of this Work;
(2) This Work is original;
(3) Any use of any work in which copyright exists was done by way of fair dealing and for permitted purposes and any excerpt or extract from, or reference to or reproduction of any copyrighted work has been disclosed expressly and sufficiently and the title of the Work and its authorship have been acknowledged in this Work;
(4) I do not have any actual knowledge, nor do I ought reasonably to know that the making of this work constitutes an infringement of any copyrighted work;
(5) I hereby assign all and every right in the copyright to this Work to the University of Malaya ("UM"), who henceforth shall be owner of the copyright in this Work and that any reproduction or use in any form or by any means whatsoever is prohibited without the written consent of UM having been first had and obtained;
(6) I am fully aware that if in the course of making this Work, I have infringed any copyright whether intentionally or otherwise, I may be subject to legal action or any other action as may be determined by UM.

Candidate's Signature Date:

Subscribed and solemnly declared before,

Witness's Signature Date:

Name:
Designation:

SYNTHESIS, CHARACTERISATION AND HIRSHFELD SURFACE ANALYSIS OF PHOSPHANECOPPER(I) ACYLTHIOUREA COMPLEXES

ABSTRACT

A series of phosphanecopper(I) complexes of acylthiourea derivatives have been synthesised and characterised by a combination of FTIR spectroscopic studies, NMR spectroscopic studies, X-ray crystallography and Hirshfeld surface analysis. One series of thirteen acylthiourea ligands of the type *N*-benzoyl-*N'*-(R-substituted phenyl)thiourea, where R is H, 3-Me, 3-OMe, 3-OH, 3-Cl, 2-Me, 2-OMe, 2-OH, 2-Cl, 4-Me, 4-OMe, 4-OH, 4-Cl denoted by **T1**-**T13** respectively, have been synthesised and verified spectroscopically. These series of ligand (**T1**-**T13**) was then followed by a complexation step with a copper(I) salt and triphenylphosphine to form the phosphanecopper(I) complexes of *N*-benzoyl-*N'*-(R-substituted phenyl)thiourea, given the complexes formula of, $[Cu(T)(I)(PPh_3)]$ designated by **CT1**-**CT13** respectively. All the complexes were characterised spectroscopically, and some were with X-ray crystallography. Results from spectroscopic data and some with crystal structure analysis show that in all complexes the acylthiourea ligands coordinated as monodentate S-donor mode. The crystallisation of complexes from acetonitrile yielded good prismatic, yellow single crystals suitable for X-ray crystallography. The complexes **CT1**-**CT7** showed a distorted tetrahedral with a single acylthiourea ligand, two triphenylphosphine act as a co-ligand and one iodide anion. The acylthiourea ligands behaved as a hypodentate S-donor ligand instead of its common O, S-bidentate nature due to the tetrahedrally favoured geometry of the copper(I) centre and the presence of two bulky group of triphenylphosphine ligand as the co-ligand. It was obtained that **CT1**-**CT4** and **CT7** crystals crystallised in the monoclinic $P2_1/c$ crystal system whereas **CT5** and **CT6** crystallised in triclinic $P\bar{1}$ crystal system. The isostructural structures of these two crystal systems illustrated almost similar crystal packing but with significantly different interactions as determined by Hirshfeld surface analysis

Keywords: Copper(I) Complexes, Acylthiourea, Hirshfeld Surface Analysis, Crystallography.

SINTESIS, PERCIRIAN DAN ANALISIS PERMUKAAN HIRSHFELD KOMPLEKS KUPRUM(I) FOSFENA ASILTIOUREA

ABSTRAK

Suatu siri kompleks kuprum(I) fosfena terbitan asiltiourea telah disintesis dan dicirikan dengan menggunakan gabungan kajian spektroskopi FTIR, kajian spektroskopi NMR, kristalografi sinar-X dan analisis permukaan Hirshfeld. Satu siri terdiri daripada 13 ligan asiltiourea jenis tiourea *N*-benzoil-*N′*-(R-fenil berganti)tiourea, di mana R adalah H, 3-Me, 3-OMe, 3-OH, 3-Cl, 2-OH, 2-OMe, 2-OH, 2-Cl, 4-Me, 4-OMe, 4-OH, 4-Cl yang disimbolkan dengan **T1-T13**, telah disintesis dan disahkan secara spektroskopik. Kemudian, siri ligan (**T1-T13**) digunakan dalam langkah pengkompleksan dengan garam kuprum(I) dan trifenilfosfena untuk membentuk kuprum(I) fosfena kompleks *N*-benzoil-*N*'-(R-fenil berganti)tiourea, dengan formula kompleks, $[Cu(T)(I)(PPh_3)]$ yang ditetapkan sebagai **CT1-CT13**. Semua kompleks telah dicirikan secara spektroskopi dan sesetengah pula dengan kristalografi sinar-X. Hasil daripada data spektroskopik dan beberapa analisis struktur kristal menunjukkan bahawa di semua kompleks ligan asiltiourea bersifat sebagai mod penderma-S monodentat. Penghabluran kompleks daripada pelarut acetonitril menghasilkan kristal tunggal prismatik yang baik untuk kristalografi sinar-X. Kompleks **CT1-CT7** menunjukkan tetrahedral terherot yang mempunyai ligan asilthiourea tunggal, dua trifenilfosfin yang bertindak sebagai ligan bersama dan satu anion iodin. Ligan asiltiourea berkelakuan sebagai ligan penderma-S hipodentate dan bukan menuruti sifat umum O, S-dwidentat kerana geometrinya lebih menyukai bentuk tetrahedral berpusat kepada kuprum(I) dan kehadiran dua kumpulan besar ligan trifenilfosfena sebagai ligand bersama. Menariknya, kristal **CT1-CT4** dan **CT7** menghablur dalam sistem kristal monoklinik $P2_1/c$ manakala **CT5** dan **CT6** didapati membentuk sebagai sistem kristal triklinik $P\bar{1}$. Struktur isostruktural dari kedua-dua sistem kristal itu menggambarkan susun atur kristal yang hampir serupa tetapi memiliki interaksi yang berbeza yang dapat ditentukan oleh analisis permukaan Hirshfeld.

Kata kunci: Kompleks Kuprum(I), Asiltiourea, Analisis Permukaan Hirshfeld, Kristallografi.

ACKNOWLEDGEMENTS

First and foremost, all praise to Allah, The Almighty God with His Mercy has granted me the strength, patience, and blessings to complete this work.

I would like to extend my deepest gratitude to my supervisors, Dr Nazzatush Shimar Jamaludin and Associate Prof Dr Siti Nadiah Abdul Halim for their obliging guidance, brilliant suggestions, unlimited tolerance and compassionate encouragement throughout my journey.

Also, sincere thanks go to all the supporting staff of Department of Chemistry, Faculty of Science, University of Malaya for their help in both academic and technical affairs that enable me to successfully complete my study. Also thanks to the Research Centre for Crystalline Materials, Sunway University for permitting the usage of the single crystal X-ray diffractometer.

I also would like to thank Research Centre for Crystalline Materials, Sunway University for permitting the usage of the single crystal X-ray diffractometer.

Not to forget, I owe my deepest gratitude appreciation to my family and friends for their love, concern and support. None of this would have been possible without them.

Finally, I would like to record my appreciation for the research grant provided by the University of Malaya, under grant Bantuan Kecil Penyelidikan (BKP086-2016) which funded and made my study possible.

TABLE OF CONTENTS

LIST OF FIGURES

LIST OF TABLES

LIST OF SCHEMES

LIST OF EQUATION

LIST OF SYMBOLS AND ABBREVIATIONS

—	:	Single bond
···	:	Weak bond
%	:	Percentage
°	:	Degree
°C	:	Degree Celsius
=	:	Double bond
^{13}C	:	Carbon-13
^{1}H	:	Proton
^{31}P	:	Phosphorus-31
Å	:	Angstrom
ACS	:	American Chemical Society
au	:	Atomic unit
ATR	:	Attenuated total reflectance
C=O	:	Carbonyl
C=S	:	Thiocarbonyl
$CDCl_3$	:	Deuterated chloroform
CIF	:	Crystallographic information files
cm^{-1}	:	Reciprocal centimetre
Cu(I)	:	Copper(I)
CuI	:	Copper iodide
d_e	:	External distance
d_i	:	Internal distance
DMSO	:	Dimethyl sulfoxide
$DMSO\text{-}d_6$	:	Deuterated dimethyl sulfoxide

d_{norm}	:	Normalised distance
FTIR	:	Fourier transform infrared
g/mol	:	Gram per mole
h	:	Hour
IR	:	Infrared
IUPAC	:	International Union of Pure and Applied Chemistry
KSCN	:	Potassium thiocyanate
L	:	Ligand
Me	:	Methyl
MeCN	:	Acetonitrile
MHz	:	Mega Hertz
ml	:	Milliliter
mmol	:	Millimole
NH_4SCN	:	Ammonium thiocyanate
NMR	:	Nuclear magnetic resonance
OH	:	Hydroxy
OMe	:	Methoxy
Ph	:	Phenyl
PPh_3	:	Triphenylphosphine
R	:	Substituent group
rt	:	Room temperature
SCXRD	:	Single Crystal X-ray Diffraction
T	:	Thiourea
ν	:	Wavenumber
π	:	Pi

LIST OF APPENDICES

CHAPTER 1: INTRODUCTION

1.1 Research Background

In the early nineteenth century, countless metal complexes were developed, synthesised but partly characterised due to the difficulties or somewhat impossible at that moment to conclusively deduce their exact chemical structures. Fundamental advancements were limited until the inventions of X-ray diffraction methods to uncover the precise structural data on solid compounds technically useful for metal complexes. These techniques were since becoming widely available, subsequently providing crystallographic data to reveal the rich potential of metal complexes (Atkins *et al.*, 2010).

Since the age of crystallography advancement, researchers were able to uncover many mysteries in the interaction and behaviour of metal complexes within the crystal structure. This has contributed and become a platform for the expansion of other extended research field such as metal organic clusters of copper and vanadium used as sensors (Faridbod *et al.*, 2008; Raizada *et al.*, 2017). Some iron(II) complexes were produced as a catalyst for selective hydrogenation of aldehydes (Gorgas *et al.*, 2016; Liu *et al.*, 2018). Others includes copper and ruthenium complexes with potential enzyme mimetic in the field medicinal (Bravo *et al.*, 2010; Vijayan *et al.*, 2017). Crystallography had also been useful in characterising novel bismuth(III) coordination polymer (Hanifehpour *et al.*, 2015; Pearson *et al.*, 2012), and some macrocycle complexes demonstrated notable anions absorption behaviour from aqueous solution (Luther & Rickard, 2005).

1.2 Problem Statement

The innovation and designing of novel metal complexes with interesting structure have been the interest for most researchers involved in the field of inorganic chemistry. The structural studies of metal complexes are crucial to truly uncover its potential properties and beneficial behaviour. However, the structural study of metal complexes cannot be simply characterised only by the mean of spectroscopy. Thus, crystal growing had always been the goal for all inorganic compounds. This is so that the crystal structures of these crystalline solids can be established through crystallography technique especially through single crystal X-ray diffraction (SCXRD) studies. Furthermore, it will provide valuable information to further study on the coordination chemistry of many metal complexes.

Additionally, the crystallography technique is not only limited for structural elucidation, it has been proved to be a powerful method in the determination of the chemical makeup, uncover the different polymorphic forms, understanding the defects or disorder within a crystal system, and also electronic properties of the metal complexes. Many new developments of instrumentation technique have emerged in the field of crystallography and the latest software has been produced for collecting, analysing, and visualising crystallographic data. One of the useful software created is the Hirshfeld surface analysis that allow us to quantify and visualise the molecular surface within a crystal system of the metal complex (Spackman & Jayatilaka, 2009).

One of the interesting class of metal complexes is the complexes of acylthiourea derivatives and they were known to coordinate to many transition metals such as copper (Wu *et al.*, 2015), cobalt (Yang *et al.*, 2012), platinum (Hernández *et al.*, 2003), and gold (Luckay *et al.*, 2010). They were synthesised and characterised with crystallographic technique to obtain the single crystal structure, but mostly were only conducted to obtain the crystal structure. Thus, with the aid of Hirschfeld surface study, it will allow the discovery of the true properties and potential of the complexes especially in understanding the surface interaction within the single crystal structure. Accurate and efficient data can be mapped out such as the electrostatic potential, curvedness, and shape index. Another important information can readily be display is the intermolecular interactions and the void spaces that can be quantified. This will overall provide a unique insight into investigation of the in-crystal environment (Spackman & Jayatilaka, 2009). These has been comprehensively studied for its application in the of field crystal engineering analysing supramolecular metal organic framework (Raizada *et al.*, 2017), coordination polymer (Seth, 2018), and the computational study of potential metallodrugs with anticancer properties (Kumar *et al.*, 2017).

1.3 Objectives

The overall goal of study the Hirshfeld surface analysis of a series of new phosphanecopper(I) acylthiourea complexes. The specific aims of this project are as listed down below:

a) To synthesise and characterise a series of new phosphanecopper(I) complexes of acylthiourea derivatives.
b) To obtain the crystals of the complexes and conduct the single crystal X-ray diffraction studies for the identification of the crystal system.
c) To assess the Hirshfeld surface analysis of the complexes based on the crystallographic data.

1.4 Research Scope

The scope of research is divided into two parts; the synthesis and characterisation of a series of phosphanecopper(I) acylthiourea complexes and followed by the crystal study of the complexes. The building block of the complex involve copper(I) metal as the metal center, acylthiourea as the ligand, and triphenylphosphine as co-ligand. The constructions of transition metal complexes with ligand containing soft donor atoms such as phosphorus, sulphur or nitrogen are known to be favourable (Garnovskii & Kharissov, 2003; Haas & Franz, 2009; Pearson, 1963). This idea led to the chemistry of acylthiourea derivatives in coordination complexes which has become an interest due to its interesting skeleton backbone of C(O)N(H)C(S)N, bearing O, N, N' and S donor atoms within it (Koch, 2001; Mertschenk *et al.*, 1995; Sumrra *et al.*, 2016).

This has inspired researches far and wide to study the versatility of acylthiourea to form complexes with d-block metals with its remarkable applications including biological sciences (Plutín *et al.*, 2014; Yaseen *et al.*, 2016), luminescent studies (Cîrcu *et al.*, 2009), electrochemical investigations (Mohamadou *et al.*, 1994) and catalytic properties (Sathishkumar *et al.*, 2018). Acylthiourea commonly exhibits an expected monoanionic O, S-bidentate coordination towards a diverse range of transition metal such as platinum (Hernández *et al.*, 2003), nickel (Selvakumaran *et al.*, 2013), copper (Hanif *et al.*, 2014), zinc (Sumrra *et al.*, 2016) and so on.

However, one interesting coordination complex that acylthiourea adopted is with copper(I) metal. Fascinatingly, acylthiourea shows unusual ability as a monodentate ligand in some mixed ligand copper(I) complexes (Gunasekaran *et al.*, 2012; Singh *et al.*, 2015), coordinating only via the sulphur atom. Commonly the acylthiourea was expected to behave exclusively as a multidentate ligand, yet it shows coordination through less than the maximum number of potential donor atoms. Hence, the term 'hypodentate' was introduced to describe this type of coordination behaviour (Gunasekaran *et al.*, 2012; Kotze *et al.*, 2017). These hypodentate manners of acylthiourea were also observed with other metals such as platinum (Kotze *et al.*, 2017), palladium (Selvakumaran *et al.*, 2011), ruthenium(Sathishkumar *et al.*, 2018) and silver (Braun *et al.*, 1985). Thus, in this project, the acylthiourea coordinated to the copper(I) centre is expected to behave as a hypodentate ligand.

The next part of the research is to analyse the crystal structure obtained by using the Crystal Explorer software in order to obtain the Hirshfeld surface analysis of the synthesised complexes by various surface maps and fingerprint plotting (Spackman & Jayatilaka, 2009). Understanding the analysis will provide an illustrative discussion on the interaction within the crystal system. Hence, providing another perspective and elaboration on the crystallographic results obtained from the series of closely related structure.

1.5 Outline of the Dissertation

The dissertation comprises of five chapters which consist of:

Chapter 1: Introduction

The first chapter provided an introductory outline of the topics of this research by elaborating on the aforementioned research that has been conducted. Through this overview, we comprehended the significance and implications in the designing of mixed ligand metal complexes containing acylthiourea ligand and its crystallographic appreciations.

Chapter 2: Literature Review

In this chapter, it consists of deliberately discussed evidence on the previous studies that have been conducted in the progress of developing and the designing of new metal complexes. From this review, we were able to develop a better understanding of the different behaviour of various thiourea derivatives as a ligand specifically as a sulphur donor ligand when coordinated to different types of the metal centre. The distinctive ability of copper(I) metal to form mixed ligand complexes with some sulphur-based ligand was also reviewed. Furthermore, it is essential to determine the suitable co-ligand to furnish the targeted mixed ligand complexes. Henceforth, these are crucial in the understanding of how the different components that built up the targeted metal complexes, would behave and their interaction within the crystal formation. Lastly, the theoretical concept of Hirshfeld surface analysis was mentioned.

Chapter 3: Methodology

This explained the methodology on how the syntheses of the acylthiourea derivatives and its novel copper(I) complexes were conducted. In this chapter, the chemical and material used were also listed and specified. Besides that, the various instrumental techniques used in the confirmation and structural elucidation of the newly synthesised compounds were listed. Therefore, this chapter provided all the behind the scene processes involved in this research.

Chapter 4: Results and Discussions

This chapter includes all the outcomes and discussion of the study. First, the general characterisation results such as CHN elemental analyser, FTIR spectroscopy, and NMR spectroscopy were presented. All of these data recorded and analysed, providing a preliminary structural illustration and confirmation of the newly formed compounds.

On top of that, we were able to produce for good quality and pure single crystal for some of the copper(I) complexes that were suitable for the SCXRD studies. Further deliberation of the Hirshfeld surface analysis was also elaborated as a distinctive discussion on each of the crystal packing. Altogether, these findings provided a clear input of the successfulness of the syntheses based on the proposed scaffold of the novel metal complexes.

Chapter 5: Conclusions and Future Works

This chapter established the research with conclusive and summarisation from the output of the experiments conducted and plausible future development and enhancement as a furtherance of this project.

On top of that the preliminary results of this work were visualised as a poster presentation at International Malaysian French Scientific Conference 2017 (IMFSC2017), and oral presentation at South East Asian Conference on Crystal Engineering (SEACCE-2). A paper on the crystal structure and the Hirshfeld surface analysis of the novel phosphanecopper(I) complexes was published in Journal of Molecular Structure.

CHAPTER 2: LITERATURE REVIEW

2.1 Thiourea

Sulphur containing organic molecule is generally known as organosulphur compounds, which are found in their abundance, notable for their versatility behaviour and diverse functionality (Kharasch, 2013). They occur in the earth crust in the form of minerals ores and also found to be essential in all living organism in the biological world. Organosulphur compound exists in many classes of plants including the strong sulphury odours of *Durio zibethinus* (Jiang *et al.*, 1998) and the pungency of allicin (Figure 2.1) from *Allium sativum* (Rybak *et al.*, 2004). Whereas in all animals, the amino acid containing sulphur *i.e.* methionine and cysteine (Figure 2.1), plays a vital role in protein structures by forming the disulphide linkage and also act as a site for metal coordination in metalloenzyme (Barrett, 2012).

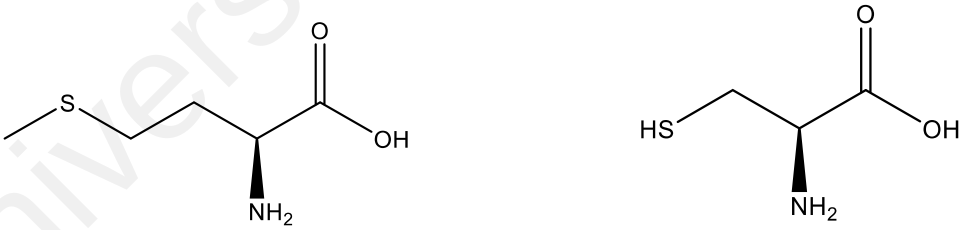

Methionine Cysteine

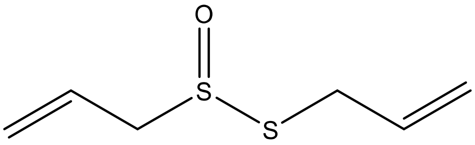

Allicin

Figure 2.1: Natural occurring organosulphur compounds.

By the discovery of the natural occurring organosulphur compounds and the advancement in experimental chemistry, countless possibility of the synthetic organosulphur compounds were produced. Astonishingly, these findings of both naturally and synthetically occurring organosulphur had led to lots of beneficial application in many different fields that includes the biocompatibility of a polysulfone membranes fabricated with potential antibacterial properties (Hayama *et al.*, 2004; Mahmoudi *et al.*, 2015), core of a penicillin-based drugs (Flynn, 2013), and that commonly known polar aprotic solvent dimethyl sulfoxide (DMSO).

One chemically interesting polyfunctional organosulfur compound is the thiourea. Thiourea is an organic compound of carbon, nitrogen, sulphur and hydrogen backbone with a chemical formula of CSN_2H_4 and the basic structure is as illustrated in Figure 2.2. Thiourea is an odourless white crystalline compound. They have interesting behaviour because of their unique combination of functional group that includes amino, imino, and thiol. The thiol group can also exist primarily as thione due to the tautomerisation (Mertschenk *et al.*, 1995). Thiourea compounds are structurally similar to that of urea (Figure 2.2), but instead, the oxygen atom of the urea is replaced by a sulphur atom.

Figure 2.2: Urea and thiourea.

Owing to the unique backbone of thiourea, the hydrogen atoms of the nitrogen atoms are easy to be substituted. These could be mono-, di-, tri- or tetra-substituted thiourea derivatives. They can also easily form heterocyclic compounds known as cyclic thiourea

(Bogatskii *et al.*, 1983). This enables thiourea to be formed into numerous possibilities of combination of substituent groups on the thiourea backbone. The nomenclature of thiourea (Figure 2.3) is based on the substituent group on the nitrogen atoms replacing the hydrogen atoms and italic letter locants can be used with relatives to the place of the substituents (Bünzli-Trepp, 2007).

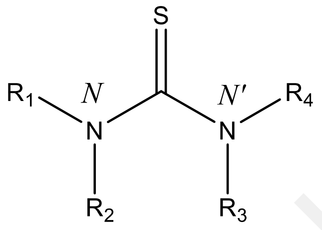

Figure 2.3: Substituted thiourea nomenclature.

2.1.1 Acylthiourea and its Derivatives

Acylthiourea is referring to *N*-(acyl/aroyl)thiourea, due to the existence of a carbonyl substituent group on the thiourea backbone. Substitution of the second nitrogen atom *N'*, will form an *N*-(acyl/aroyl)-*N'*-(mono-substituted)thiourea and *N*-(acyl/aroyl)-*N'*,*N'*-(di-substituted)thiourea, which the substituent group may be an alkyl, aryl, aralkyl or heterocyclic substituent (Saeed *et al.*, 2014). Acylthiourea derivatives have become a great interest because of its chemical properties and they are reasonably simple to synthesise and can be produced with satisfying yield with less by-product (Han *et al.*, 2013; Koca *et al.*, 2016).

2.1.2 Preparation of Acylthiourea

Many different methods have been developed in order to synthesise thiourea and specifically acylthiourea derivatives. One of the most outstanding synthetic routes is by the utilisation of acyl chloride and the salt of thiocyanate to form an acyl isothiocyanate, then continued with the addition of any primary or secondary amines of interest as shown in Scheme 2.1 (Brito *et al.*, 2015). This method usually can be done by refluxing in acetone as solvent. It is then followed by a simple cold forced precipitation of the final product. The crude product can then be further purified through recrystallisation. This method is useful to produce *N*-benzoyl-*N'*-phenylthiourea and other related acylthiourea derivatives. The reaction mechanism is as illustrated in Scheme 2.2.

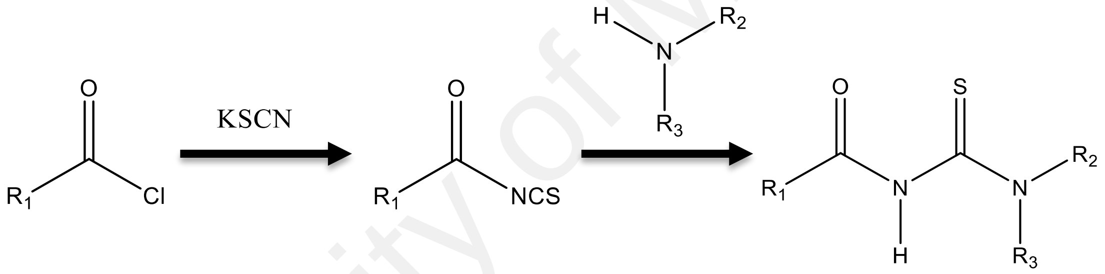

Scheme 2.1: Synthesis of acylthiourea derivatives via acyl isothiocyanate and amine.

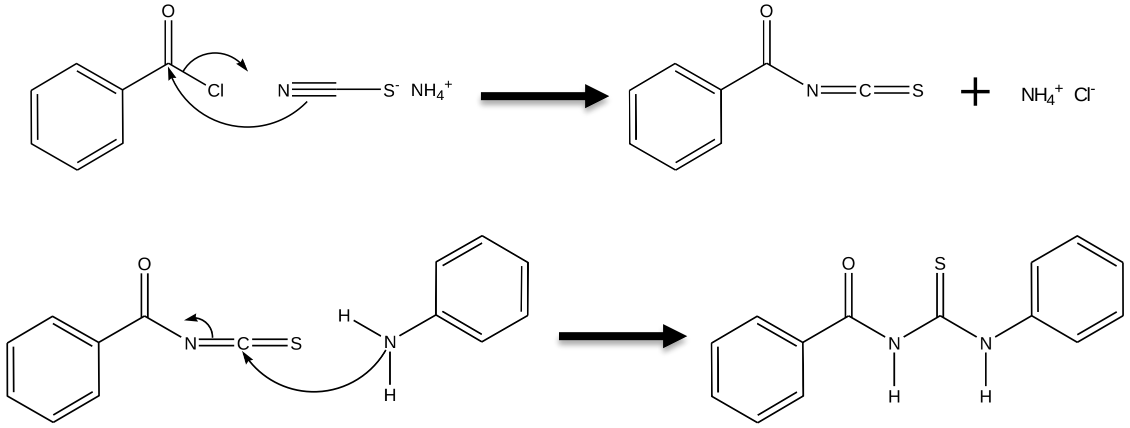

Scheme 2.2: Reaction mechanism of *N*-benzoyl-*N'*-phenylthiourea derivatives.

Another methodology adopted to produce the acylthiourea is via microwave irradiation (Scheme 2.3). It has been successfully applied in the synthesis of benzoic acid with *N,N*-disubstituted thiourea in the presence of solid support (Márquez *et al.*, 2000). This result in a substantial amount of yield and a shorter synthesis time.

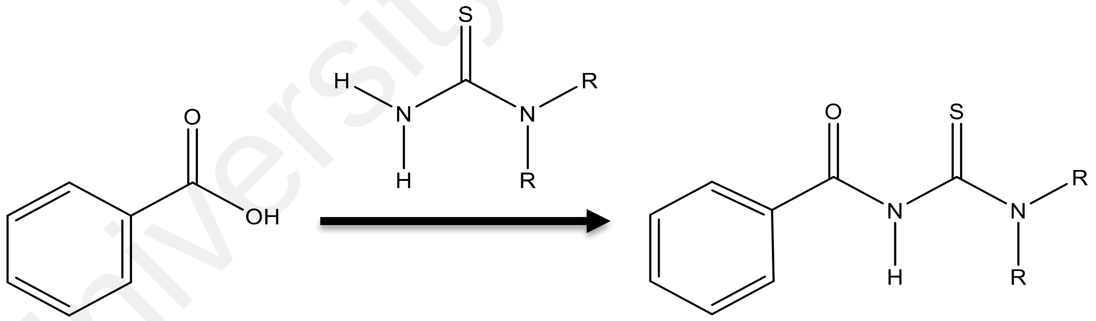

Scheme 2.3: Synthesis of acylthiourea derivatives by microwave assisted.

2.1.3 Unique Conformation

Theoretically, the acylthiourea are able to adopt a number of different types of conformers, contributed by several functional groups available that form its unique backbone. Hence, based on computational simulation and calculation reported, the acylthiourea could be fashioned into four types of stable conformation, that is M, S, U, and Z (Figure 2.4). The alphabet illustrates the location of C=O and C=S bonds. Depending on the electron density of the R group substituted on both of the nitrogen atoms, the four conformers may be interchangeable to take on the most stable conformers. Besides, it is noted that the presence of lone pair electrons on all the heteroatoms N, O and S may affect the rotation of the C—N bonds. Although suggested in illustration as in Figure 2.4, all the conformation do not necessarily consider to be planar (Woldu & Dillen, 2008).

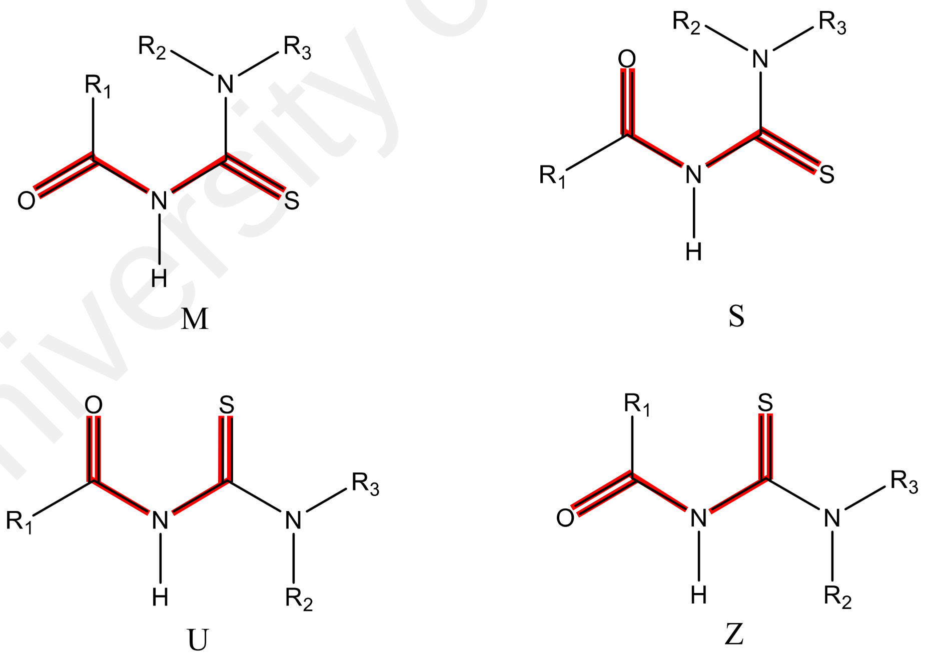

Figure 2.4: Four stable conformations of acylthiourea backbone.

2.1.4 Thione-Thiol Tautomerism

N-acyl-*N'*-(monosubstituted)thiourea could interconvert between the thione form and its less common thiol form in rapid equilibrium. This is a result of the functional group situated side-by-side on the acylthiourea backbone. Collectively, it is reported that the thione tautomers are regularly the preferred form. However, in some cases of acylthiourea derivatives may employ a thiol form. Evidence from some studies suggested that the IR band at around 2438 cm^{-1} designated to the ν(SH) were observed (Yang *et al.*, 2007). Therefore, it indicates that the thione–thiol tautomerism (Scheme 2.3) is in accordance with the existence of a thiol functional group.

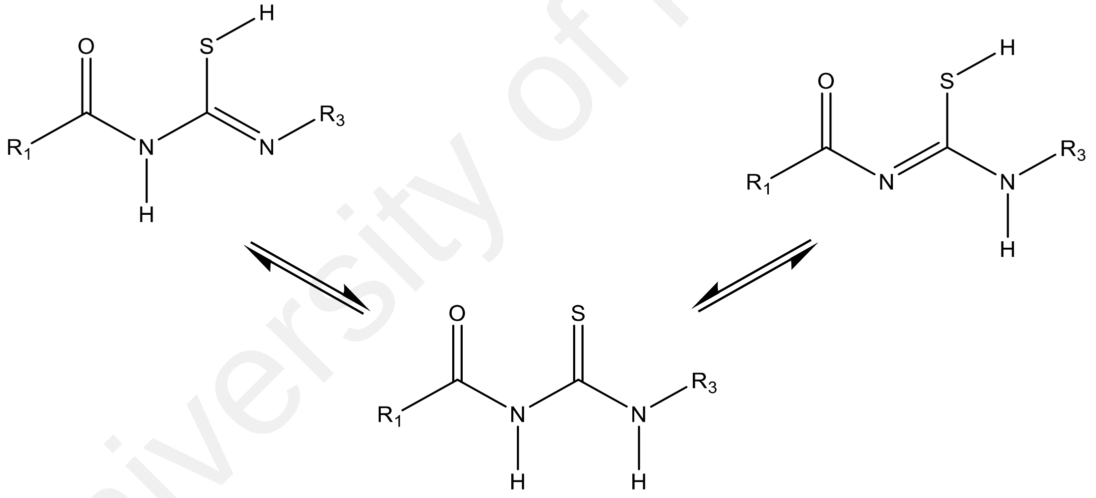

Scheme 2.4: Thione-thiol tautomerism of acylthiourea.

2.1.5 Versatile Applications of Acylthiourea

Over the years of studies, the interest of acylthiourea has expanded in term of the applications for the versatility of the thiourea backbone as some example were tabulated in Table 2.1. Research reported that some new long alkyl chain acylthiourea derivatives showed liquid crystalline properties (Iliş *et al.*, 2017). Besides, acylthiourea derivative was developed as organocatalyst for the catalysis of the Michael addition reaction (Androvič *et al.*, 2016; Wang *et al.*, 2016). Another study reported the activity of acylthiourea group as a benzene sensing material with enhanced sensing properties. By advance computational modelling and calculation, the preferred binding sites for interaction with benzene were situated at the active acylthiourea backbone (Khairul *et al.*, 2017).

Other than physical applications, acylthiourea derivatives were studied in the field of biology. A series of acylthiourea were investigated for its soil urease inhibitory properties for the interest in agriculture (Brito *et al.*, 2015). On top of that, a class of antiparasitic acylthiourea were also proved beneficial to agriculture (Chang *et al.*, 2017). Acylthiourea derivatives were also thoroughly explored for its medicinal value such as enzyme inhibitor (Saeed *et al.*, 2014; Yun *et al.*, 2016), fungicidal (Ming-Yan *et al.*, 2015), antitumor (Anuta *et al.*, 2014) and as a good antimicrobial potency against more susceptible Gram-positive bacteria (Oyeka *et al.*, 2018). An acylthiourea derivative known as tenovin-6 was tested progressively because of its promising anticancer properties (Dai *et al.*, 2016; MacCallum *et al.*, 2013; Yuan *et al.*, 2017).

Table 2.1: Example of acylthiourea and their properties.

	Acylthiourea compounds	Properties
a)	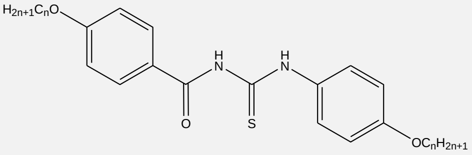 n = 10 or 12	The long alkyl chain at both phenyl group shows the mesomorphic behavior and the acylthiourea act as a site for metal coordination in the formation of metallomesogen (Iliş *et al.*, 2017).
b)	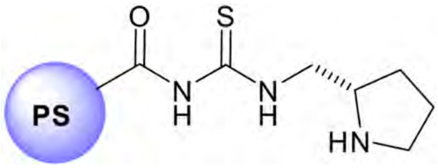 PS= polystyrene resin	The activation of the reaction is due to the ability to form hydrogen bonding between the polystyrene supported acylthiourea fragment and the reaction component (Androvič *et al.*, 2016; Wang *et al.*, 2016).
c)	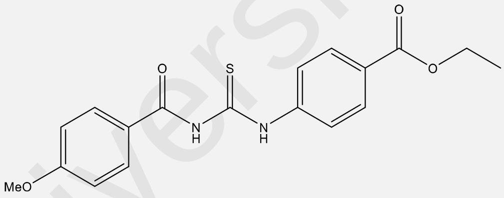	The molecular docking studies conducted shows that the acylthiourea molecule were able to adapt into the Z conformation to allow the interactions within the urease enzymes site. Thus, held by hydrogen bond and metal interactions (Saeed *et al.*, 2014).
d)	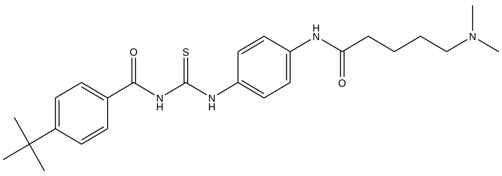	Tenovin-6 act as inhibitors of the NAD$^+$-dependent family of the protein deacetylases known as the sirtuins. It is also a more water-soluble acylthiourea based compound (Yuan *et al.*, 2017).

2.2 Transition Metal Complexes of Acylthiourea

Acylthiourea may coordinate with various transition metals through the oxygen and/or sulphur atoms forming its corresponding metal complexes. For that reason, this group of ligands are able to bind and form stable complexes with a variety of metal ions in different coordination modes, that includes nickel(II) (Selvakumaran *et al.*, 2013), copper(I) (Iliş & Cîrcu, 2018), ruthenium(II) (Barolli *et al.*, 2017; Sathishkumar *et al.*, 2018), palladium(II) (Khan *et al.*, 2018), zinc(II) (Sumrra *et al.*, 2016), cobalt(III) (Yaseen *et al.*, 2016), copper(II) (Wu *et al.*, 2015), platinum(II) (Cîrcu *et al.*, 2009), and mercury(II) (Okuniewski *et al.*, 2015). Acylthiourea can even be coordinated to some lanthanides like uranium (Noufele *et al.*, 2018) . Some of the selected examples of the metal complexes of acylthiourea and their properties are as tabulated in Table 2.2.

Table 2.2: Example of metal complexes of acylthiourea and their properties

	Acylthiourea Complexes	Properties
a)	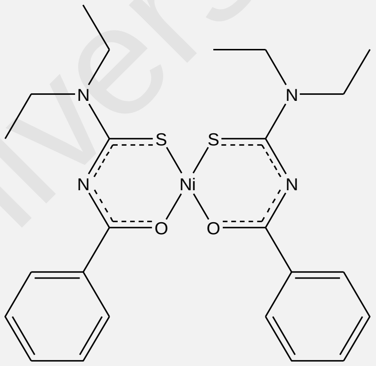	The acylthiourea ligand show the common S,O-bidentate coordination to form a homoleptic square planar nickel(II) complexes. They were found to be more potent than the parent ligands (Selvakumaran *et al.*, 2013).

	Acylthiourea Complexes	Properties
b)	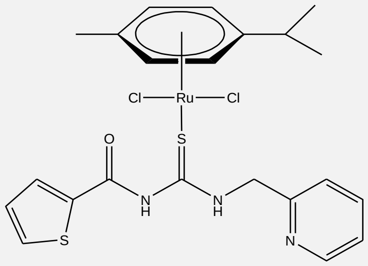	The hypodentate acylthiourea ruthenium(II) complexes were reported to be efficient pre-catalysts for the transfer hydrogenation of carbonyl compounds and nitroarenes (Sathishkumar *et al.*, 2018).
c)	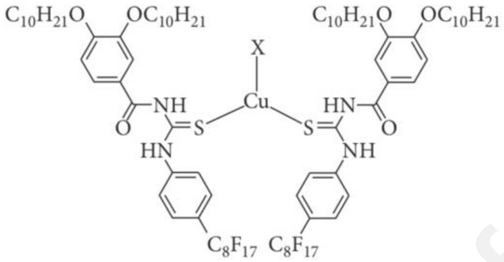 X= Cl or Br	The combination between the long alkyl chain of the acylthiourea ligands and the coordination flexibility of the copper(I) ion resulting in a three coordinated metallomesogen with mesomorphic properties (Iliş & Cîrcu, 2018)
d)	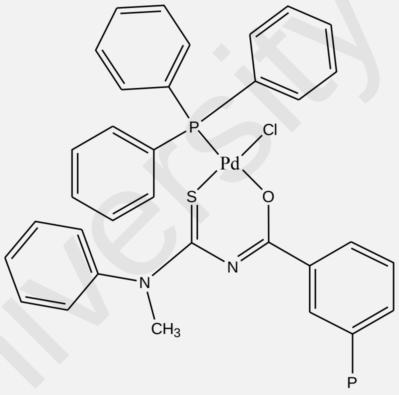	The acylthiourea ligand behave as a bidentate ligand forming a heteroleptic square planar palladium(II) complexes with potential cytotoxic activity. The complex adopted a triclinic crystal system (Khan *et al.*, 2018).
f)	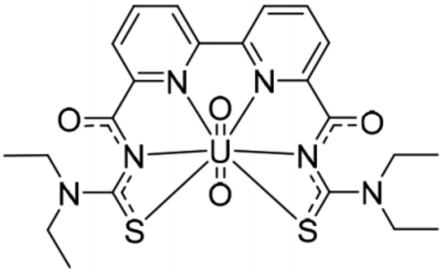	The acylthiourea act as a hexadentate ligand to the uranyl moiety via four nitrogen and two sulfur atoms, giving a hexagonal bipyramidal coordination upon the metal ion. Thus, showing a S,N coordination mode of the acylthiourea.

Table 2.2, continued.

2.2.1 Coordination Behaviour and X-Ray Crystal Packing

The coordination behaviour of substituted acylthiourea having N, O, and S as donor atoms have been widely investigated by the aid of X-ray crystallographic methods and the outcome can be structurally interesting and diversify (Figure 2.5). They usually adopt the coordination modes through the anionic O, S-bidentate form (Plutín *et al.*, 2016; Selvakumaran *et al.*, 2013).

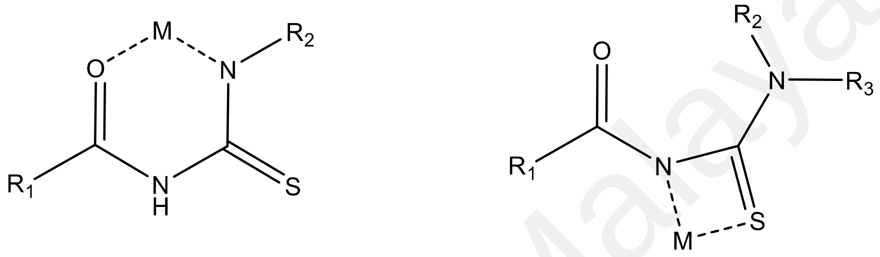

O, N-bidentate

S, N-bidentate

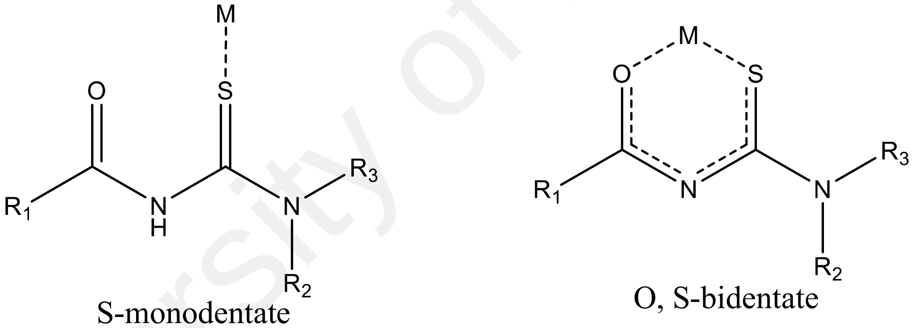

S-monodentate

O, S-bidentate

Figure 2.5: Four coordination modes of acylthiourea metal complexes.

Sometimes they can behave as a hypodentate ligand through a neutral S-monodentate coordinating solely through sulphur with metal centre such as copper(I) (Gunasekaran *et al.*, 2012; Iliş & Cîrcu, 2018; Luckay *et al.*, 2010; Singh *et al.*, 2015), gold(I) (Luckay *et al.*, 2010), palladium(II) (Rohini *et al.*, 2018; Selvakumaran *et al.*, 2011) and silver(I) (Wei *et al.*, 2017). The third, very rare, is coordination through S, N-bidentate forming a distorted four-membered chelate ring with the metal centre (Noufele *et al.*, 2018; Shen *et* *al.*, 1998). Lastly, a more unusual case is that of O, N-coordination features (Che *et al.*, 1999).

Acylthiourea complex forms a homoleptic complex, forming a slightly distorted square planar bis-chelate six-membered ring. The chelation is in such that two oxygen atoms and two sulphur atoms coordinated to the metal centre in a *cis*-fashioned, achieving near planarity of the six-membered chelate rings. This was observed in a triclinic copper(II) complexes (Sumrra *et al.*, 2016; Wu *et al.*, 2015) and monoclinic nickel(II) complexes (Selvakumaran *et al.*, 2013). However, a tetrahedral coordinate structure of zinc(II) (Armstrong *et al.*, 2004) and cobalt(II) (Yang *et al.*, 2012) acylthiourea complexes were also reported.

Some homoleptic metal complexes chelated by three acylthiourea ligands, each of which coordinates in the bidentate S, O mode (Yang *et al.*, 2012). For instance, the acylthiourea cobalt(III) complex formed a slightly distorted octahedral geometry which also deviated from the known triclinic and monoclinic structure, rather they crystallised in a trigonal crystal system, which was rarely observed in this class of compound (Yaseen *et al.*, 2016).

Nonetheless, in many cases, acylthiourea complexes can form stable heteroleptic complexes. This particularly can be observed in the formation of acylthiourea metal complexes with a bipyridine moiety as a co-ligand (Barolli *et al.*, 2017; Shen *et al.*, 1998), while some with phosphine (Gunasekaran, 2018; M. R. Khan *et al.*, 2018; Sathishkumar *et al.*, 2018) and so on. Other unique metal complexes of acylthiourea is that they can form dimeric and polymeric coordination complexes with mercury(II) (Estévez-Hernández *et al.*, 2015; Okuniewski *et al.*, 2015) and lead(II) (Schwade *et al.*, 2013).

2.3 Copper

Copper is situated in the 11th group of the periodic table, together with the other precious metals that are silver and gold. Apart from gold, copper is the only characteristic coloured metal exist in nature and they are the first metal to be mastered and crafted by human since the ancient time (Atkins *et al.*, 2010). Copper can be inert, it oxidises in the air very slowly into copper oxide, unlike other common metals. As a highly versatile metal, copper is one of the important element that had driven the technological transformation, mainly due to its high thermal and electrical conductivity (Callister Jr & Rethwisch, 2012). Copper is massively mined in Chile, in the form of copper sulphide minerals ore such as chalcopyrite ($CuFeS_2$) chalcocite (Cu_2S) and covellite (CuS) (Büchel *et al.*, 2008).

Copper complexes exhibit a variety of coloured compounds and their chemistry based on, the interactions between structural formations and reactivity behaviour has been broadly explored. Most copper(I) compounds are fairly readily oxidised to the common stable copper(II) compounds, but it is more unstable to further oxidised it to copper(III). Due to its various oxidation state, copper complexes are able to form various different coordination complexes with unlimited combinations of ligand (Atkins *et al.*, 2010). Copper(I) are commonly found as four-coordinated complexes, adopting the tetrahedral geometry (Gunasekaran *et al.*, 2012), whereas some formed a three-coordinated copper(I) complexes (Kakizoe *et al.*, 2017). Whereas copper(II) compounds are affected by Jahn-Teller distortions can custom into various coordination mode including the common mononuclear eight-coordinated copper(II) complexes (Veidis *et al.*, 1969), multinuclear copper(II) formation (Roy *et al.*, 2008) and polymeric copper(II) supramolecular structures (Chu & Zhang, 2017). The restricted stability of copper(III) complexes has resulted in less research exploration in the past years. However, modern approach shows that the formation of copper(III) complexes are in accordance with its d^8 electronic configuration which is the square-planar or square-pyramidal geometries (Casitas & Ribas, 2013).

2.3.1 Classification of Copper(I) Complexes

Many syntheses and structural studies of copper(I) compounds have been conducted (Gunasekaran *et al.*, 2012; Iliş & Cîrcu, 2018; Luckay *et al.*, 2010; Singh *et al.*, 2015),. Most of the syntheses have involved a direct reaction between a copper(I) halide and the appropriate ligand in a non-aqueous solvent (Gunasekaran *et al.*, 2017). Others involve the reduction of a copper(II) salt in the presence of a ligand, serving as both ligand and reducing agent (Bodio *et al.*, 2014).

A mononuclear copper(I) metal can form two-coordinated complexes (Chou *et al.*, 2008), with its coordination geometry approximately linear; L—Cu—L angles between 170°-180°. The more commonly formed three-coordinated copper(I) complex preferred a trigonal planar formation (Li et al., 2003) and their bond length and bond angle varies depending on the torsional and steric nature of its ligands. The most common copper(I) complex are those with four-coordinated tetrahedral geometry that is usually distorted subjected to the different nature of ligands bonded to the metal centre.

A mononuclear copper(I) complex coordinated to the multidentate ligand may result in cyclometalated complexes (Crispini *et al.*, 2018; Devkule & Chavan, 2017). Thus, the bond angles have consequentially deviated with respect to ring strain. While, in the case of unidentate ligands, the effects of the steric hindrance for several different donor atoms may result in the elongation of the Cu—L bonds (Khan *et al.*, 2018). On the other hand, torsional hindrance may have an effect on both bond angles and bond lengths.

In cases of a binuclear copper(I) complexes, the formation of Cu—Cu (Engelhardt *et al.*, 1991), bridging or Cu—L—Cu bridging (Xu *et al.*, 2018) can be observed. In cases of Cu—L—Cu, the bridging bond lengths and angles varies in correspond to the type of ligands, atomic radii and the nature of the bridging atoms (Khandar *et al.*, 2010). Other expanded multinuclear copper(I) complexes (Hu *et al.*, 2014) and coordination polymer copper(I) complexes (Sugimoto *et al.*, 2018) have been reported with elaborated structural properties.

2.4 Phosphine

Phosphine is a group of compounds with the formula PR_3 (where R can be H or an organic group) and throughout the years has become one of the most important classes of organophosphorus compounds. One of the most known and commonly used organophosphorus compounds is triphenylphosphine (PPh_3) (Figure 2.6). They are usually prepared by reacting halophosphines and organometallic compounds, alkyl halides with metal phosphides or by reduction of phosphorus compounds or hydrophosphination (Levason, 1990). However, with modern advancement, many new methods of synthesising a new type of phosphine have been developed through catalytic procedures (Wauters *et al.*, 2014). Most phosphines are highly oxidisable to its corresponding phosphine oxide, which has become a major concern in its synthesis as well as storage. Thus, some phosphine is available in its oxide form and reduction process is required to convert phosphine oxide to phosphine (Li *et al.*, 2012).

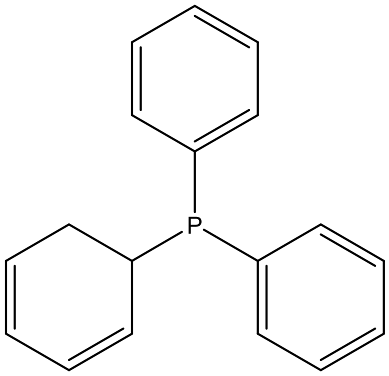

Figure 2.6: Triphenylphosphine

The complexation of tertiary phosphines is the most studied organophosphorus compound that acts as a ligand to form metal complexes due to its stability. However, the research of primary and secondary phosphines was at a slower pace (Brynda, 2005; Nell & Tyler, 2014). The interest has risen since the development of metal complexes with phosphine ligands for its catalytic properties for the application of cross-coupling reactions (Fu *et al.*, 2017; Kollár & Keglevich, 2010; Martin & Buchwald, 2008). The various types of phosphine have led to the discovery of vast compilations of metal complexes with phosphine ligands. This includes macrocyclic phosphine complexes (Swor & Tyler, 2011), heteroleptic tris-chelate ruthenium(II) complexes containing phosphine as a co-ligand (Barolli *et al.*, 2017), a palladium(II) complex with phosphine ligands (Gunasekaran, 2018; Khan *et al.*, 2018) and so on.

2.5 Hirshfeld Surface Analysis

The Hirshfeld surface analysis was developed to explain the space occupied by a molecule in a crystal structure by partitioning the crystal electron density into molecular fragments. Hirshfeld surfaces were named in honour of F. L. Hirshfeld, who proposed the stockholder partitioning scheme for defining atoms in molecules, consequently, led to the extension of expressing a molecule in a crystal space (Hirshfeld, 1977; Spackman & Jayatilaka, 2009).

Hirshfeld surface has since become a unique tool in the prediction and study of crystal structure and its packing behaviour. This method is so-called analysis; because it has proven to be a better method in uncovering the minute factors and features that contribute to a specific crystal characteristic, unlike by just examining the classical crystal packing diagrams (Spackman & McKinnon, 2002). Clearer rationale for distinguishing a various types of non-bonding interactions (such as; van der Waals forces, hydrogen bonding, intermolecular contacts to halogen atoms, $\pi \cdots \pi$ stacking interaction and so on (Desiraju *et al.*, 2011)) and their impact within the crystal system can be understood.

Generally, it is generated based on the theory of space partitioning in a crystal, relating to the electron distribution calculated as the sum of spherical atom belong to the molecule, (promolecule) dominates the corresponding sum over the crystal (procrystal). This gives rise in the analogy with Hirshfeld's idea, defined as the molecular weight function $w(r)$ (Equation 2.1) (Chopra, 2018; Spackman & Jayatilaka, 2009).

$$w(r) = \frac{\rho_{promolecule(r)}}{\rho_{procrystal(r)}} = \frac{\sum_{\mathrm{A}\epsilon promolecule} \rho_{\mathrm{A}}(r)}{\sum_{\mathrm{A}\epsilon procrystal} \rho_{\mathrm{A}}(r)}$$

Equation 2.1: Molecular weight function.

Where $w(r)$ is a continuous function with $0<w(r)<1$, $\rho_A(r)$ is the spherically averaged atomic electron density centred on nucleus A. Therefore, the Hirshfeld surface is the region surrounding the molecule in the crystal where $w(r) \geq 0.5$. It is the region where the ratio of promolecule contribution to the procrystal electron density exceeds from all other molecules in the crystal (Spackman & Jayatilaka, 2009).

Each molecule has its own unique set of spherical atomic electron density; thus, no two molecules have the same Hirshfeld surface. Spackman and co-worker also stated that:

> "… the Hirshfeld surface envelops the molecule and defines the volume of space where the promolecule electron density exceeds that from all neighbouring molecules. It guarantees maximum proximity of neighbouring molecular volumes, but the volumes never overlap because of the nature of the weight function." (Spackman & Jayatilaka, 2009)

2.5.1 Properties of Various Surfaces and Fingerprint Plots

Apart from being ecstatically pleasing, the interesting feature of Hirshfeld surface is that all information regarding the intermolecular interaction is easily achievable based on various functions of distance and curvature map. There are five main functions described, that is d_e, d_i, d_{norm}, shape index and curvedness (Spackman & Jayatilaka, 2009). All this information can be obtained using the CrystalExplorer17 software (Turner *et al.*, 2017; Wolff *et al.*, 2012). This is practically useful in the crystal studies and the packing characteristic of structurally closely related molecules.

Two distances are defined for every point on the surface; d_i is the distance to the nearest nucleus internal to the surface while d_e is the distance from the point to the nearest nucleus external to the surface. Based on the contact distances of both d_e and d_i and their relationship with the van der Waals radii of the atom, we can obtain the normalised contact distance (d_{norm}). This facilitates the association of the regions that are significant to the intermolecular interactions of a crystal. When intermolecular contacts are longer or shorter than the van der Waals separations, the value becomes positive or negative respectively. The Hirshfeld surface mapped for d_{norm} shows plotting of red, white and blue colour scheme, where red indicates shorter contacts, white specifies the contacts around the van der Waals separation and blue representing the longer contacts (Wolff *et al.*, 2012).

Shape index mapping of the Hirshfeld surface has very practical features representing the nature of the self-complementary pairs in the crystal packing, where the two shape-indices differs only by a sign. This mapping represented as such that for the negative value, in red, indicating hollows or concave surface, while the convex or bumps surface showing a positive value, in blue (Spackman & Jayatilaka, 2009). Consequently, they create a mapping showing two molecular surfaces touching one another like a stamp and mould. Shape index is a measurement of "which shapes" of the surface and it can be sensitive to very minute changes in surface shape, particularly in areas where the total curvature (or the curvedness) is very low (Wolff *et al.*, 2012).

Curvedness can also be mapped out, where sharp region shows evidence of high curvedness and flat region of a surface representing low curvedness. Curvedness is expressed as a function of the root-mean-square curvature of the surface. A typical curvedness map shows a largely flat region mapped in green and separated by comparatively dark blue edges indicating a large positive curvature (Sim *et al.*, 2014; Spackman & Jayatilaka, 2009). Curvedness is a measure of "how much shape". The sharp curvature region possesses a high curvedness, tend to divide the surface into patches associated with contacts between neighbouring molecules (Chopra, 2018). While surfaces with low curvedness give some indication regarding the molecular geometry. A flat surface having a low curvedness and planar to the aromatic ring may be an indication of the presence of π···π stackings (Gumus *et al.*, 2018).

Another useful approach is the electrostatic potential of the electron density on the Hirshfeld surface. This information established an instant display of the property relating to the electrostatic potential of each molecule inside a crystal system. The electrostatic interaction between neighbouring molecules is indicated by red (electronegative) and blue (electropositive) region (Turner *et al.*, 2017).

The 2D fingerprint plot outcome of Hirshfeld surface has become a convenient and straightforward summary in the classification, identification and quantification of the nature of intermolecular interactions in a certain crystal systems (Mahmoudi *et al.*, 2016; Spackman & McKinnon, 2002). As discussed by Spackman and co-workers, the 2D histogram was employed by the combination of d_e and d_i values. The binning pairs with the intervals of 0.01 Å were represented by colouring each bin (respectively a pixel), resembling as a function of every single fraction of surface points. Different colours of each point indicating the contribution of each d_e and d_i, where the uncoloured region shows no contributions. The blue region representing small contributions, while the region with more contribution and greatest contribution is signified with the colour green and red respectively (Safin *et al.*, 2016; Seth *et al.*, 2011; Spackman & Jayatilaka, 2009).

CHAPTER 3: METHODOLOGY

3.1 Materials

Common organic solvents were used for the syntheses, purification and crystal growing of the ligands and complexes. Chemical needed for the synthesis work were: benzoyl chloride (ACS reagent, 99 %, Sigma-Aldrich), ammonium thiocyanate (Crystalline/Certified ACS, Fisher Chemical), aniline (Certified ACS, Fisher Chemical), 2-aminophenol (99 %, Merck), 2-chloroaniline (98 %, Sigma-Aldrich), 2-anisidine (99 %, Sigma-Aldrich), and 2-toluidine (99 %, Sigma-Aldrich), 3-aminophenol (98 %, Merck), 3-chloroaniline (99 %, Sigma-Aldrich), 3-anisidine (97 %, Sigma-Aldrich), and 3-toluidine (99 %, ACROS Organics), 4-aminophenol (99 %, Merck), 4-chloroaniline (98 %, Sigma-Aldrich), 4-anisidine (99 %, Sigma-Aldrich), and 4-toluidine (99.6 %, Sigma-Aldrich). Other chemical used includes triphenylphosphine (99 %, Sigma-Aldrich), and copper(I) iodide (98 %, Sigma-Aldrich). All chemicals were used without further treatment.

All solvent used such as acetone, methanol, ethanol, diethyl ether, and acetonitrile were reagent grades and purchased from Merck, Friedemann Schmidt Chemicals, Fischer and J. T. Baker. Other deuterated solvents such as DMSO-d_6, $CDCl_3$-d_1, and acetone-d_6 were purchased from Merck and Sigma Aldrich.

3.2 Instrumental Technique

3.2.1 Fourier Transform Infrared (FTIR) Spectroscopy

The IR measurement for all the synthesised compounds was conducted in the frequency range of 450-4000 cm^{-1} using Perkin Elmer FTIR-Spectrum 400 equipped with the attenuated total reflectance (ATR) polarisation accessory.

3.2.2 Melting Point

The melting point was measured with MEL-TEMP II melting point apparatus. Glass capillary sample tubes were used.

3.2.3 Nuclear Magnetic Resonance (NMR) Spectroscopy

The ^{1}H NMR and ^{13}C NMR spectra of ligands (**TI-T13**) were recorded in deuterated dimethyl sulfoxide, DMSO-d_6. The ^{1}H NMR, ^{13}C NMR and ^{31}P NMR spectra of the copper(I) phosphine complexes (**CT1-CT13**) were recorded in deuterated chloroform, $CDCl_3$. The ^{1}H NMR and ^{13}C NMR were referenced to internal tetramethylsilane (TMS) whereas the ^{31}P NMR was externally referred to 85 % phosphoric acid. All the NMR experiment was conducted on a JEOL ECA 400 MHz instrument.

3.2.4 Elemental (CHN) Analyser

The composition of C, H, and N for all the complexes (**CT1-CT13**) was analysed on a Perkin Elmer CHN Analyser 2400. The samples were packed in a standard size solid sample tin capsule.

3.2.5 Single Crystal X-Ray Crystallography (SCXRD)

X-ray quality crystals were produced for all the phosphanecopper(I) complexes of acylthiourea derivatives (**CT1-CT7**). Yellow crystals of dimension and structure suitable for X-ray diffraction analysis for all complexes **CT1-CT7** were grown by slow evaporation of the acetonitrile mother liquors.

X-ray single crystal determinations of the complexes **CT1-CT7** were carried out using the Agilent Oxford Supernova Single Crystal Dual Wavelength X-ray Diffractometer and XtaLAB Synergy, Dualflex, AtlasS2 Rigaku Oxford Diffractometer using CuK_{α} (λ = 1.54184 Å) radiation. High-quality crystals were chosen using a polarising microscope and mounted on glass fibres.

Data processing and absorption correction were performed using a multi-scan method within CrysAlis PRO. Empirical absorption correction using spherical harmonics, as implemented in the SCALE3 ABSPACK scaling algorithm, (Oxford Diffraction) was carried out. The structures were solved by a direct method using SHELXS. All data were refined by full matrix least-squares refinement against $|F^2|$ using SHELXL 2017, (Sheldrick, 2015) and the final refinements were done that includes atomic positions for all the atoms, anisotropic thermal parameters for all the non-hydrogen atoms, and isotropic thermal parameters for the hydrogen atoms. The programs Olex2 (Dolomanov *et al.*, 2009), PLATON, (Spek, 2009) and Mercury (Macrae *et al.*, 2008) were used to process the data.

The Hirshfeld surface analysis was conducted and their 2D fingerprint plots were obtained using CrystalExplorer17 software (Turner *et al.*, 2017). The software reads the solved Crystallographic Information Files (CIF) for each of the single crystal structure obtained. Thus, the surface was generated and mapped out.

3.3 Syntheses

3.3.1 Synthesis of Acylthiourea Ligands (T1-T13)

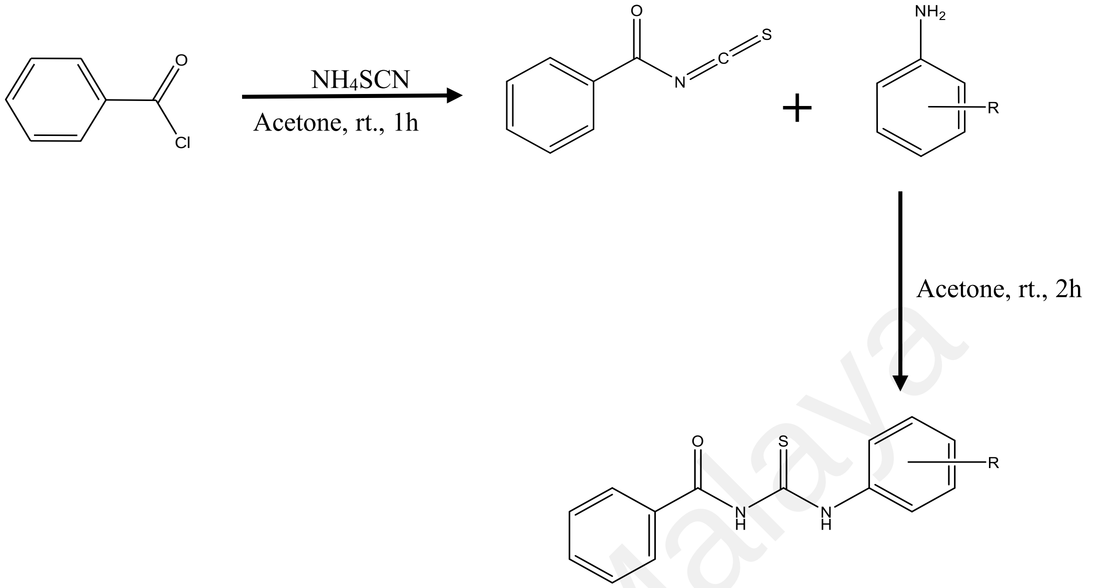

R= H, 3-Me, 3-OMe, 3-OH, 3-Cl, 2-Me, 2-OMe, 2-OH, 2-Cl, 4-Me, 4-OMe, 4-OH, 4-Cl

Scheme 3.1: Preparation of acylthiourea derivatives: *N*-benzoyl-*N*'-(R-substituted phenyl) thiourea.

The *N*-benzoyl-*N'*-phenylthiourea (**T1**) were synthesised by adapting the literature method (Brito *et al.*, 2015) as follows: Potassium isothiocyanate (15 mmol, 1.13 g) was dissolved in acetone (5.00 ml) and slowly treated with benzoyl chloride (10 mmol, 1.15 ml) in acetone (5.00 ml). The mixture was stirred for 1 hour, and then the ammonium chloride precipitate formed was filtered. Aniline or substituted aniline (10 mmol, 0.90 ml) was then added slowly into the yellow filtrate at room temperature. The mixture was stirred for 2 hours and then poured into crack ice. The precipitate formed was then collected via suction and washed with cold ethanol and followed by cold diethyl ether. The precipitate can be recrystallised from acetonitrile:acetone or alcohol:acetone mixtures. The reaction route is as in Scheme 3.1 and similar method was used to prepare other ligands (**T2-T13**).

3.3.2 Synthesis of Acylthioureas Complexes (CT1-CT13)

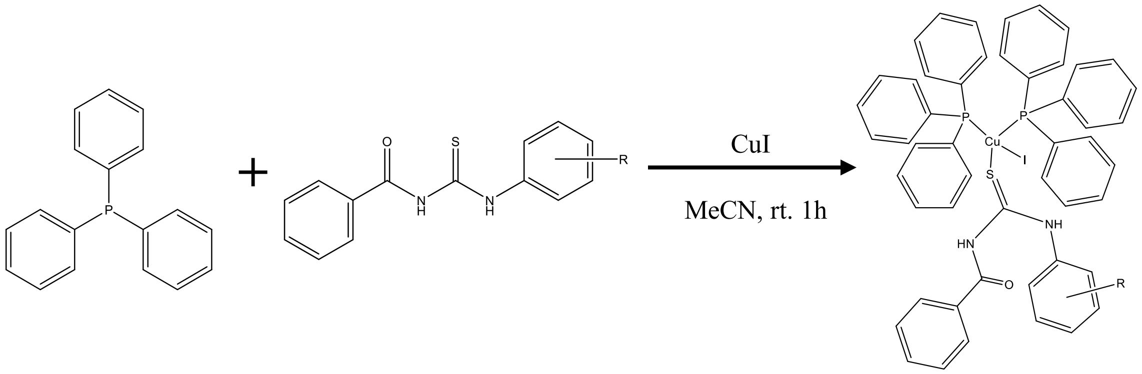

R= H, 3-Me, 3-OMe, 3-OH, 3-Cl, 2-Me, 2-OMe, 2-OH, 2-Cl, 4-Me, 4-OMe, 4-OH, 4-Cl

Scheme 3.2: Preparation of *N*-benzoyl-*N’*-(R-substituted phenyl)thiourea phosphanecopper(I) complexes.

CT1 complex was prepared by modifying previously described procedure (Scheme 3.2) (Anastasiadou *et al.*, 2016; Gunasekaran *et al.*, 2017). Triphenylphosphine (20 mmol, 5.23 g) was dissolved in acetonitrile (10.00 ml) and was stirred vigorously before copper(I) iodide solid (10 mmol, 1.90 g) was added into the stirring solution. The reaction mixture was left stirring for 1 hour and the solid formed (phosphanecopper(I) precursor) was isolated upon filtration with excess acetonitrile and methanol. The dried phosphanecopper(I) precursor, without any purification or characterisation, was directly reacted with the solid thiourea (**T1**) (10 mmol) *in-situ* followed by addition of acetonitrile (5 ml) to give a yellow precipitate in a clear yellow solution. The clear yellow solution was allowed to stand at room temperature, for a day up to a week to form pure yellow, prismatic crystals. A similar method was applied to obtained **CT2**-**CT13**.

CHAPTER 4: RESULTS AND DISCUSSION

4.1 Physical Characterisation

Result tabulated in Table 4.1 summarised the chemical formula, molecular weight (g/mol), percentage yield (%), melting point (℃), colour and CHN data for the synthesised phosphanecopper(I) complexes (**CT1-CT13**). The molecular weight of the complexes was calculated from the proposed chemical formula as in Figure 4.1. The percentage yield of the compounds was considered to be fairly good and as predicted, based on molecules with a similar scaffold (Gunasekaran *et al.*, 2017).

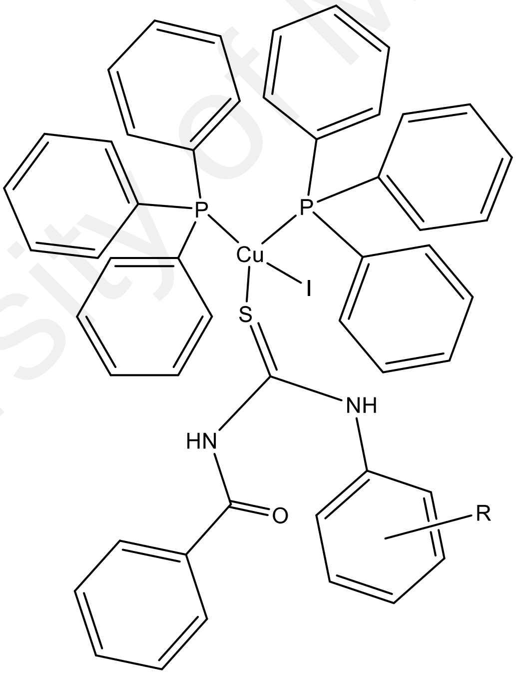

R= H, 3-Me, 3-OMe, 3-OH, 3-Cl, 2-Me, 2-OMe, 2-OH, 2-Cl, 4-Me, 4-OMe, 4-OH, 4-Cl

Figure 4.1: Phosphanecopper(I) complex (CT1-CT13).

Table 4.1: Physical data of phosphanecopper(I) complexes (CT1-CT13).

Compound	Chemical Formula	R	Molecular Weight (g/mol)	Yield (%)	Melting Point (°C)	C		H		N	
						Calc	Found	Calc	Found	Calc	Found
CT1	$C_{50}H_{42}CuIN_2OP_2S$	H	971.36	81	154-156	61.82	61.53	4.36	4.37	2.88	2.87
CT2	$C_{51}H_{44}CuIN_2OP_2S$	3-Me	985.38	79	155-158	62.16	61.96	4.50	4.37	2.84	2.66
CT3	$C_{51}H_{44}CuIN_2O_2P_2S$	3-OMe	1000.09	82	152-154	61.25	61.38	4.43	4.29	2.80	2.71
CT4	$C_{50}H_{42}CuIN_2O_2P_2S$	3-OH	987.08	85	156-158	60.84	60.93	4.29	4.02	2.84	2.73
CT5	$C_{50}H_{41}ClCuIN_2OP_2S$	3-Cl	1005.8	89	166-168	59.71	59.91	4.11	4.01	2.79	2.79
CT6	$C_{51}H_{44}CuIN_2OP_2S$	2-Me	985.38	75	172-174	62.16	62.30	4.50	4.48	2.84	2.65
CT7	$C_{51}H_{44}CuIN_2O_2P_2S$	2-OMe	1000.09	80	171-173	61.25	61.11	4.43	4.37	2.80	2.69
CT8	$C_{50}H_{42}CuIN_2O_2P_2S$	2-OH	987.08	73	170-172	60.84	61.08	4.29	4.16	2.84	2.63
CT9	$C_{50}H_{41}ClCuIN_2OP_2S$	2-Cl	1005.8	79	176-178	59.71	60.01	4.11	4.37	2.79	2.49
CT10	$C_{51}H_{44}CuIN_2OP_2S$	4-Me	985.38	77	115-117	62.16	61.86	4.50	4.20	2.84	2.69
CT11	$C_{51}H_{44}CuIN_2O_2P_2S$	4-OMe	1000.09	83	132-134	61.25	61.07	4.43	4.60	2.80	2.53
CT12	$C_{50}H_{42}CuIN_2O_2P_2S$	4-OH	987.08	74	147-148	60.84	60.59	4.29	4.16	2.84	2.71
CT13	$C_{50}H_{41}ClCuIN_2OP_2S$	4-Cl	1005.8	86	108-110	59.71	59.85	4.11	4.13	2.79	2.68

4.2 FTIR Spectra

The most significant IR bands for thioureas (**T1-T13**) and their complexes (**CT1-CT13**) are presented in Table 4.2 with their tentative assignments. The IR spectrum of ligand **T1** as shown in Figure 4.2, while the spectrum of complex **CT1** is shown in Figure 4.3. The spectra of other ligands and complexes are included in Appendix A. A polyfunctional group compound; acylthiourea tend to show very complex spectroscopic data. Based on studies conducted by using the FTIR and computational simulation and calculations, the molecular vibrational analysis of acylthiourea derivatives can be understood (Arslan *et al.*, 2007).

The IR spectra for all free ligands (**T1-T13**) presented significant vibrational bands with medium intensity in the wavenumber (v) at 3350-3200 cm^{-1} regions, attributable to v(N—H) stretching modes and correspond the hydrogen bond of the NH group (Yusof *et al.*, 2010). This band diminished in the metal complex indicating the changes of the hydrogen bonding of the amine group (Aydin *et al.*, 2010). The thiourea derivatives (**T1-T13**) can exist in the thiocarbonyl or thiol form. In the solid state of these compounds, the reduction of the v(S—H) band at about 2570 cm^{-1} and the presence of the v(N—H) bands in the range of 3000-3300 cm^{-1} in the IR spectra revealed the evidence for thiocarbonyl tautomer formation (Tadjarodi *et al.*, 2007).

The C=O bonds can be very distinctive towards its chemical environment. Thus, at region 1670 cm^{-1} may come from ordinary amide carbonyl absorption. Nonetheless, in many cases of *N'*-mono-substituted acylthiourea, an intramolecular N—H···O=C hydrogen bond may result in slight shifting in the IR spectra (Cairo *et al.*, 2017).

The other vibrational bands at lower region can be tricky to understand experimentally because of multiple overlapping of the thioamide groups. However, studies on some substituted acylthiourea with the aid of the animation of GaussView 3.0

graphical interface for gaussian programs (Arslan *et al.*, 2007) can be helpful. It was classified into four characteristic thioamide bands (I-IV) (Plutín *et al.*, 2016; Saeed *et al.*, 2015; Yang *et al.*, 2007) which have contributions from the thioamide group HN—C=S, namely; I: *v*(C—N) asymmetric stretching and *v*(C—C) of the phenyl ring at about 1500 cm^{-1}; II: *v*(C=S) vibrations and *v*(C—N) stretching at about 1300-1200 cm^{-1}; III: *v*(C—H) in-plane bending vibrations and *v*(C=S) vibration at about 1200-1050 cm^{-1}; IV: *v*(C=S) stretching at about 800-700 cm^{-1}.

Table 4.2: FTIR spectral assignments of ligands (T1-T13) and phosphanecopper(I) complexes (CT1-CT13).

Compound	**Wavenumber, *v* (cm^{-1})**					
	N-H	C=O	Thioamide bands			
			I	II	III	IV
T1	3257.25 (m)	1671.54 (m)	1526.39 (st)	1357.40 (st)	1141.92 (st)	793.27 (m)
CT1	3049.03 (w)	1669.47 (m)	1517.77 (st)	1311.95 (w)	1143.89 (st)	741.63 (st)
T2	3323.81 (m)	1667.59 (m)	1519.09 (st)	1353.65 (st)	1137.99 (st)	792.57 (m)
CT2	3048.65 (w)	1667.60 (m)	1514.77 (st)	1310.74 (w)	1139.24 (st)	741.79 (st)
T3	3270.57 (m)	1671.77 (m)	1522.07 (st)	1357.38 (st)	1140.08 (st)	784.87 (m)
CT3	3206.26 (w)	1668.63 (m)	1518.13 (st)	1313.29 (m)	1142.55 (st)	742.00 (st)
T4	3320.67 (m)	1670.54 (m)	1518.50 (st)	1327.19 (st)	1140.23 (st)	735.15 (m)
CT4	3051.29 (w)	1670.69 (m)	1514.88 (st)	1307.55 (w)	1138.95 (st)	741.94 (st)
T5	3287.13 (m)	1668.87 (m)	1516.94 (st)	1344.28 (st)	1140.86 (st)	792.00 (m)
CT5	3051.11 (w)	1667.26 (m)	1508.62 (st)	1327.93 (w)	1146.98 (st)	742.84 (st)

*w = weak, m = medium, st = strong

Compound	**Wavenumber, *ν* (cm^{-1})**					
	N-H	C=O	Thioamide bands			
			I	II	III	IV
T6	3258.02 (m)	1668.63 (m)	1517.80 (st)	1337.59 (st)	1151.07 (st)	742.56 (st)
CT6	3053.36 (w)	1667.53 (m)	1510.84 (st)	1337.24 (m)	1148.00 (st)	740.11 (st)
T7	3267.41 (m)	1674.35 (m)	1538.75 (st)	1353.68 (st)	1151.26 (st)	750.70 (st)
CT7	3047.42 (w)	1673.41 (m)	1503.31 (st)	1312.52 (w)	1148.48 (st)	742.12 (st)
T8	3288.18 (m)	1654.95 (m)	1521.53 (st)	1316.04 (st)	1142.02 (st)	747.62 (st)
CT8	3050.85 (w)	1670.60 (m)	1515.27 (st)	1308.38 (m)	1138.97 (st)	741.44 (st)
T9	3309.91 (m)	1670.78 (st)	1514.58 (st)	1330.33 (st)	1154.63 (st)	792.83 (st)
CT9	3054.34 (w)	1672.10 (m)	1508.04 (st)	1327.76 (m)	1146.96 (st)	741.82 (st)
T10	3309.91 (m)	1670.78 (st)	1508.27 (st)	1353.32 (st)	1142.58 (st)	792.83 (st)
CT10	3046.91 (w)	1667.25 (m)	1514.58 (st)	1323.14 (w)	1151.90 (st)	736.66 (st)
T11	3227.00 (m)	1668.06 (m)	1509.98 (st)	1339.37 (m)	1150.96 (st)	791.31 (m)
CT11	3049.79 (w)	1666.84 (m)	1510.90 (st)	1377.76 (w)	1151.83 (m)	739.15 (st)
T12	3355.38 (m)	1672.37 (m)	1511.65 (st)	1322.63 (st)	1145.96 (st)	742.87 (m)
CT12	3049.64 (w)	1665.61 (m)	1512.29 (st)	1307.87 (w)	1130.54 (m)	740.98 (st)
T13	3258.63 (m)	1673.76 (m)	1522.95 (st)	1333.99 (st)	1141.79 (st)	761.74 (st)
CT13	3052.67 (w)	1671.19 (m)	1508.75 (st)	1315.18 (w)	1158.00 (st)	737.53 (st)

Table 4.2, continued, *w = weak, m = medium, st = strong

All the bands have considerable changes in frequency upon coordination with copper(I). The coordination of the ligands **T1-T13** with phosphanecopper(I) is confirmed by comparing the IR spectra of the free ligands with those of the complexes. The IR vibrational bands II for the complexes showed obvious changes as the strong (st) *ν*(C=S) bands at the region 1400-1200 cm^{-1} were reduced in intensity and shifted (Figure 4.3) (Gunasekaran *et al.*, 2017). This is a significant indication that the sulphur atom of the thiourea ligand were involved in the coordination with copper(I) metal. Other noticeable observation is that the IR bands at region 3300-3400 cm^{-1} and 1670-1690 cm^{-1} attributed to v(N—H) and v(C=O) respectively (Haribabu *et al.*, 2015; Panicker *et al.*, 2010), which remained similar in both of the IR spectra of the ligands and their complexes. This ruled out the involvement of the carbonyl nor the amine group in the coordination with the metal centre.

Based on the other thioamide characteristic bands, they also supported the coordination. According to the thioamide characteristic bands I at about 1500 cm^{-1}, generally appears to have slight reduction in intensity in the spectra of the complexes, compared to the spectra of the respective free ligands. While, the absorptions at 800-730 cm^{-1}in the spectra of free ligands (**T1-T13)**, attributed to the v(C—S) stretching vibrations, and it had shown some shifting consistently in the spectra to the range of 741-743 cm^{-1} in the spectra of the complexes. These slights variations were cause by the changes of the molecular environment between the free ligand and its complex. (Plutín *et al.*, 2016). However, the bands of thioamide III, as expected, their changes in terms of the shifting and intensity which were found to be less significant nor uniform. (Aslanidis *et al.*, 2012). Thus, these support that the acylthiourea ligands behaved as monodentate S-donor ligands in the coordination.

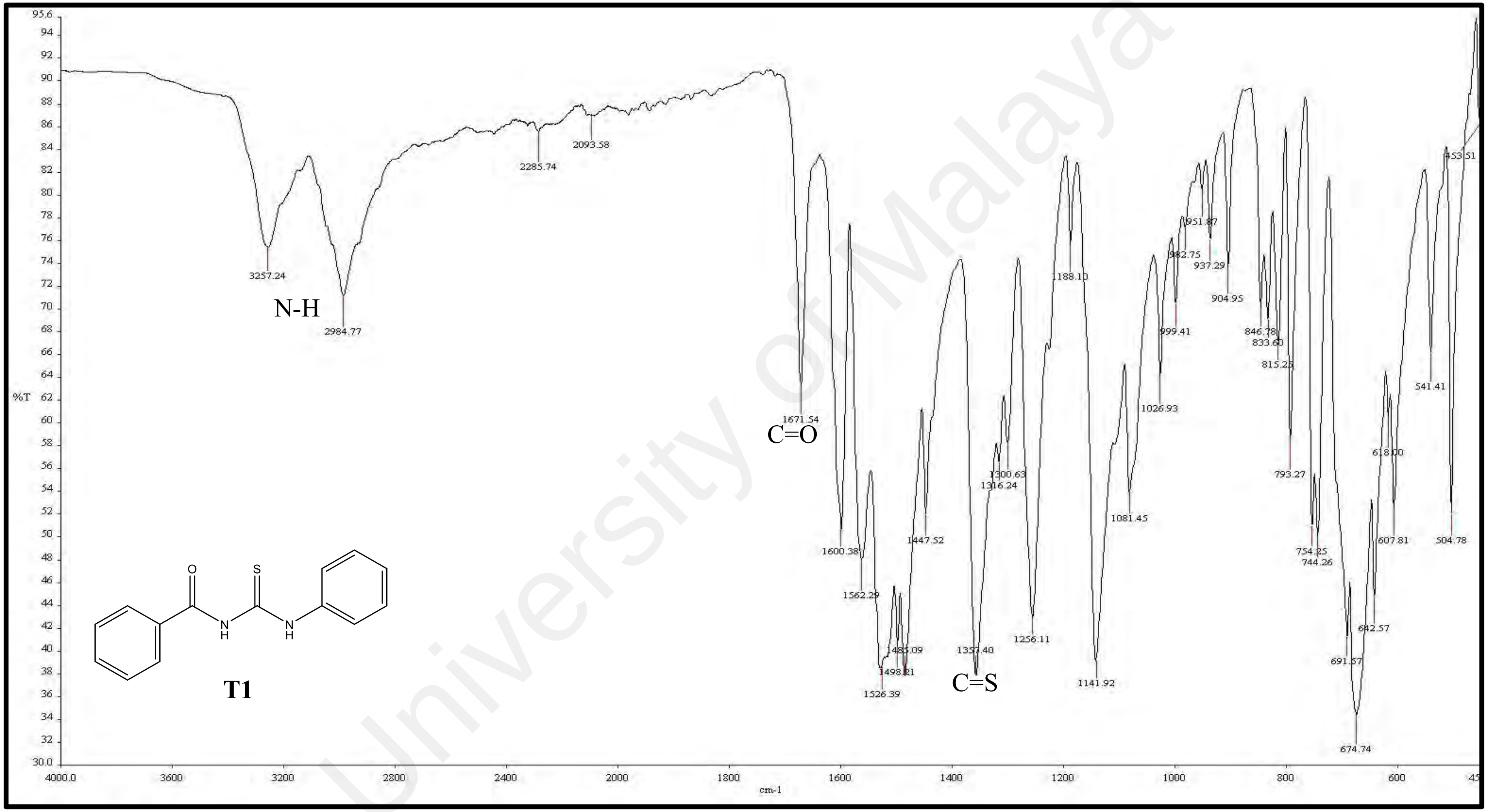

Figure 4.2: FTIR spectrum of T1.

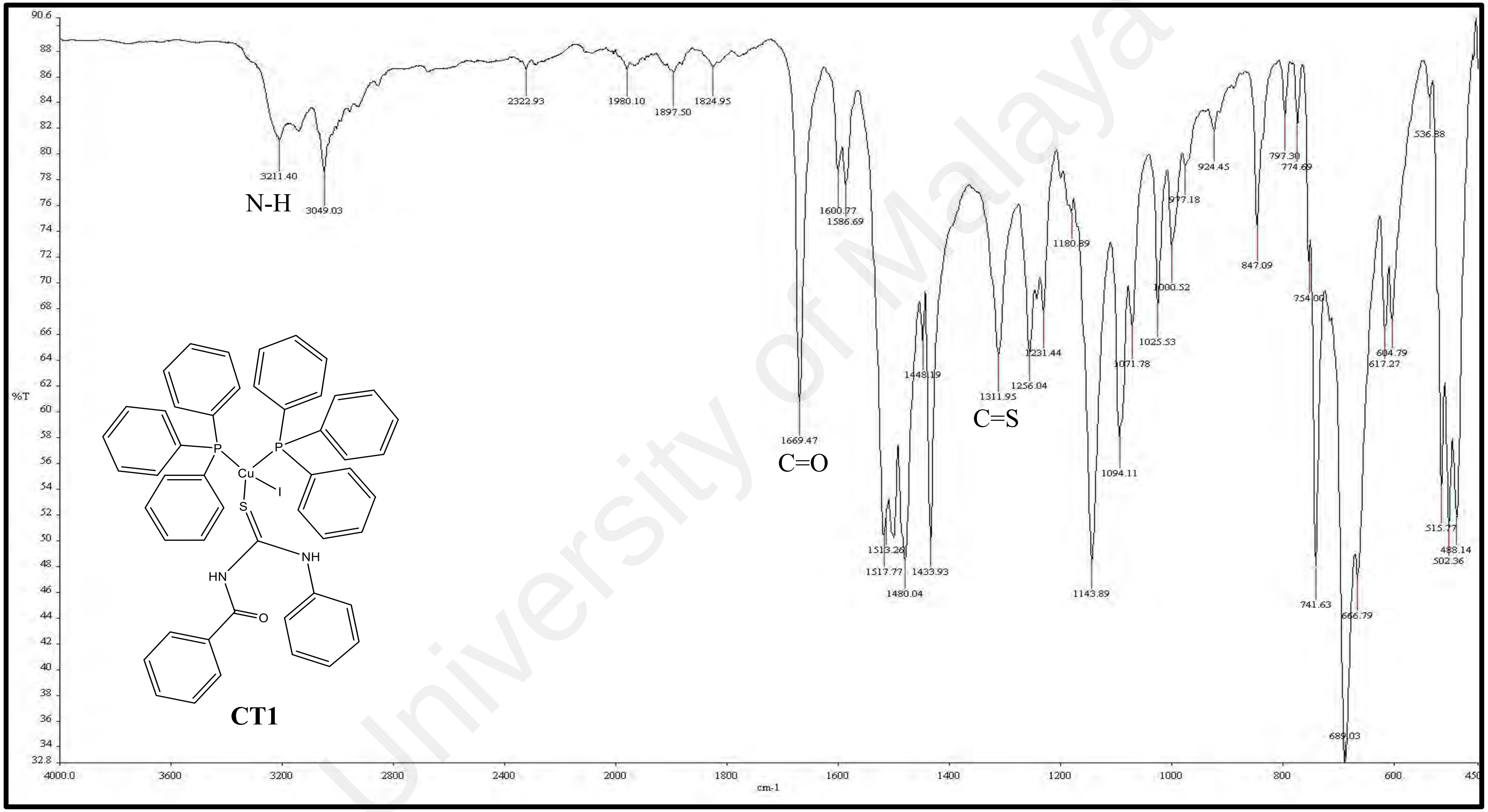

Figure 4.3: FTIR spectrum of CT1.

4.3 NMR Spectra

4.3.1 ^{1}H NMR Spectra

The ^{1}H NMR spectra of **T1** and **CT1** are given in Figures 4.4 and 4.5 respectively. Tentative assignments of the ^{1}H NMR spectra of the acylthiourea ligands and their complexes are given in Table 4.3. The ^{1}H NMR spectrum of complex **CT1** shows multiplets at the aromatic region, which integrates as 40 hydrogens at 8.04-7.19 ppm due to the aromatic protons of two phenyl rings of the ligand and the aromatic protons of two triphenylphosphine molecules attached to the metal. Similar multiplicities were also observed in the ^{1}H NMR spectra of complexes **CT2-CT13** (Appendix B) that also shows multiplets at the aromatic region, which integrates as 39 hydrogens at the range of 8.70-6.80 ppm.

In the ^{1}H NMR spectra of complexes, the N(1)H appeared at the range of 10.00-9.60 ppm and has shifted downfield compared to the free ligands at 11.90-11.40 ppm. This is due to the changes in the molecular environment as a result of complexation with the metal, based on consistent observation of all the complexes (Chetana *et al.*, 2016). These results are in good agreement suggesting that the nitrogen is not involved in the coordination with copper(I) for all of the complexes. Hence, leaving the coordination occur exclusively through the sulphur atom.

Table 4.3: ^{1}H NMR assignments of ligands (T1-T13) and phosphanecopper(I) complexes (CT1-CT13).

Compound	Chemical Shifts, δ(ppm)		
	N(1)H	Aromatic	Others
T1	11.53 (s, 1H)	7.95 (d, 2H), 7.64 (m, 3H), 7.50 (t, 2H), 7.39 (t, 2H), 7.24 (t, 1H)	-
CT1	9.86 (s, 1H)	8.04-7.19 (m, 40H)	-
T2	11.55 (s, 1H)	7.99 (d, 2H), 7.66 (t, 1H), 7.54 (m, 4H), 7.31 (t, 1H), 7.10 (d, 1H)	2.33 (s, 3H) -Me
CT2	9.92 (s, 1H)	8.04-7.18 (m, 39H)	2.34 (s, 3H) -Me
T3	11.54 (s, 1H)	7.93 (d, 2H), 7.62 (t, 1H), 7.50 (t, 2H), 7.41 (s, 1H), 7.29 (t, 1H), 7.19 (d, 1H), 6.82 (d, 1H)	3.73 (s, 3H) -OMe
CT3	9.81 (s, 1H)	8.03-6.80 (m, 39H)	3.76 (s, 3H) -OMe
T4	11.47 (s, 1H)	7.92 (d, 2H), 7.61 (t, 1H), 7.49 (t, 2H), 7.24 (s, 1H), 7.15 (t, 1H), 7.01 (d, 1H), 6.63 (d, 1H)	9.60 (s, 1H) -OH
CT4	9.61 (s, 1H)	7.98-6.74 (m, 39H)	5.14 (s, 1H) -OH
T5	11.66 (s, 1H)	7.97 (t, 3H), 7.67 (t,1H), 7.54 (m, 3H), 7.45 (t,1H), 7.35 (d, 1H)	-
CT5	9.93 (s, 1H)	8.05-7.19 (m, 39H)	-
T6	11.61 (s, 1H)	7.80 (d, 2H), 7.67 (t, 1H), 7.56 (m, 3H), 7.25 (m, 3H)	2.27 (s, 3H) -Me
CT6	9.95 (s, 1H)	8.05-7.19 (m, 39H)	2.28 (s, 3H) -Me
T7	11.56 (s, 1H)	8.57 (d, 1H), 7.99 (d, 2H), 7.67 (t, 1H), 7.54 (t, 2H), 7.25 (t, 1H), 7.16 (d, 1H), 7.00 (t, 1H)	3.89 (s, 3H) -OMe
CT7	9.61 (s, 1H)	8.52-7.21 (m, 39H)	3.92 (s, 3H) -OMe
T8	11.87 (s, 1H)	8.11 (d, 1H), 8.00 (m, 3H), 7.80 (t, 1H), 7.68 (t, 1H), 7.56 (m, 3H)	-
CT8	9.87 (s, 1H)	8.64-7.22 (m, 39H)	-
T9	11.81 (s, 1H)	8.03 (m, 3H), 7.67 (t, 1H), 7.59 (m, 3H), 7.42 (t, 1H), 7.34 (t, 1H)	-
CT9	9.72 (s, 1H)	8.18-7.19 (m, 39H)	-
T10	11.53 (s, 1H)	7.99 (d, 2H), 7.66 (t, 1H), 7.55 (m, 4H), 7.24 (d, 2H)	2.32 (s, 3H) -Me
CT10	9.66 (s, 1H)	8.00-7.21 (m, 39H)	2.36 (s, 3H) -Me
T11	11.47 (s, 1H)	7.93 (d, 2H), 7.62 (t, 1H), 7.51 (m, 4H), 6.94 (d, 2H)	3.74 (s, 3H)-OMe
CT11	9.82 (s, 1H)	8.00-6.88 (m, 39H)	3.82 (s, 3H)-OMe
T12	11.78 (s, 1H)	8.28 (d, 2H), 8.08 (d, 2H), 7.98 (d 2H), 7.68 (t, 1H), 7.55 (t, 2H)	-
CT12	9.56 (s, 1H)	7.97-6.83 (m, 39H)	-
T13	11.58 (s, 1H)	7.93 (d, 2H), 7.67 (d, 2H), 7.60 (t, 1H), 7.50 (t, 2H), 7.44 (d, 2H)	-
CT13	9.83 (s, 1H)	8.02-7.18 (m, 39H)	-

*s= single, d= doublet, t= triplet, m= multiplet

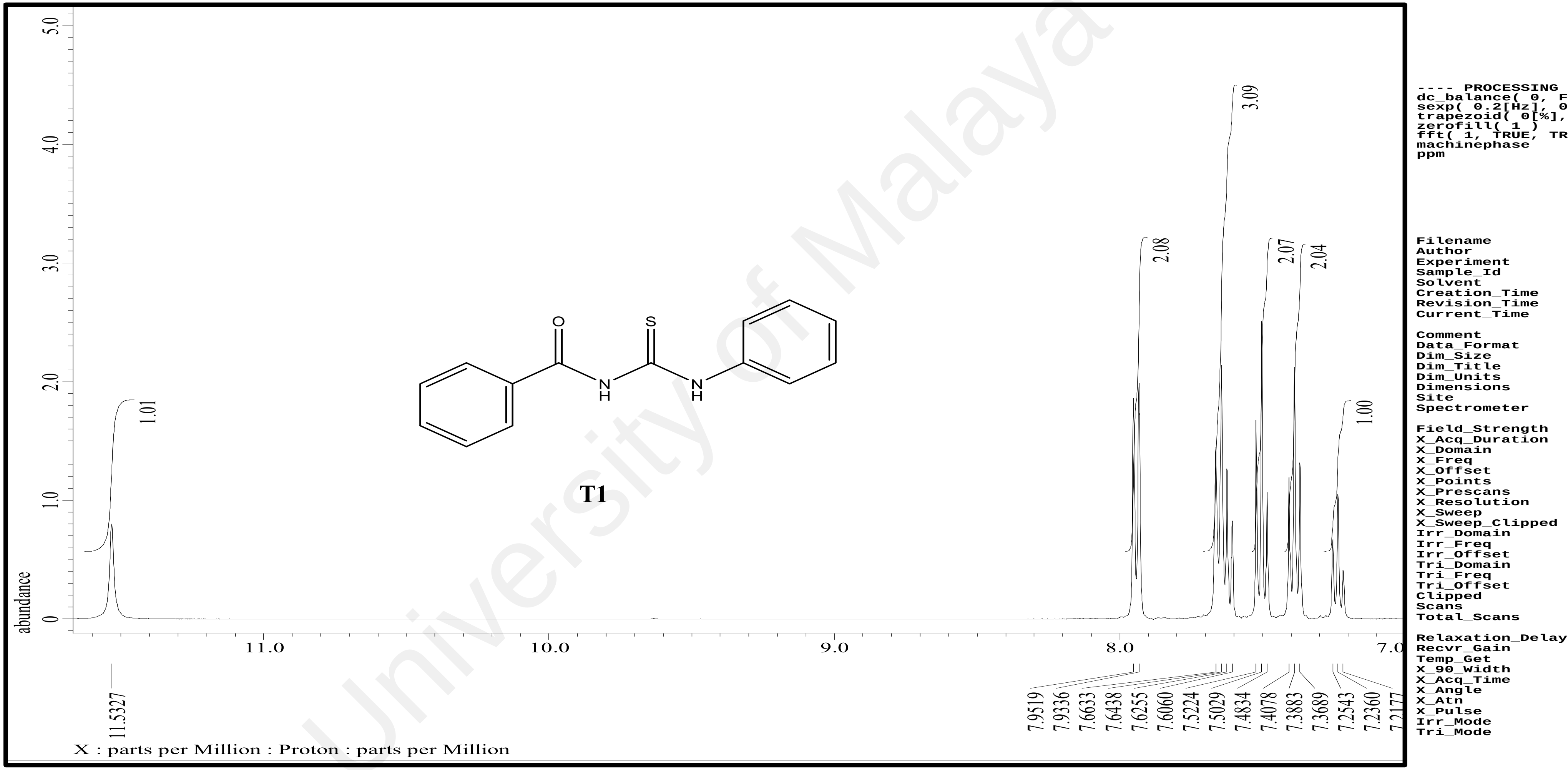

Figure 4.4: ^{1}H NMR spectrum of T1.

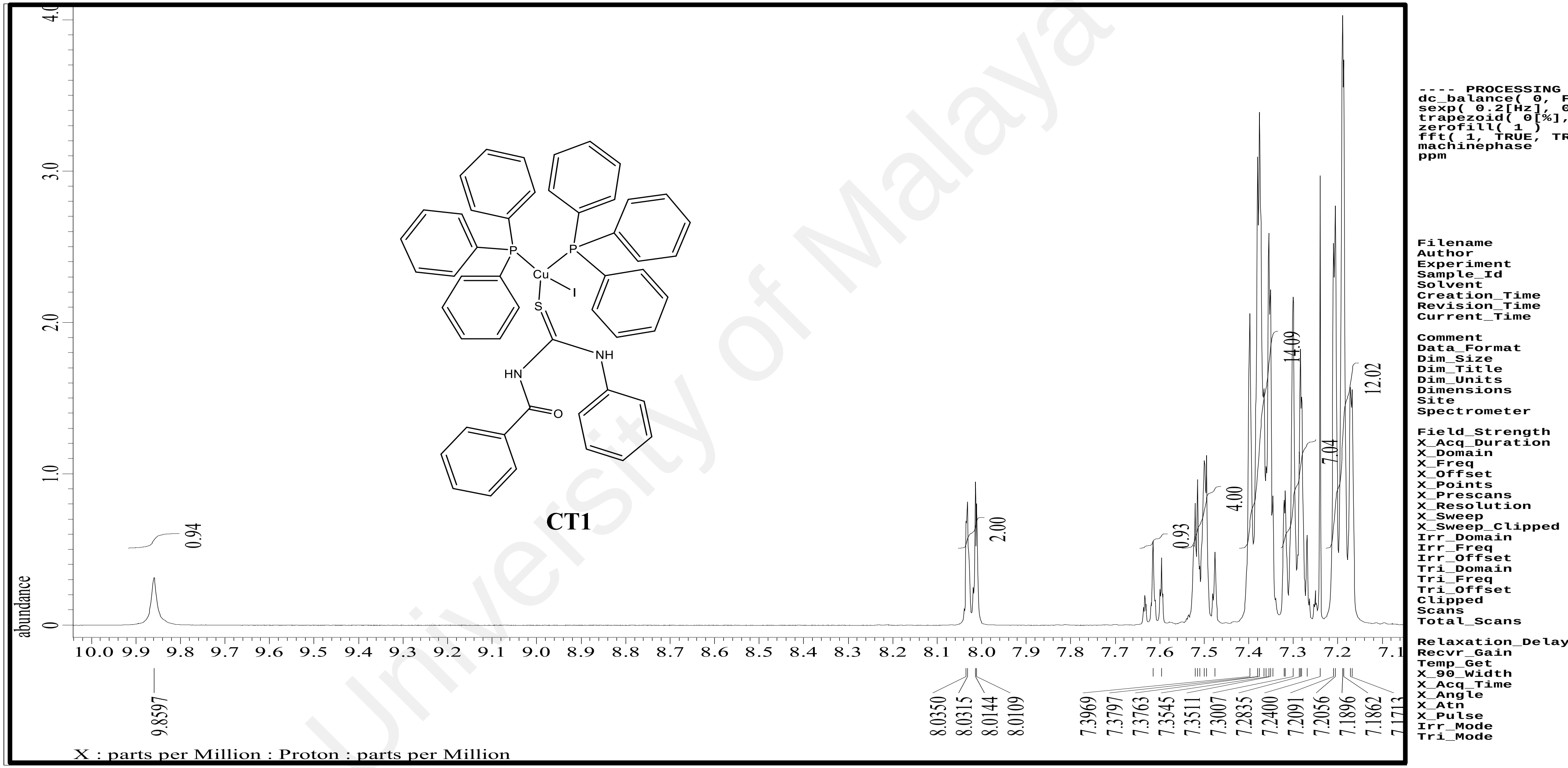

Figure 4.5: ^{1}H NMR spectrum of CT1.

4.3.2 ^{13}C NMR Spectra

^{13}C NMR spectra of the ligand **TI** and its complex **CT1** are given in Figures 4.6 and 4.7 respectively. The ^{13}C NMR chemical shifts for the acylthiourea and its phosphanecopper(I) complexes are presented in Tables 4.4. The proton-decoupled ^{13}C NMR spectra for complexes showed significant chemical shifts compared with the free ligands. The ^{13}C NMR spectra of these complexes (Appendix C) showed the presence of 13 carbon signals in complex **CT1** and **CT13**. As for **CT12,** it has 14 signals while 15 signals were observed for **CT8**, **CT9**, **CT10** and **CT11**. Whereas, there were 16 carbon signals for complexes **CT4** and **CT5**, and for complexes, **CT2**, **CT3**, **CT6** and **CT7** have 17 carbon signals.

The C=S carbon atom resonance was observed in the farthest low field at the range between 179.37-179.99 ppm in the ^{13}C NMR spectrum of the free ligands, resultant of the conjugative effect of the C=O—N(1)—C=S—N(3) thiourea skeleton. This signal underwent a slight upfield shift to 177.91-178.33 ppm in all complexes. This is possibly due to the electron delocalisation induced from the coordination of copper(I) with the ligand through the thiourea sulphur (Gunasekaran *et al.*, 2012).

The carbon atoms of the phenyl rings in triphenylphosphine are observed in the aromatic region with a higher abundance. It was also noticed that the signals split into doublets by the magnetic field of phosphorus atoms. This splitting occurred even in the proton-decoupled spectrum; this is expected because carbon-phosphorus coupling is not turned off (Pavia *et al.*, 2008). Meanwhile, the aromatic carbons of the phenyl ring belonging to the thiourea were observed in the aromatic region with respect to the free ligands. However, in the case of **CT8**, **CT9** and **CT13**, the number of carbon signal of the phenyl ring attributed to the ligand is observed to be less than the predicted result of the free ligand. This is due to some overlapping of the acylthiourea carbon signal and the triphenylphosphine ligand. Thus, the ^{13}C NMR spectra observed for the phosphanecopper(I) complexes provided direct information about the carbon skeleton of the compounds; where the total numbers of the signals in the ^{13}C NMR spectra of the complexes are in good accordance with the proposed structures and are in coherent with the formulation of each complexes containing one acylthiourea ligand molecules and two triphenylphosphine molecules.

Table 4.4: ^{13}C NMR assignments of ligands (T1-T13) and phosphanecopper(I) complexes (CT1-CT13).

Compound	Chemical shifts, δ (ppm)				
	C=S	C=O	Aromatic due to acylthiourea	Aromatic due to PPh_3	Others
T1	179.65	168.83	138.52, 133.67, 132.68, 129.22, 128.99, 126.87, 124.88	-	-
CT1	178.24	168.01	137.36, 133.88, 133.32, 133.06, 131.31, 127.12, 124.67	134.18, 129.69, 128.94, 128.47	-
T2	179.48	168.88	178.66, 138.41, 133.68, 132.67, 129.21, 129.04, 128.99, 127.54, 125.19, 121.87	-	21.47 -Me
CT2	178.09	168.09	138.92, 137.22, 133.85, 133.36, 133.09, 131.30, 128.99, 127.93, 125.20, 121.77	134.18, 129.68, 128.74, 128.56	21.49 -Me
T3	179.37	168.84	159.86, 139.58, 133.69, 132.66, 130.02, 129.22, 128.99, 116.82, 112.42, 110.24	-	55.77 -OMe
CT3	177.92	167.96	159.93, 138.43, 133.90, 133.25, 132.99, 131.31, 129.64, 116.60, 113.18, 109.74	134.17, 129.72, 129.05, 128.58	55.51 -OMe

Compound	Chemical shifts, δ (ppm)				
	C=S	C=O	Aromatic due to acylthiourea	Aromatic due to PPh_3	Others
T4	179.07	168.84	158.05, 139.43, 133.65, 132.69, 130.00, 129.21, 128.97, 115.05, 113.89, 111.39	-	-
CT4	177.91	167.73	155.95, 138.51, 133.16, 132.89, 131.35, 130.01, 128.25, 116.52, 114.14, 111.37	134.16, 129.78, 129.13, 128.63	-
T5	179.99	168.73	140.00, 133.74, 133.23, 132.58, 130.84, 129.25, 129.00, 126.69, 124.62, 123.72	-	-
CT5	178.33	168.15	138.44, 134. 43, 133.29, 133.03, 131.09, 129.89, 128.61, 127.14, 124.64, 122.71	134.16, 129.71, 129.06, 128.57	-
T6	180.56	168.87	137.49, 133.99, 133.69, 132.62, 130.97, 129.26, 128.99, 127.62, 127.18, 126.70	-	18.21 - Me
CT6	179.15	168.10	136.00, 133.91, 133.63, 133.08, 132.79, 131.19, 130.86, 127.91, 126.61, 126.48	134.22, 129.76, 128.94, 128.57	18.09 - Me
T7	178.49	169.00	151.19, 133.68, 132.61, 129.27, 128.96, 127.35, 127.25, 123.79, 120.32, 111.87	-	56.57 - OMe
CT7	176.58	167.63	151.16, 134.05, 133.12, 132.85, 131.58, 128.21, 127.14, 126.88, 123.73, 120.20	134.19, 129.76, 128.99, 128.58	56.07 - OMe
T8	181.48	168.78	144.73, 134.36, 133.67, 132.67, 132.40, 130.57, 129.35, 129.03, 128.46, 125.42	-	-
CT8	178.77	168.18	148.39, 138. 55, 133.17, 132.90, 130.98, 130.25, 129.67, 121.57, 119.36	134.14, 129.76, 129.18, 128.59	-
T9	180.81	169.12	135.91, 133.83, 132.42, 130.06, 129.35, 129.00, 128.89, 128.76, 128.61, 127.84	-	
CT9	178.66	167.60	134.87, 133.49, 133.03, 132.75, 131.24, 128.41, 127.96, 126.93, 126.75	134.19, 129.79, 129.09, 128.60	

Table 4.4, continued.

Compound	Chemical shifts, δ (ppm)				
	C=S	C=O	Aromatic due to acylthiourea	Aromatic due to PPh_3	Others
T10	179.51	168.83	136.21, 135.94, 133.66, 132.69, 129.65, 129.20, 128.98, 124.77	-	21.16 - Me
CT10	178.33	167.76	137.09, 134.85, 133.83, 133.18, 132.91, 131.47, 128.28, 124.55	134.16, 129.75, 129.09, 128.61	21.24 - Me
T11	179.68	168.78	157.98, 133.63, 132.71, 131.37, 129.19, 128.98, 126.53, 114.33	-	55.82 - OMe
CT11	178.50	167.99	158.43, 133. 82, 133.23, 132.96, 131.40, 130.28, 126.29, 114.11	134.18, 129.72, 129.02, 128.58	55.59 - OMe
T12	179.83	168.64	144.85, 144.56, 133.82, 132.51, 129.31, 129.01, 124.85, 125.54	-	-
CT12	178.61	167.77	133.86, 133.46, 133.21, 131.44, 130.39, 128.28, 126.44, 115.69	134.15, 129.67, 129.10, 128.58	-
T13	179.91	168.73	137.52, 133.70, 132.63, 130.80, 129.23, 129.12, 128.99, 126.78	-	-
CT13	178.45	167.83	135.95, 133. 44, 133.18, 132.43, 131.26, 128.29, 125.81	134.15, 129.68, 129.15, 128.56	-

Table 3.4, continued.

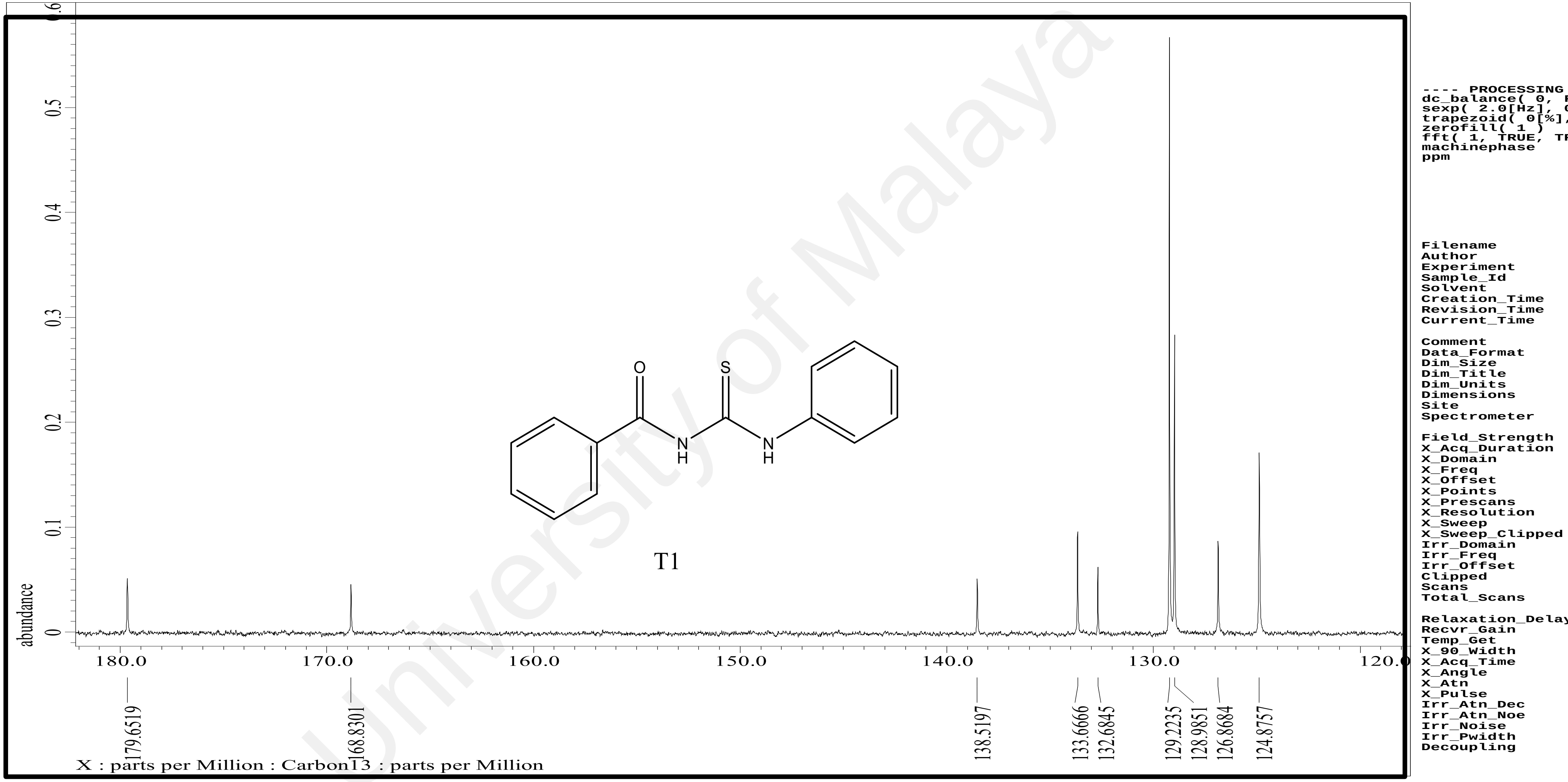

Figure 4.6: ^{13}**C NMR spectrum of T1.**

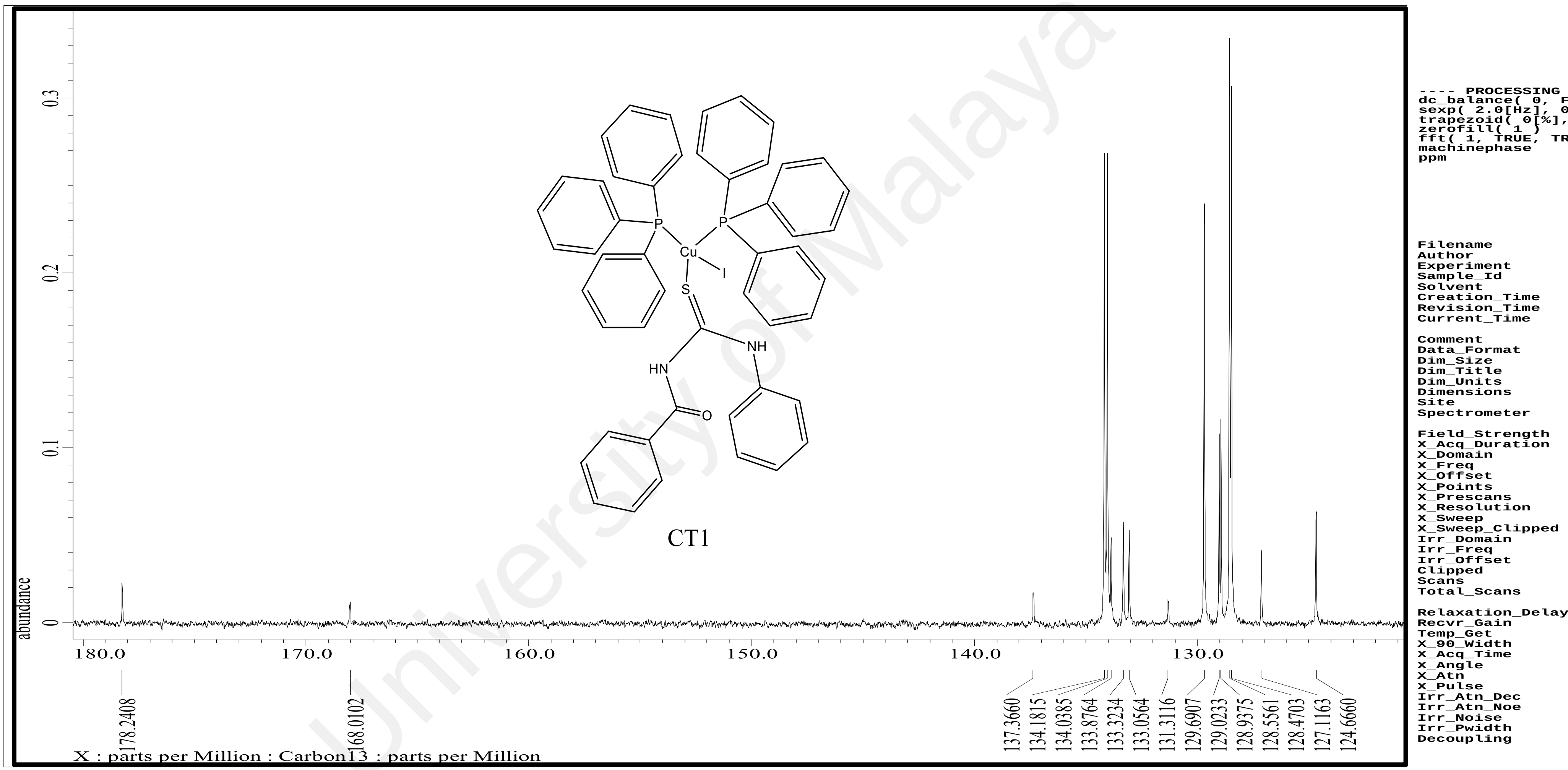

Figure 4.7: ^{13}C NMR spectrum of CT1.

4.3.3 ^{31}P NMR Spectra

The ^{31}P signals for the phosphanacopper(I) complexes of acylthiourea are presented in Table 4.5. The ^{31}P NMR spectra of the complexes **CT1-CT13** in $CDCl_3$-d_1 exhibited only one signal at around -5.00 ppm indicating the presence of the triphenylphosphine (Shakhatreh *et al.*, 2012). A single resonance signal is observed because the chemical environment of the phosphorus atom from the two triphenylphosphine groups is similar (Qiu *et al.*, 2014). The ^{31}P NMR spectrum of complex **CT1** is given in Figure 4.9 and **CT2-CT13** (Appendix D).

Table 4.5: ^{31}P NMR assignments of phosphanecopper(I) complexes (CT1-CT13).

Compound	Chemical shifts, δ (ppm)
CT1	-5.38
CT2	-5.41
CT3	-5.30
CT4	-5.09
CT5	-5.38
CT6	-5.33
CT7	-5.41
CT8	-5.25
CT9	-5.60
CT10	-5.12
CT11	-5.36
CT12	-5.14
CT13	-5.36

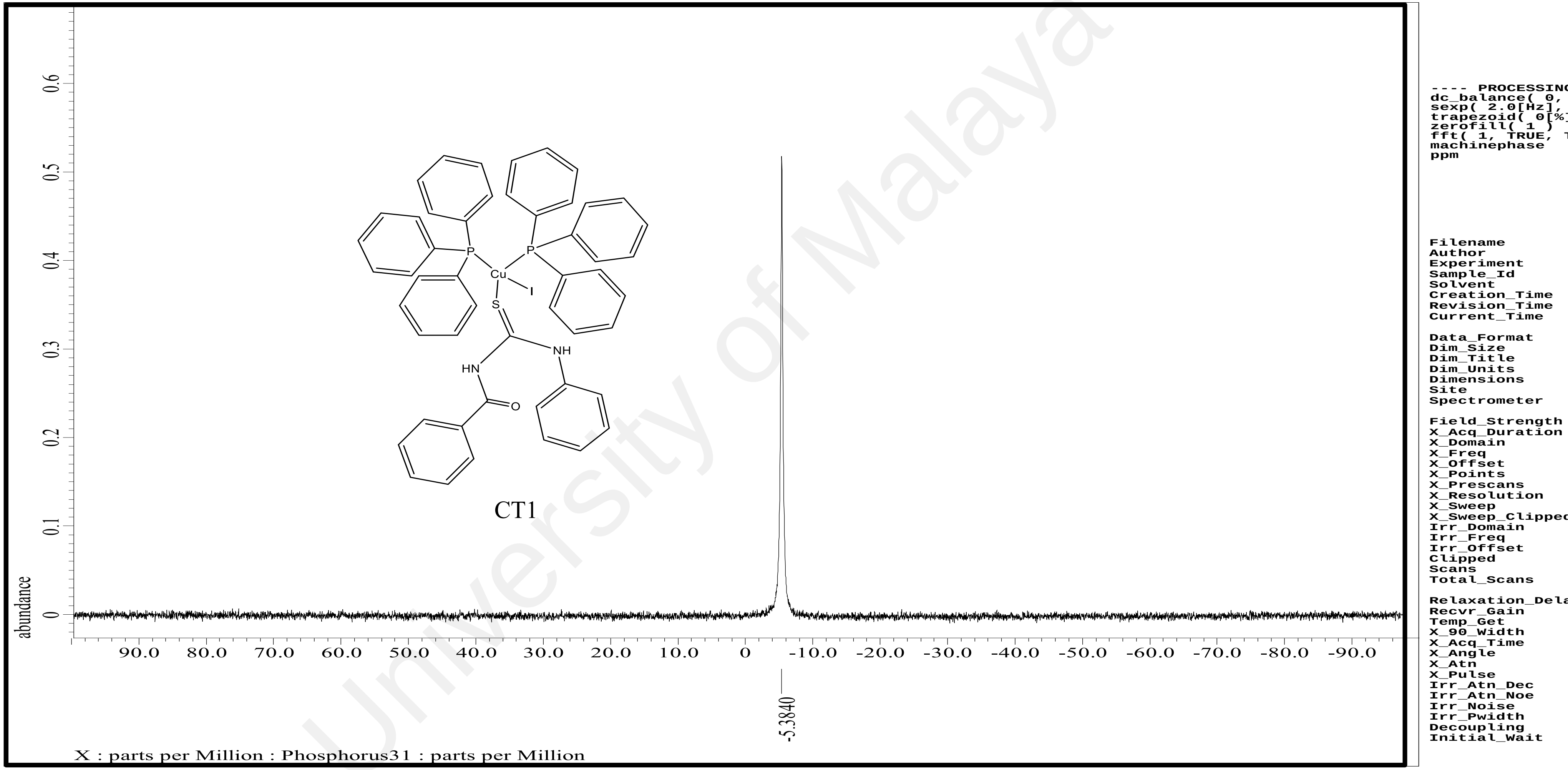

Figure 4.8: ^{31}P NMR spectrum of CT1..

4.4 X-ray Crystallography

The single crystal X-ray diffraction (SCXRD) studies of phosphanecopper(I) complexes with substituted acylthiourea ligand have been conducted to evaluate the coordination behaviour of these polyfunctional group ligands when forming complexes with copper(I) metal centre. The steric effect of the bulky phosphine co-ligands, which can modify the compound geometry and behaviour was also explored (Wang *et al.*, 2017).

Prismatic yellow coloured crystals of **CT1**-**CT7** were grown from its acetonitrile solution by slow evaporation method at ambient atmosphere and were collected to conduct the SCXRD analysis. The crystallographic data and structural refinement details and parameters obtained from X-ray diffraction analysis for all the crystals **CT1**-**CT7** are listed in Table 4.6. The result revealed that all the phosphanecopper(I) complexes, **CT1**-**CT7** are isostructural, adopting the geometry of a distorted tetrahedral form with one monodentate acylthiourea ligand, iodide anion and two PPh_3 moieties. Compounds **CT1**, **CT2**, **CT3**, **CT4** and **CT7** shows isomorphism as they crystallised in the monoclinic system with space group $P2_1/c$, while **CT5** and **CT6** crystallised in the triclinic system with space group $P\bar{1}$.

Significant bond lengths and angles are shown in Table 4.7 and Table 4.8 respectively. It is noteworthy that all efforts to produce crystallographic quality crystals of compounds **CT8**-**CT13** were unsuccessful. It seems that they either preferred to be in the amorphous form or the crystal formed was not of good quality.

Table 4.6: Crystal data and refinement details for phosphanecopper(I) complexes (CT1-CT7).

Parameter	CT1	CT2	CT3	CT4	CT5	CT6	CT7
CCDC No	1865948	1865949	1875061	1874984	1865944	1865945	1865946
Empirical formula	$C_{50}H_{42}CuIN_2OP_2S$	$C_{51}H_{44}CuIN_2OP_2S$	$C_{51}H_{44}CuIN_2O_2P_2S$	$C_{50}H_{42}CuIN_2O_2P_2S$	$C_{50}H_{41}Cl_1CuIN_2OP_2S$	$C_{51}H_{44}CuIN_2OP_2S$	$C_{51}H_{44}CuIN_2O_2P_2S$
Formula weight	971.30	985.32	1001.32	987.30	1005.03	985.33	1001.32
Temperature/ K	293(2)	293(2)	293(2)	293(2)	293(2)	293(2)	293(2)
Wavelength	CuK_α (λ = 1.54178)	CuK_α (λ = 1.54178)	CuK_α (λ = 1.54178)	CuK_α (λ = 1.54178)	CuK_α (λ = 1.54178)	CuK_α (λ = 1.54178)	CuK_α (λ = 1.54178)
Crystal system	Monoclinic	Monoclinic	Monoclinic	Monoclinic	Triclinic	Triclinic	Monoclinic
Space group	$P2_1/c$	$P2_1/c$	$P2_1/c$	$P2_1/c$	P-1	P-1	$P2_1/c$
a/ Å	10.4262(3)	10.7295(5)	10.2510	10.3834(10)	11.7876(10)	11.6335(6)	10.4317(5)
b/ Å	22.6541(6)	22.7196(10)	22.8713(10)	22.3572(10)	12.7342(12)	12.5117(6)	22.8237(12)
c/ Å	18.8774(6)	18.6290(8)	19.0029(10)	18.7591(10)	17.6274(15)	18.0259(8)	19.1489(10)
α/ °	90.000	90.000	90.000	90.000	79.475(7)	88.279(4)	90.000
β/ °	90.491(3)	91.489(4)	91.230	91.400	74.273(7)	71.833(4)	90.266(5)
γ/ °	90.000	90.000	90.000	90.00	65.999(9)	67.611(5)	90.000
Volume/ $Å^3$	4458.60(2)	4539.70(4)	4454.44(3)	4353.51(5)	2318.8(4)	2293.3(2)	4559.1(4)
Z	4	4	4	4	2	2	4
ρ_{calc}, g/cm^3	1.536	1.536	1.495	1.506	1.438	1.395	1.459
μ/ mm^{-1}	7.583	7.583	7.585	7.753	7.781	7.324	7.411
F (000)	2088	2088	2036	2000	1014	980	2032

Parameter	CT1	CT2	CT3	CT4	CT5	CT6	CT7
2Θ range for data collection/°	7.80 to 148.02	7.78 to 148.34	6.04 to 153.08	6.16 to 153.2	7.62 to 147.78	7.68 to 148.044	7.74 to 147.66
Reflections collected	19369	19651	57755	56828	16134	15880	11884
Independent reflections	7863 [Rint=0.0385, Rsigma=0.0365]	8943 [Rint=0.0525, Rsigma=0.0558]	9308 [Rint=0.0287, Rsigma=0.0179]	9073 [Rint=0.0320, Rsigma=0.0194]	9097 [Rint=0.0918, Rsigma=0.0287]	8904 [Rint=0.0859, Rsigma=0.0789]	7312 [Rint=0.0292, Rsigma=0.0417]
Data/ restraints/ parameters	7863/0/524	8943/0/534	9308/0/542	9073/0/529	9097/0/533	8904/0/534	7312/0/543
Goodness-of-fit on F2	1.023	1.021	1.046	0.990	1.052	1.136	1.028
Final R indices [I>=2σ (I)]	R1 = 0.0557, wR2 = 0.1480	R1 = 0.0588, wR2 = 0.1529	R1 = 0.0207, wR2 = 0.0517	R1 = 0.0274, wR2 = 0.0738	R1 = 0.0745, wR2 = 0.1848	R1 = 0.0782, wR2 = 0.2036	R1 = 0.0457, wR2 = 0.1249
Final R indices (all data)	R1 = 0.0592, wR2 = 0.1535	R1 = 0.0649, wR2 = 0.1622	R1 = 0.0212, wR2 = 0.0520	R1 = 0.0283, wR2 = 0.0747	R1 = 0.0819, wR2 = 0.1983	R1 = 0.0858, wR2 = 0.2221	R1 = 0.0504, wR2 = 0.1319
Largest diff. peak/ hole/ e.Å-3	1.20/-1.94	1.31/-1.98	0.28/-0.89	1.44/-1.23	2.45 /-1.95	2.12/-2.80	1.10/-1.18

Table 4.6, continued

Table 4.7: Selected bond lengths (Å) for phosphanecopper(I) complexes (CT1-CT7).

Atom	**Atom**	**Length/Å**						
		CT1	CT2	CT3	CT4	CT5	CT6	CT7
Cu1	S1	2.3745(9)	2.3588(9)	2.3266(4)	2.3426(5)	2.4089(14)	2.4095(16)	2.3550(10)
Cu1	I1	2.6350(6)	2.6369(6)	2.6106(2)	2.6520(3)	2.6462(8)	2.6349(8)	2.6330(6)
Cu1	P1	2.2883(9)	2.2886(10)	2.2912(4)	2.2786(5)	2.2836(13)	2.2870(15)	2.3061(10)
Cu1	P2	2.2840(9)	2.2833(9)	2.2801(4)	2.2730(5)	2.2989(13)	2.2915(16)	2.2966(10)

Table 4.8: Selected bond angles (˚) for phosphanecopper(I) complexes (CT1-CT7).

Atom	Atom	Atom	Angle/˚						
			CT1	CT2	CT3	CT4	CT5	CT6	CT7
P1	Cu1	S1	99.71(3)	101.52(3)	99.93(15)	99.77(2)	108.50(5)	106.69(6)	99.62(4)
P1	Cu1	I1	104.93(3)	105.92(3)	105.03(13)	103.73(17)	104.02(4)	101.49(4)	106.16(3)
P1	Cu1	P2	123.46(4)	123.37(4)	124.24(16)	124.12(2)	123.42(6)	122.53(6)	123.52(4)
P2	Cu1	S1	104.14(4)	103.73(4)	106.88(16)	104.75(2)	102.19(6)	103.75(6)	106.87(4)
P2	Cu1	I1	109.07(3)	108.63(3)	107.83(12)	108.85(16)	110.62(4)	115.58(5)	107.50(3)
S1	Cu1	I1	115.84(3)	113.75(3)	112.88(12)	116.06(16)	107.26(4)	115.58(5)	113.18(3)

It is noted that the angle between the phenyl rings of the acylthiourea ligands shows some differences i.e. the phenyl ring appeared to be planar in CT5 and CT6, while perpendicular in the others. The presence of intramolecular hydrogen bond N—H···O=C (with the formation of a '6-membered ring') represented as the blue dotted lines in Figure 4.9 and Figure 4.10. Hence, explained the stability in forming a monodentate S behaviour acylthiourea ligand of all the complexes.

4.4.1 Crystal structure of CT1, CT2, CT3, CT4 and CT7

The molecular structure obtained for complex **CT1** is depicted in Figure 4.9 the H atoms of the PPh_3 were omitted for clarity. This is a monomeric compound, crystallises in the monoclinic space group $P2_1/c$, that consists of four independent [Cu(**TI**)(I)($(PPh_3)_2$)] molecular units accommodated per unit cell (Appendix E). The asymmetric unit of complex **CT1** showed that it is a mononuclear and four-coordinated with one iodide anion, two triphenylphosphine units and one acylthiourea ligand, that is *N*-benzoyl-*N'*-phenylthiourea (**T1**), as a monodentate ligand coordinating via the sulphur, (S1) atom to the copper(I), (Cu1) atoms. Again, **CT1** is isostructural with **CT2**, **CT3**, **CT4** and **CT7** (Appendix E).

Coordination bonds are listed in Table 4.7. It shows that the range for Cu—S bond distance are from (2.3266 (4)-2.4095 (16)) Å, are consistent with the distances usually found for tetrahedrally coordinated copper(I) complexes with S-donors ligands (Aslanidis *et al.*, 2012; Gunasekaran *et al.*, 2017; Shakhatreh *et al.*, 2012). The Cu—P distances ranges from (2.2730 (5)-2.3061 (10)) Å are similar to Cu—P distances in previous reported analogous complexes (Gunasekaran *et al.*, 2012; Wang *et al.*, 2017). The Cu—I bond ranges from (2.6106 (2)-2.6520 (3)) Å is less than the sum of the ionic radii of copper and iodine, that is 2.97 Å, agrees to other reported copper(I) halide complexes (Anastasiadou *et al.*, 2016; Lobana *et al.*, 2005; Walia *et al.*, 2015).

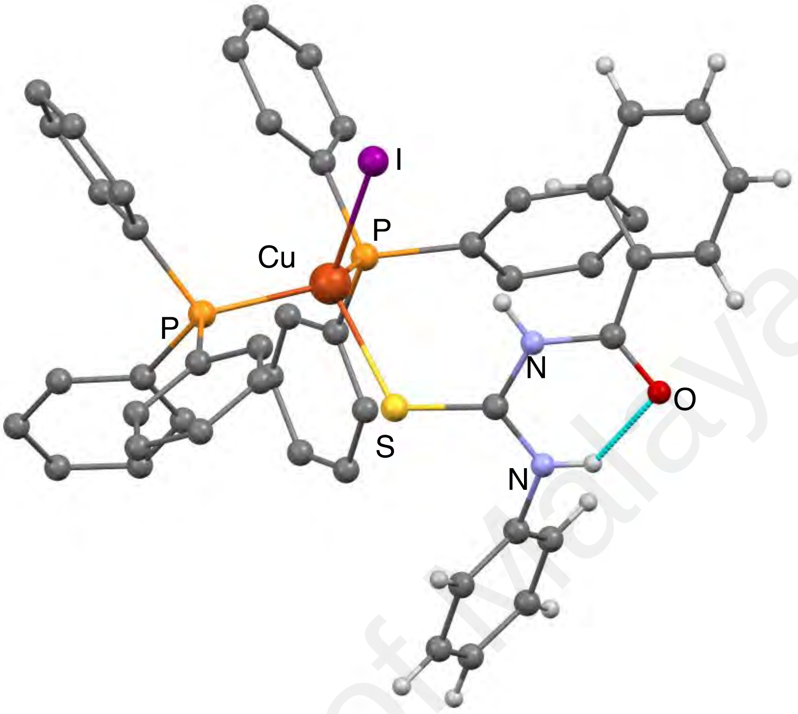

Figure 4.9: Three-dimensional structure of CT1.

The bond angles around the copper(I) atom is in the range of (99.62 (4)-124.24 (16))° as shown in Table 4.8. The deviation from an ideal tetrahedral bond angle of 109.5° is most significant at the P1—Cu1—P2 angle, that is above 120°**;** (122.53-124.24)°, subtended by the bulky triphenylphosphine ligands (Anastasiadou *et al.*, 2016). This reveals a distorted tetrahedral coordination environment around each copper(I) atom in the mononuclear complex. The distorted tetrahedral geometry is also reported in the copper(I) halide complexes with mixed PPh_3/sulphur-based ligands (Anastasiadou *et al.*, 2016; Aslanidis *et al.*, 1993; Nimthong *et al.*, 2008).

4.4.2 Crystal structure of CT5 and CT6

Figure 4.10 shows the molecular structure of complex **CT5** and the H atoms of the PPh_3 were omitted for clarity. This is a monomeric compound, crystallises in the triclinic space group $P\bar{1}$, that consists of two independent [CuI(**T5**)$(PPh_3)_2$] molecular units accommodated per unit cell (Appendix E). The asymmetric unit of complex **CT5** showed that it is mononuclear and four-coordinated with a single iodine atom, and one monodentate acylthiourea ligands, that is *N*-benzoyl-*N'*-(3-chlorophenyl)thiourea (**T5**), coordinating through the sulphur, (S1) atom of the thiourea. The other two coordination site is occupied by two triphenylphosphine units. Again, **CT5** is isostructural with **CT6** (Appendix E).

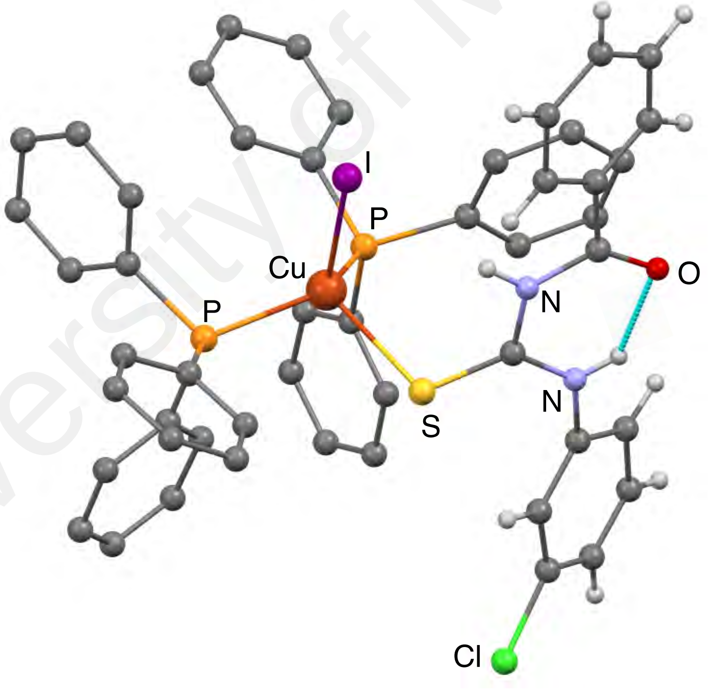

Figure 4.10: Three-dimensional structure of CT5.

Table 4.7 shows the coordination bond length of the complexes **CT5** and **CT6**. The Cu—S bond distance ranges from (2.2832(14)-2.6456(9)) Å which are in the range for tetrahedrally coordinated copper(I) complexes with monodentate S-donor ligands (Aslanidis *et al.*, 2012; Gunasekaran *et al.*, 2017; Shakhatreh *et al.*, 2012). In the case of the two Cu—P bond length, the ranges are from (2.2832(14)-2.2979(14)) Å which are similar to those found in other phosphanecopper(I) complexes (Gunasekaran *et al.*, 2012; Wang *et al.*, 2017). The Cu—I distances are from (2.6456(9)-2.6520(3)) Å is likewise less than the sum of the ionic radii of copper and iodine, 2.97 Å. Thus, they are almost similar as other reported coordinated copper(I) iodide complexes (Anastasiadou *et al.*, 2016; Lobana *et al.*, 2005; Walia *et al.*, 2015).

The bond angles of **CT5** and **CT6** are in the range of (101.49(4)-123.42(6))° deviated from the tetrahedral value as shown in Table 4.8. This revealed a distorted tetrahedral geometry around each copper(I) atom in the phosphanecopper(I) complex. This distorted tetrahedral geometry was also found in other related copper(I) halide complexes with mixed PPh_3/sulphur-based ligands (Anastasiadou *et al.*, 2016; Aslanidis *et al.*, 1993; Nimthong *et al.*, 2008). It is significant to observe the P1—Cu1—P2 internal bond angle of 123.42(6)° and 122.53(6)° respectively, which is much greater than 109.5°; making the tetrahedral figure distorted. This demonstrated that the two triphenylphosphine ligands exerted significant steric effects on the coordination geometry of both **CT5** and **CT6** complexes (Anastasiadou *et al.*, 2016).

4.5 Hirshfeld Surface Analysis

In order to exemplify the interactions of the crystal structures in this series of closely related molecules, the Hirshfeld surface analysis was conducted and their 2D fingerprint plots were established using CrystalExplorer17 software (Turner *et al.*, 2017). All the Hirshfeld surfaces were generated for all the structure of the phosphanecopper(I) complexes **CT1**-**CT7**. There were four different Hirshfeld surfaces obtained, namely: d_{norm}, shape index, curvedness and electrostatic potential. Since the complex **CT1**-**CT7** are all closely related structures (where they only differ by a few atoms or a small group of atoms), their Hirshfeld surface analysis results in a somewhat analogous but still differ considerably.

All the Hirshfeld surfaces and the 2D fingerprint plots were represented and tabulated in Table 4.9 and Table 4.10 respectively. All the Hirshfeld surfaces were elucidated as transparent to permit visualisation of the molecular structure and the positioning of each of the complexes was set individually in accordance with the specific and significant orientation of interest. Such information is crucial to fully understand and appreciate the interaction based on the crystal packing as in Appendix E of each of the complexes (**CT1**-**CT7**).

Table 4.9: Hirshfeld surface analysis maps of phosphanecopper(I) complexes (CT1-CT7).

Complex	CT1	CT2	CT3	CT4	CT5	CT6	CT7
Shape index	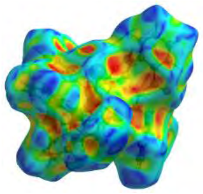	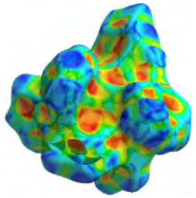	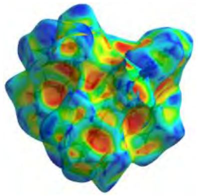	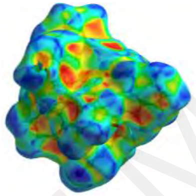	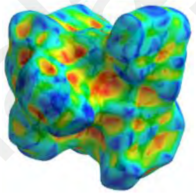	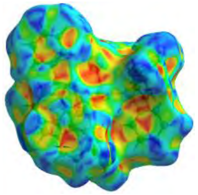	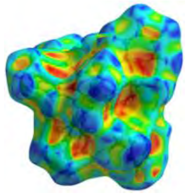
Curvedness	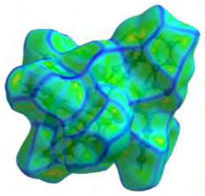	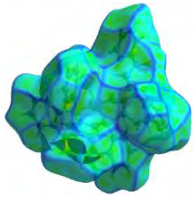	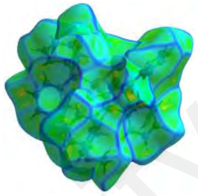	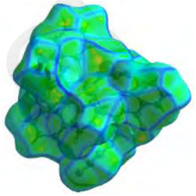	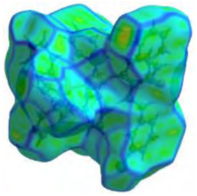	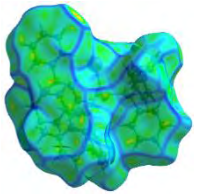	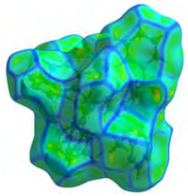
Electrostatic potential		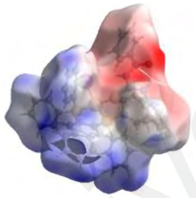	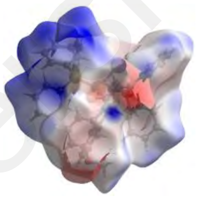	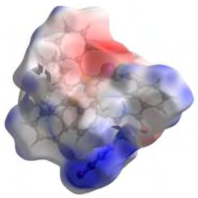	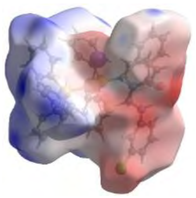	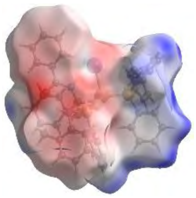	
***d*norm**	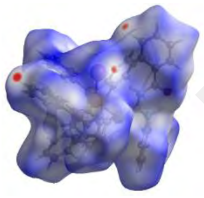	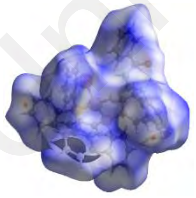	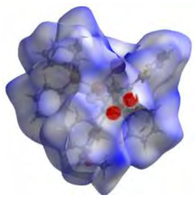	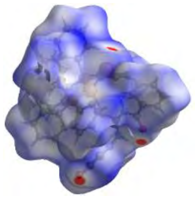	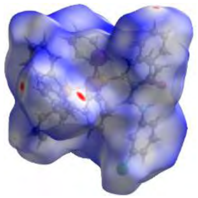	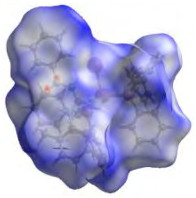	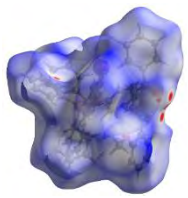

4.5.1 The Hirshfeld Surface Maps

The Hirshfeld surface mapped with shape index function illustrated the consistent pattern of adjacent blue and red triangles for complexes **CT5** and **CT6** as in Figure 4.11 and Figure 4.12 respectively. They showed a planar stacking arrangement of the molecules, a typical characteristic for a planar geometry aromatic hydrocarbon rings arranged in such a way. This is obvious when associated to the d_e and d_i range, which is within the van der Waals radii separation (clearly seen as the large white region in the d_{norm} mapping surrounding the planar surface of the ligand) (Spackman & Jayatilaka, 2009). The alternating red and blue region represented the concave and convex structure correspondingly, indicating that the neighbouring molecule participated in a π···π stacking interaction in these crystal structures (Seth *et al.*, 2011). However, there is no such existence of participation in complexes **CT1**, **CT2**, **CT3**, **CT4** and **CT7**.

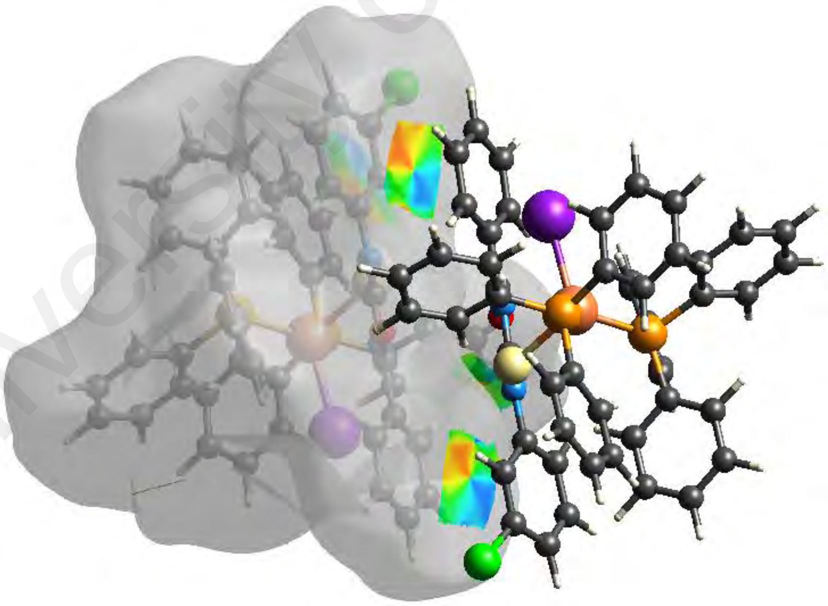

Figure 4.11: Complementary patches on the shape index surface of CT5.

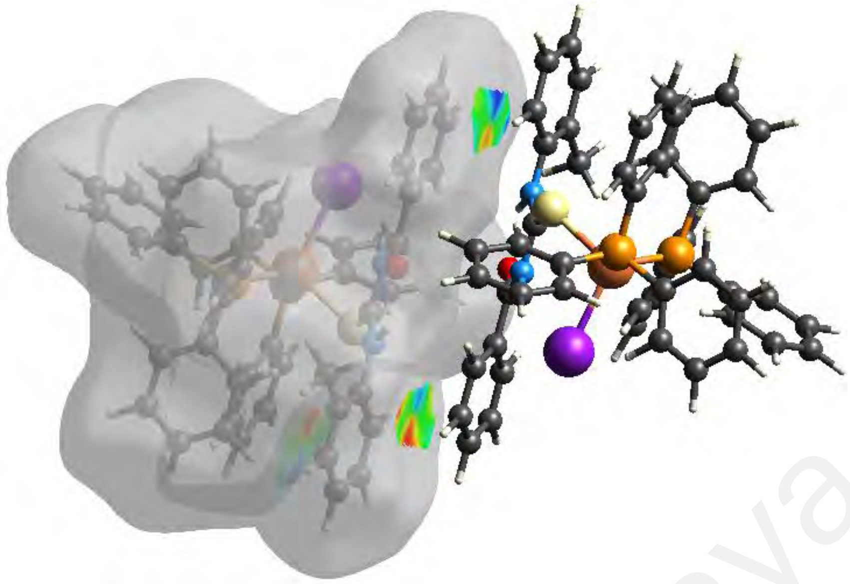

Figure 4.12: Complementary patches on the shape index surface of CT6.

This is further proven by the evidence observed on the curvedness mapping of the Hirshfeld surface. This gives insight into the different acylthiourea surface geometry resulting in different crystal packing. Complexes **CT5** and **CT6** showed relatively large green plane at the region of the acylthiourea ligand and **CT5** was observed to be more planar than **CT6**. This deduction is based on the fine blue lines on the **CT6,** surface around the acylthiourea ligand. This is due to the presence of the tetrahedral methyl group on the acylthiourea ligand. Instead, obvious sharp edges and flat green surface were observed on the surface surrounding the acylthiourea in **CT5** because the chlorine atom is planar to the aromatic ring. The curvedness mapping provided a convincing suggestion of the planarity of **CT5** and **CT6** and that give rise to the π···π stacking interaction between the crystal molecules resulting in a triclinic crystal packing (Gumus *et al.*, 2018). Whereas all the complexes **CT1**, **CT2**, **CT3**, **CT4**, and **CT7** showed many sharp edge faces and no such flat surfaces on the aromatic rings of the acylthiourea ligand. The differences between these phosphanecopper(I) complexes were due to their distinctive conformations affected by the small different substituent groups (Spackman & Jayatilaka, 2009).

The molecular electrostatic potentials mapped on Hirshfeld surfaces is over the range of -0.09 to 0.04 au for all the molecules. In specific, the blue (electropositive) and red (electronegative) mapping provided a very strong indication of the theory of electrostatic complementarity. The complexes presented a rather dramatic fashion and clear distinction can be observed between them. This proved on how small substituent groups on the acylthiourea affected the electrostatic potential of the complexes. The intermolecular hydrogen bonding (green dotted lines) of N—H···O=C interaction that was observed in **CT3**, **CT4** and **CT7** as in Appendix E is signified based on the electrostatic environment on the surface that resulted in the dipole moments of the molecule.

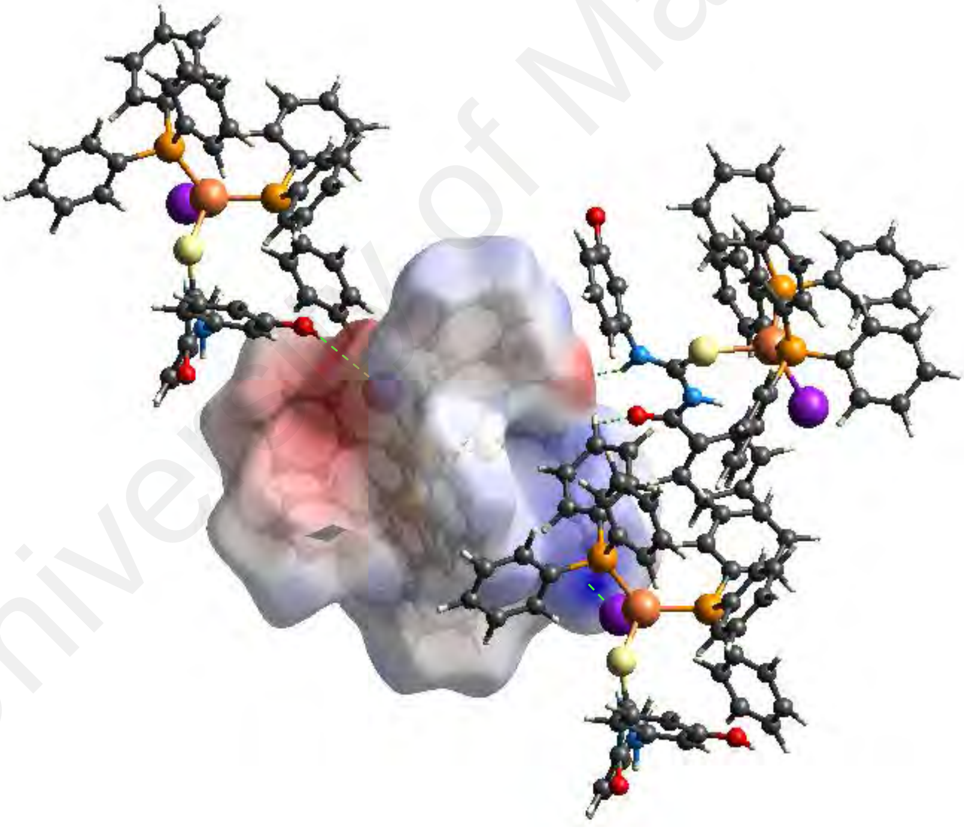

Figure 4.13: Electrostatic potential mapping of CT4.

For instance, Figure 4.13 illustrated the electrostatic potential mapping of complex **CT4**. The presence of a hydroxy group (dominated with a blue surface) on the acylthiourea ligand consequently involved in electrostatic complementary interaction with the iodine (enveloped with a red surface) of the adjacent molecule. Thus, forming a polymeric crystal chain interaction (Appendix E). Observing at the electrostatic potential mapping of complexes **CT1** and **CT2**, it indicates similar electrostatic potential distribution. This is where the area enveloping the triphenylphosphine group appeared to be blue and the region for the acylthiourea ligand is overall red. Therefore, in the complexes (**CT1-CT2**) crystal packing (Appendix E), they arranged themselves accordingly by obeying the electrostatic complementarity.

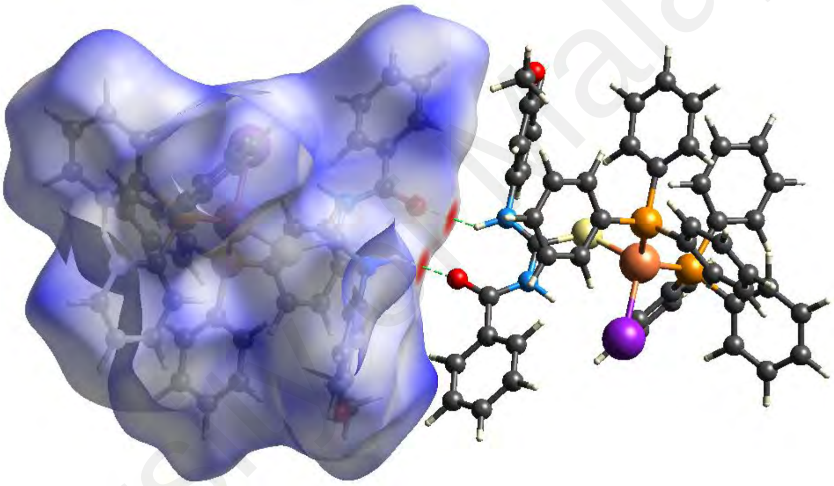

Figure 4.14: d_{norm} mapping of CT3.

The d_{norm} (-0.5 to 1.5) Å mapping of the Hirshfeld surface revealed several red spots with different sizes and intensity. The red spots proved that the intramolecular distance to be notably shorter than the sum of the van der Waals radii. Larger and more intensify red spots noticed on complex **CT3** and **CT7** as in Figure 4.14 and 4.15 respectively, corresponding to a close and strong intermolecular hydrogen bonding (green dotted lines) and they are consistent with the crystal structures. They showed the dominant interactions at the thiourea backbone between the hydrogen of the amine and its adjacent oxygen of the carbonyl atoms (N—H···O=C), forming a dimeric arrangement (Appendix E) in the crystal packing. Thus, it built the stability of the unit cell packing. For complex **CT4**, apart from the N—H···O=C interaction, there is also additional intense red spot representing the intermolecular hydrogen bonding due to the presence of hydrogen of the hydroxy group and the iodine atom (O—H···I—Cu). In the case of **CT1**, **CT2**, **CT5** and **CT6**, they were only dotted with small and paler red spots representing weaker close contacts (Mohamadou *et al.*, 1994).

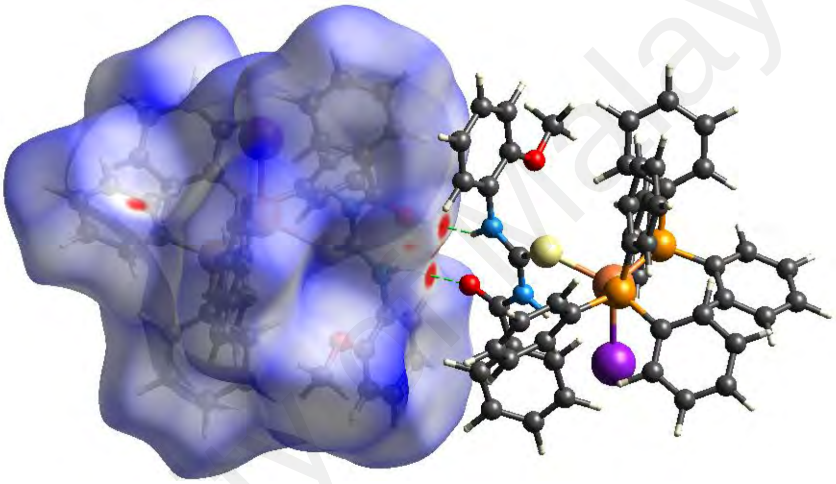

Figure 4.15: d_{norm} mapping of CT7.

4.5.2 2D Fingerprint Plot

The full coloured, 2D fingerprint plots of the Hirshfeld surface is as shown in Table 4.10, was plotted over the range 0.4-2.8 Å in each of d_i and d_e. Whereas, Figure 4.16 illustrated the selected percentage contributions of the Hirshfeld surface area. They represented the summarisation of the quantitative information of intermolecular interactions "fingerprint" contained in the molecular crystals of the phosphanecopper(I) complexes (**CT1-CT7**). Each fingerprint plot was decomposed into specific pairs of atom-types contributions to highlight all their interactions (including H···H, H···C, H···O, H···I, H···S, H···N and C···C), allowing the relationship and their contributions towards the different intermolecular interaction types within the crystal packing (Desiraju *et al.*, 2011). For each plot, the outline of the original fingerprint plots is represented as a grey shadow and the reciprocal contacts were included.

Each Hirshfeld surface of the complexes does not generate the same 2D plotting and there are distinguishable likenesses and differences that could be discussed. For all the complexes (**CT1-CT7**), they showed a large number and a great spread of points (d_e and $d_{i)}$ displayed as tailed structures; as seen at the top right of the plots where they nearly filled up all the available plotting area. These regions also described that d_e is generally greater than d_i, indicating that voids exist around the molecule in the crystal packing are very small. This type of points distribution was observed and reported in other benzene and phenyl-containing compounds, showing both d_e and d_i points covering much greater ranges in the fingerprint plots (Mondal *et al.*, 2017; Safin *et al.*, 2016; Spackman & McKinnon, 2002). This also supported the large blue areas surrounding the aromatic rings in the d_{norm} mapping, corresponding to the longer contact distances contributed by the bulky phosphine group.

The intermolecular H···H contacts are in accordance to the Hirshfeld surface analysis for all the molecules, containing from 52.6 to 67.3 % of the total number of contacts. They are major contributors to the crystal packing. The characteristic spikes representing the shortest H···H contacts are converging along the diagonal line in the fingerprint plots at $d_e + d_i \approx 2.2\text{-}2.4$ Å. Accordingly, it showed obvious short head-to-head H···H contacts (Spackman & McKinnon, 2002).

The structures of all molecules are also dominated by H···C contacts, including from 20.4 to 34.5 % of the total Hirshfeld surface areas. The presence of 'wings' at the bottom right and top left of each plot in the fingerprint plots are a typical representation of a C···H contact. In all the complexes, the shortest $d_e + d_i \approx 2.6–2.7$ Å are documented as characteristic of a C—H···π interaction. The wing at the top left representing $d_i < d_e$ relates to points on the surface around the C—H donor. While, the bottom right plotting where $d_e < d_i$ corresponds to the surface throughout the π acceptor (Spackman & McKinnon, 2002). All plots contain one or more C—H···π interactions because of the presence of the multiple aromatic rings (Safin *et al.*, 2016).

The spikes of H···O and H···I contacts corresponded to the presence of interactions in all of the complexes. However, throughout the series, only **CT3**, **CT4** and **CT7** showed a higher contribution of H···O contacts which is above 4 %. The sharpest point featured a closer contact of $d_e + d_i \approx 2.2–2.4$ Å which is in the range that is in agreeable to the intermolecular hydrogen bonding between N—H donor and O=C acceptor (N—H···O=C) (Desiraju *et al.*, 2011). All the complexes showed a trend for the H···I contact in the range of 3-4 % of the surface area. **CT4** showed the shortest contact of $d_e + d_i \approx 2.8–3.0$ Å that allowed intermolecular hydrogen bonding. This is expected for interaction engaged between strong hydrogen bond donor O—H and a strong hydrogen bond acceptor I—Cu (O—H···I—Cu) (Brammer *et al.*, 2001).

A particular observation worth discussing from the fingerprint plots is the interests in the relative areas associated with C···C contacts and correlated with the presence of planar stacking arrangement of aromatic π···π interaction (Spackman & McKinnon, 2002). This is observed in complexes **CT5** and **CT6** with the contribution of 3.7 % and 2.9 % respectively but there is a negligible amount of contribution, with less than 1 % in the rest of the series. The structures are further presented by a smaller insignificant proportion of H···S and H···N interactions, contributes a very small percentage of the molecular surfaces, that is less than 1.4 %. Thus, their contacts are almost insignificant throughout the whole series.

Figure 4.16 illustrated the selected percentage contributions of the Hirshfeld surface area. They represented the summarization of the quantitative information of intermolecular interactions contained in the molecular crystals (**CT1-CT7)**. They all show almost similar pattern except for **CT5** show a larger percentage of other contacts, this is majorly contributed by the H···Cl contacts.

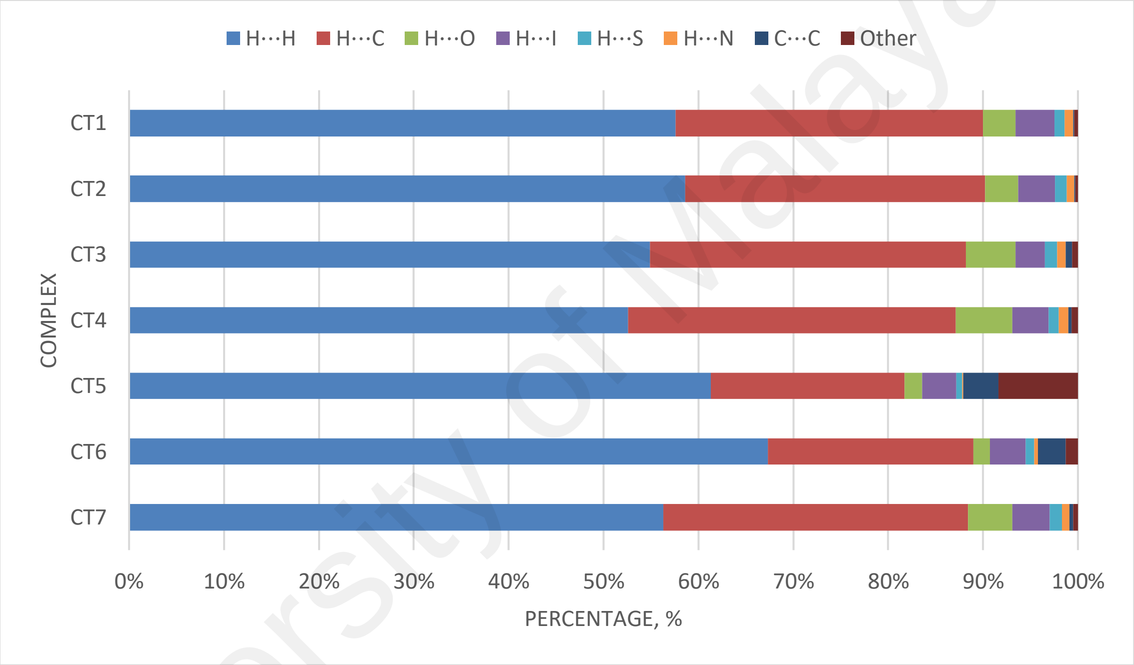

Figure 4.16: Percentage contributions of the Hirshfeld surface area for phosphanecopper(I) complexes (CT1-CT7).

Table 4.10: 2D fingerprint plots of phosphanecopper(I) complexes (CT1-CT7).

Complex	CT1	CT2	CT3	CT4	CT5	CT6	CT7
Fingerprint Plot- Full	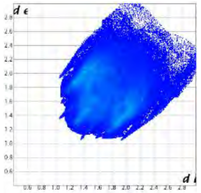	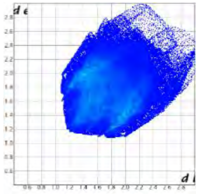	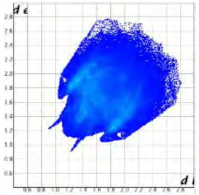	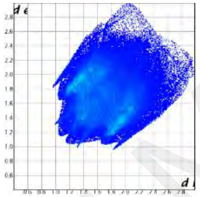	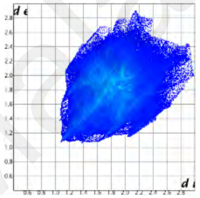	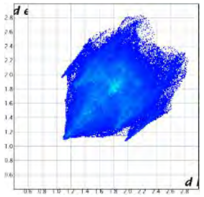	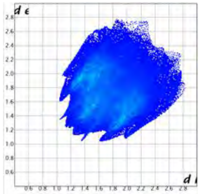
Fingerprint Plot-H···H	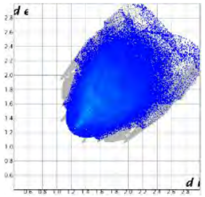	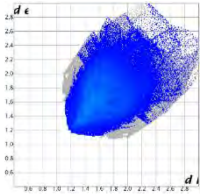	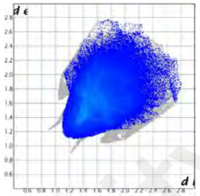	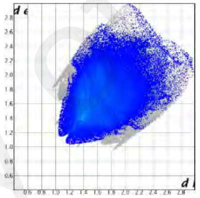	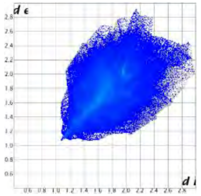	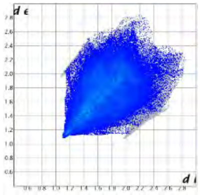	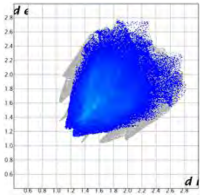
Fingerprint Plot-H···C	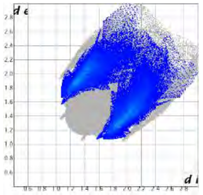	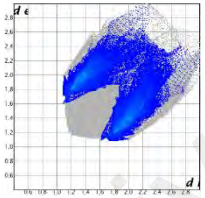	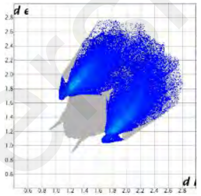	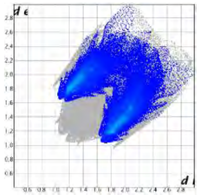	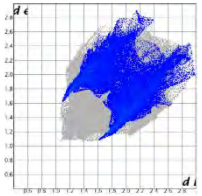	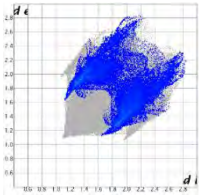	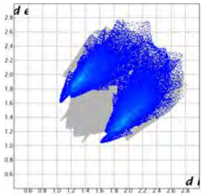
Fingerprint Plot-H···O	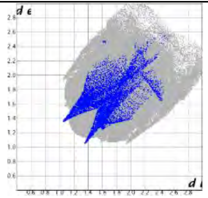	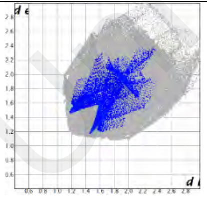	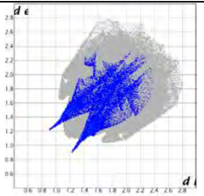	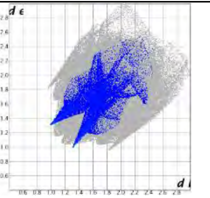	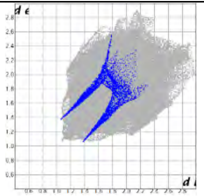	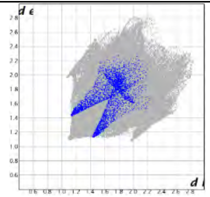	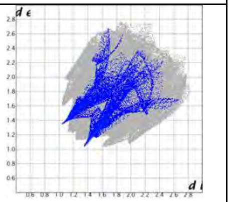

Complex	CT1	CT2	CT3	CT4	CT5	CT6	CT7
Fingerprint Plot-H···I	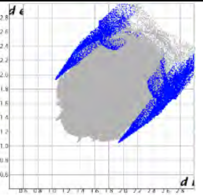	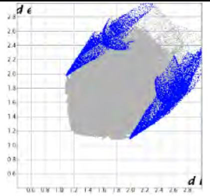	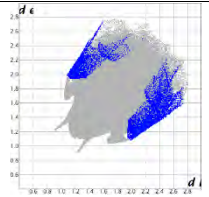	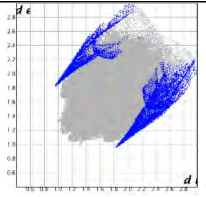	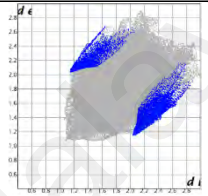	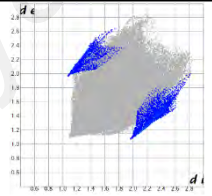	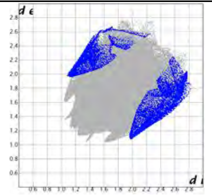
Fingerprint Plot-H···S	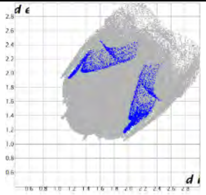	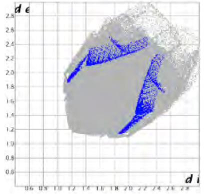	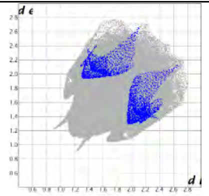	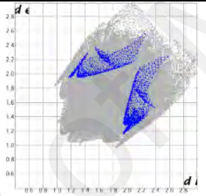	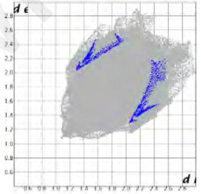	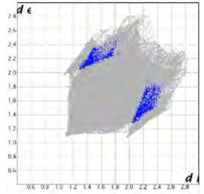	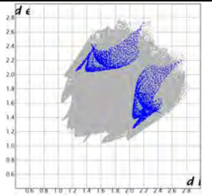
Fingerprint Plot-H···N	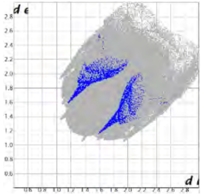	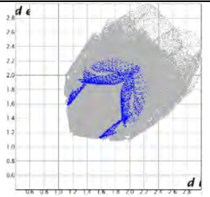	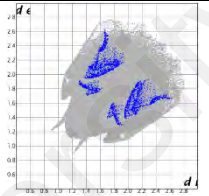	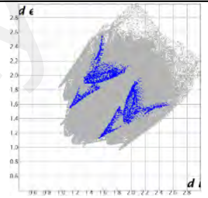	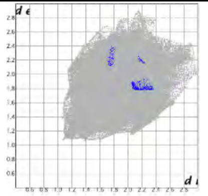	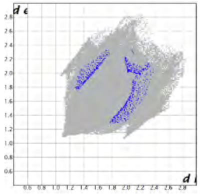	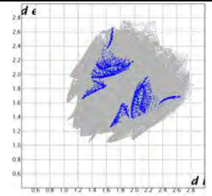
Fingerprint Plot-C···C	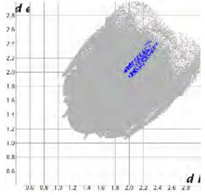	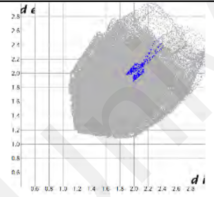	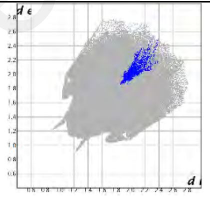	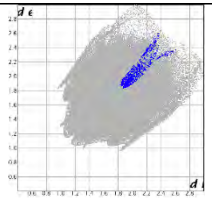	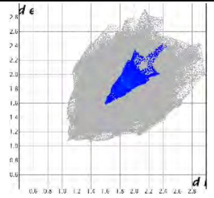	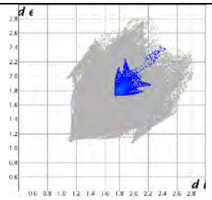	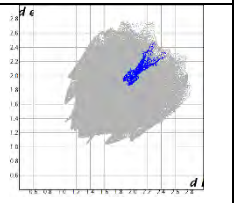

Table 4.10, continued.

CHAPTER 5: CONCLUSION

5.1 Conclusion

This thesis describes the syntheses, structural characterisations and the Hirshfeld surface analysis of phosphanecopper(I) complexes of a series of S-donor acylthiourea ligands. Thirteen known acylthiourea ligands (**T1-T13**) were used to coordinate with copper(I) metal. Thirteen novel series of phosphanecopper(I) complexes (**CT1-CT13**) with the general formulation of [Cu(**T**)(I)(PPh_3)$_2$] have been prepared by the reaction of acylthiourea (**T1-T13**) with copper(I) iodide and triphenylphosphine. These complexes have been characterised by elemental analysis, IR and NMR. The structures for some of the complexes (**CT1-CT7**) have been solved by single crystal X-ray crystallography. The results from spectroscopic data and crystal structure analysis showed that the mixed ligand complexes are mononuclear tetrahedrally-coordinated with one monodentate acylthiourea ligands, two PPh_3 moieties and one iodine occupied the fourth coordination site.

Interestingly, this new series of the closely related structure are isostructural, yet they crystallised in two different crystal systems. Complexes **CT1**, **CT2**, **CT3**, **CT4** and **CT7** crystallised in a $P2_1/c$, monoclinic manner. While the complexes **CT5** and **CT6** adopted the $P\bar{1}$, triclinic crystal structure. They exhibited interesting examples of S-monodentate of an acylthiourea by coordination of sulphur to copper(I) metal. With the aid of Hirshfeld surface analysis, the effects of substituent groups on the aromatic of the acylthiourea upon the formation of crystal structure were able to be understood. The analysis we able to clearly illustrate significant differences on the characteristic of the series of complexes (**CT1- CT7**) within the crystal system. However, many attempts to prepare the single crystals of complexes **CT8-CT13** were unsuccessful.

5.2 Future Work

The initial objective of this research was accomplished. A new copper(I) complexes of acylthiourea ligands with interesting S-donor coordination and crystal packing behaviours were successfully designed, synthesised and structurally characterised. However, the complexes deserved a chance in further development for its potential applications. Future work to be considered will focus on the bioactivity assays which can be carried out to evaluate the potential medicinal properties of these complexes.

As noted, complexes **CT8-CT13** did not form good quality crystals to carry out the single X-ray diffraction studies, accordingly. Thus, other recrystallisation methods such as recrystallisation al low temperature could be conducted to improve the quality of the crystals in order to obtain the X-ray structure of these complexes. Additionally, it would be interesting to extend the Hirshfeld surface analysis study of the whole complete series.

Moreover, it would be very significant to design other mixed ligand metal complexes of this series of substituted acylthiourea. Ideally, other types of phosphine could also be used as co-ligand or in fact, a different type of metals could be experimented on to develop new combinations of the heteroleptic complexes of this class of ligands. This may give rise to far and wide structural studies, both experimentally and computationally.

CHAPTER 6: REFERENCES

Anastasiadou, D., Psomas, G., Lalia-Kantouri, M., Hatzidimitriou, A. G., & Aslanidis, P. (2016). Copper(I) halide complexes of 2,2,5,5-tetramethyl-imidazolidine-4-thione: Synthesis, structures, luminescence, thermal stability and interaction with DNA. *Materials Science and Engineering: C, 68*, 241-250.

Androvič, L., Drabina, P., Svobodová, M., & Sedlák, M. (2016). Polystyrene supported benzoylthiourea—pyrrolidine organocatalyst for the enantioselective Michael addition. *Tetrahedron: Asymmetry, 27*(16), 782-787.

Anuta, V., Nitulescu, G. M., Dinu-Pîrvu, C. E., & Olaru, O. T. (2014). Biopharmaceutical profiling of new antitumor pyrazole derivatives. *Molecules, 19*(10), 16381-16401.

Armstrong, K. E., Crane, J. D., & Whittingham, M. (2004). Structural insight into the different reactivities towards ligand S-ethylation with iodoethane of the tetrahedral zinc(II) complexes of 1,1,5,5-tetramethyl-2-thiobiuret and 1,1,5,5-tetramethyl-2,4-dithiobiuret. *Inorganic Chemistry Communications, 7*(6), 784-787.

Arslan, H., Flörke, U., Külcü, N., & Binzet, G. (2007). The molecular structure and vibrational spectra of 2-chloro-*N*-(diethylcarbamothioyl)benzamide by Hartree–Fock and density functional methods. *Spectrochimica Acta Part A: Molecular and Biomolecular Spectroscopy, 68*(5), 1347-1355.

Aslanidis, P., Hadjikakou, S. K., Karagiannidis, P., Gdaniec, M., & Kosturkiewicz, Z. (1993). Four-coordinate copper(I) iodide complexes with triphenylphosphine and heterocyclic thione ligands. The crystal structure of [Cu(PPh_3)$_2$(pymtH)I]. *Polyhedron, 12*(18), 2221-2226.

Aslanidis, P., Kyritsis, S., Lalia-Kantouri, M., Wicher, B., & Gdaniec, M. (2012). Copper(I) halide complexes of 2-thiohydantoin and 5,5-diphenyl-2-thiohydantoin. *Polyhedron, 48*(1), 140-145.

Atkins, P. W., Rourke, J. P., Weller, M. T., Armstrong, F. A., & Overton, T. (2010). *Shriver and Atkins' inorganic chemistry* (5th ed.). USA: Oxford University Press.

Aydin, F., Ünver, H., Aykaç, D., & Ocak İskeleli, N. (2010). Spectroscopic studies and structure of 4-(3-benzoylthioureido)benzoic acid. *Journal of Chemical Crystallography, 40*(12), 1082-1086.

Barolli, J. P., Maia, P. I. S., Colina-Vegas, L., Moreira, J., Plutin, A. M., Mocelo, R., Deflon, V. M., Cominetti, M. R., Camargo-Mathias, M. I., & Batista, A. A. (2017). Heteroleptic tris-chelate ruthenium(II) complexes of *N*,*N*-disubstituted-*N'*-acylthioureas: Synthesis, structural studies, cytotoxic activity and confocal microscopy studies. *Polyhedron, 126*, 33-41.

Barrett, G. (2012). *Chemistry and biochemistry of the amino acids* (G. Barrett Ed.). UK: Springer Science & Business Media.

Bodio, E., Boujtita, M., Julienne, K., Le Saec, P., Gouin, S. G., Hamon, J., Renault, E., & Deniaud, D. (2014). Synthesis and characterization of a stable copper (I) complex for radiopharmaceutical applications. *ChemPlusChem, 79*(9), 1284-1293.

Bogatskii, A. V., Luk'yanenko, N. G., & Kirichenko, T. I. (1983). Cyclic thioureas (review). *Chemistry of Heterocyclic Compounds, 19*(6), 577-589.

Brammer, L., Bruton, E. A., & Sherwood, P. (2001). Understanding the behavior of halogens as hydrogen bond acceptors. *Crystal Growth & Design, 1*(4), 277-290.

Braun, U., Richter, R., Sieler, J., Yanovsky, A. I., & Struchkov, Y. T. (1985). Kristall- und Molekülstruktur von Tris(1,1-diethyl-3-benzoylthioharnstoff)silber(I)-hydrogensulfid. *Zeitschrift für anorganische und allgemeine Chemie, 529*(10), 201-208.

Bravo, J., Bolaño, S., Gonsalvi, L., & Peruzzini, M. (2010). Coordination chemistry of 1, 3, 5-triaza-7-phosphaadamantane (PTA) and derivatives. Part II. The quest for tailored ligands, complexes and related applications. *Coordination Chemistry Reviews, 254*(5-6), 555-607.

Brito, T. O., Souza, A. X., Mota, Y. C. C., Morais, V. S. S., de Souza, L. T., de Fátima, Â., Macedo, F., & Modolo, L. V. (2015). Design, syntheses and evaluation of benzoylthioureas as urease inhibitors of agricultural interest. *RSC Advances, 5*(55), 44507-44515.

Brynda, M. (2005). Towards “user-friendly” heavier primary pnictanes: Recent developments in the chemistry of primary phosphines, arsines and stibines. *Coordination Chemistry Reviews, 249*(19-20), 2013-2034.

Büchel, K. H., Moretto, H.-H., & Werner, D. (2008). *Industrial inorganic chemistry*. Federal Republic of Germany: John Wiley & Sons.

Bünzli-Trepp, U. (2007). *Systematic nomenclature of organic, organometallic and coordination chemistry: Chemical-abstracts guidelines with IUPAC recommendations and many trivial names*. Switzerland: EPFL Press.

Cairo, R. R., Stevens, A. M. P., de Oliveira, T. D., Batista, A. A., Castellano, E. E., Duque, J., Soria, D. B., Fantoni, A. C., Corrêa, R. S., & Erben, M. F. (2017). Understanding the conformational changes and molecular structure of furoyl thioureas upon substitution. *Spectrochimica Acta Part A: Molecular and Biomolecular Spectroscopy, 176*, 8-17.

Callister Jr, W. D., & Rethwisch, D. G. (2012). *Fundamentals of materials science and engineering: An integrated approach*. Federal Republic of Germany: John Wiley & Sons.

Casitas, A., & Ribas, X. (2013). The role of organometallic copper (III) complexes in homogeneous catalysis. *Chemical Science, 4*(6), 2301-2318.

Chang, Y., Zhang, J., Chen, X., Li, Z., & Xu, X. (2017). Synthesis and nematicidal activities of 1,2,3-benzotriazin-4-one derivatives containing thiourea and acylthiourea against Meloidogyne incognita. *Bioorganic & Medicinal Chemistry Letters, 27*(11), 2641-2644.

Che, D.-J., Li, G., Yao, X.-L., Wu, Q.-J., Wang, W.-L., & Zhu, Y. (1999). Photochemical generation of a novel (O, N′, N″) coordinated iron(II) complex [Fe(FT–py)$_2$] from a ferrocenoyl-functionalized thiourea ligand: *N*-ferrocenylcarbonyl-*N*′-(2-pyridyl)thiourea (HFT–py): crystal and molecular structures of HFT–py and [Fe(FT–py)$_2$]. *Journal of Organometallic Chemistry, 584*(1), 190-196.

Chetana, P. R., Srinatha, B. S., Somashekar, M. N., & Policegoudra, R. S. (2016). Synthesis, spectroscopic characterisation, thermal analysis, DNA interaction and antibacterial activity of copper(I) complexes with N, N′- disubstituted thiourea. *Journal of Molecular Structure, 1106*, 352-365.

Chopra, D. (2018). *Understanding intermolecular interactions in the solid state: Approaches and techniques* (Vol. 26). UK: Royal Society of Chemistry.

Chou, C.-C., Liu, H.-J., & Su, C.-C. (2008). The first stereochemically nonrigid monomeric two-coordinate copper (I) complexes with homoleptic and heteroleptic "N2" donor set. *Dalton Transactions, 25*, 3358-3362.

Chu, X., & Zhang, K. L. (2017). Preparation and characterization of two new Cu(II) supramolecular coordination polymers incorporating sulfobenzoate and flexible heterocyclic ligands. *Acta crystallographica Section C: Structural Chemistry 73*(Pt 12), 1087-1097.

Cîrcu, V., Ilie, M., Iliş, M., Dumitraşcu, F., Neagoe, I., & Păsculescu, S. (2009). Luminescent cyclometallated platinum(II) complexes with *N*-benzoyl thiourea derivatives as ancillary ligands. *Polyhedron, 28*(17), 3739-3746.

Crispini, A., Cretu, C., Aparaschivei, D., Andelescu, A. A., Sasca, V., Badea, V., Aiello, I., Szerb, E. I., & Costisor, O. (2018). Influence of the counterion on the geometry of Cu(I) and Cu(II) complexes with 1,10-phenanthroline. *Inorganica Chimica Acta, 470*, 342-351.

Dai, W., Zhou, J., Jin, B., & Pan, J. (2016). Class III-specific HDAC inhibitor Tenovin-6 induces apoptosis, suppresses migration and eliminates cancer stem cells in uveal melanoma. *Scientific Reports, 6*, 22622.

Desiraju, G. R., Vittal, J. J., & Ramanan, A. (2011). *Crystal engineering: A textbook*. Singapore: World Scientific.

Devkule, S. S., & Chavan, S. S. (2017). Copper(I) complexes of N-(2-quinolynylmethylene)-1H-benzimidazole and triphenylphosphine: Synthesis, characterization, luminescence and catalytic properties. *Inorganica Chimica Acta, 466*, 122-129.

Dolomanov, O. V., Bourhis, L. J., Gildea, R. J., A Howard, J. A. K., & A Puschmann, H. (2009). OLEX2: a complete structure solution, refinement and analysis program. *Journal of Applied Crystallography, 42*(3), 339-341.

Engelhardt, L. M., Jacobsen, G. E., Patalinghug, W. C., Skelton, B. W., Raston, C. L., & White, A. H. (1991). Synthesis and structure of copper (I), silver (I) and zinc (II) amides [Cu $_2$ (mpsa) $_2$],[Cu $_6$ X $_2$ (mpsa) $_4$](X= Cl or Br),[Ag $_4$ (mpsa) $_4$] and [(ZnEt) $_2$ (mpsa) $_2$][mpsa= 2-N (SiMe $_3$) C $_5$ H $_3$ N-6-Me]. *Journal of the Chemical Society, Dalton Transactions, 11*, 2859-2868.

Estévez-Hernández, O., Duque, J., Rodríguez-Hernández, J., & Reguera, E. (2015). Dinuclear and polymeric Hg(II) complexes with 1-(2-furoyl)thiourea derivatives: Their crystal structure and related properties. *Polyhedron, 97*, 148-156.

Faridbod, F., Ganjali, M. R., Dinarvand, R., Norouzi, P., & Riahi, S. (2008). Schiff's bases and crown ethers as supramolecular sensing materials in the construction of potentiometric membrane sensors. *Sensors, 8*(3), 1645-1703.

Flynn, E. H. (2013). *Cephalosporins and penicillins: Chemistry and biology*. USA: Elsevier.

Fu, L., Mighion, J. D., Voight, E. A., & Davies, H. M. (2017). Synthesis of 2, 2, 2,-Trichloroethyl Aryl-and Vinyldiazoacetates by Palladium-Catalyzed Cross-Coupling. *Chemistry–A European Journal, 23*(14), 3272-3275.

Garnovskii, A. D., & Kharissov, B. I. (2003). *Synthetic coordination and organometallic chemistry*. UK: CRC Press.

Gorgas, N., Stöger, B., Veiros, L. F., & Kirchner, K. (2016). Highly efficient and selective hydrogenation of aldehydes: a well-defined Fe (II) catalyst exhibits noble-metal activity. *ACS catalysis, 6*(4), 2664-2672.

Gumus, I., Solmaz, U., Binzet, G., Keskin, E., Arslan, B., & Arslan, H. (2018). Hirshfeld surface analyses and crystal structures of supramolecular self-assembly thiourea derivatives directed by non-covalent interactions. *Journal of Molecular Structure, 1157*, 78-88.

Gunasekaran, N. (2018). Palladium(II) complexes with 2,4-dichloro-*N*-[di(alkyl/aryl)carbamothioyl]benzamide derivatives and triphenylphosphine as effective catalysts for oxidation of alcohols in ionic liquid. *Inorganic Chemistry Communications, 89*, 55-59.

Gunasekaran, N., Bhuvanesh, N. S. P., & Karvembu, R. (2017). Synthesis, characterization and catalytic oxidation property of copper(I) complexes containing monodentate acylthiourea ligands and triphenylphosphine. *Polyhedron, 122*, 39-45.

Gunasekaran, N., Ng, S. W., Tiekink, E. R. T., & Karvembu, R. (2012). Hypodentate coordination of *N*,*N*-di(alkyl/aryl)-*N′*-acylthiourea derivatives in Cu(I) complexes. *Polyhedron, 34*(1), 41-45.

Haas, K. L., & Franz, K. J. (2009). Application of metal coordination chemistry to explore and manipulate cell biology. *Chemical reviews, 109*(10), 4921-4960.

Han, J., Dong, H., Xu, Z., Wang, J., & Wang, M. (2013). Synthesis and activity of novel acylthiourea with hydantoin. *International Journal of Molecular Sciences, 14*(10), 19526-19539.

Hanif, M., Chohan, Z. H., Winum, J. Y., & Akhtar, J. (2014). Metal-based carboxamide-derived compounds endowed with antibacterial and antifungal activity. *Journal of Enzyme Inhibition and Medicinal Chemistry, 29*(4), 517-526.

Hanifehpour, Y., Mirtamizdoust, B., Hatami, M., Khomami, B., & Joo, S. W. (2015). Synthesis and structural characterization of new bismuth (III) nano coordination polymer: A precursor to produce pure phase nano-sized bismuth (III) oxide. *Journal of Molecular Structure, 1091*, 43-48.

Haribabu, J., Subhashree, G. R., Saranya, S., Gomathi, K., Karvembu, R., & Gayathri, D. (2015). Synthesis, crystal structure, and in vitro and in silico molecular docking of novel acyl thiourea derivatives. *Journal of Molecular Structure, 1094*, 281-291.

Hayama, M., Yamamoto, K.-i., Kohori, F., & Sakai, K. (2004). How polysulfone dialysis membranes containing polyvinylpyrrolidone achieve excellent biocompatibility? *Journal of Membrane Science, 234*(1), 41-49.

Hernández, W., Spodine, E., Carlos Muñoz, J., Beyer, L., Schröder, U., Ferreira, J., & Pavani, M. (2003). Synthesis, characterization and antitumor activity of *cis*-bis(acylthioureato) platinum(II) complexes, *cis*-[PtL$_2$] [HL=*N*,*N*-diphenyl-*N*'-benzoylthiourea or HL=*N*,*N*-diphenyl-*N*'-(*p*-nitrobenzoyl)thiourea]. *Bioinorganic chemistry and applications, 1(3-4)*, 271-284.

Hirshfeld, F. L. (1977). Bonded-atom fragments for describing molecular charge densities. *Theoretica chimica acta, 44*(2), 129-138.

Hu, J., Yao, H., Bai, Y., Zhao, D., Chen, S., & Zhao, J. a. (2014). Multinuclear-based copper coordination architectures constructed from pyridyl-1H-benzimidazol-derived flexible tripodal connector and the magnetic behaviors. *Polyhedron, 78*, 1-9.

Iliş, M., & Cîrcu, V. (2018). Discotic Liquid Crystals Based on Cu (I) Complexes with Benzoylthiourea Derivatives Containing a Perfluoroalkyl Chain. *Journal of Chemistry, 2018*.

Iliş, M., Micutz, M., Pasuk, I., Staicu, T., & Cîrcu, V. (2017). Synthesis and liquid crystalline properties of novel fluorinated *N*-benzoyl thiourea compounds. Effect of perfluoroalkyl chains on the thermal behavior and smectic phases stability. *Journal of Fluorine Chemistry, 204*, 84-89.

Jiang, J., Choo, S. Y., Omar, N., & Ahamad, N. (1998). GC-MS analysis of volatile compounds in durian (Durio zibethinus Murr.). In E. T. Contis, C. T. Ho, C. J.

Mussinan, T. H. Parliment, F. Shahidi, & A. M. Spanier (Eds.), *Developments in Food Science* (Vol. 40, pp. 345-352). The Netherlands: Elsevier.

Kakizoe, D., Nishikawa, M., Fujii, Y., & Tsubomura, T. (2017). Photophysical properties of three coordinated copper (i) complexes bearing 1, 10-phenanthroline and a monodentate phosphine ligand. *Dalton Transactions, 46*(43), 14804-14811.

Khairul, W. M., Daud, A. I., Mohd Hanifaah, N. A., Arshad, S., Razak, I. A., Zuki, H. M., & Erben, M. F. (2017). Structural study of a novel acetylide-thiourea derivative and its evaluation as a detector of benzene. *Journal of Molecular Structure, 1139*, 353-361.

Khan, A., Jasinski, J. P., Smolenski, V. A., Hotchkiss, E. P., Kelley, P. T., Shalit, Z. A., Kaur, M., Paul, K., & Sharma, R. (2018). Enhancement in anti-tubercular activity of indole based thiosemicarbazones on complexation with copper(I) and silver(I) halides: Structure elucidation, evaluation and molecular modelling. *Bioorganic Chemistry, 80*, 303-318.

Khan, M. R., Zaib, S., Khan, A., Badshah, A., Rauf, M. K., Imtiaz ud, D., Tahir, M. N., Shahid, M., & Iqbal, J. (2018). Pd(II)-based heteroleptic complexes with N-(acyl)-N′, N′-(disubstituted)thioureas and phosphine ligands: Synthesis, characterization and cytotoxic studies against lung squamous, breast adenocarcinoma and Leishmania tropica. *Inorganica Chimica Acta, 479*, 189-196.

Khandar, A. A., Butcher, R. J., Abedi, M., Hosseini-Yazdi, S. A., Akkurt, M., & Tahir, M. N. (2010). Synthesis, characterization and crystal structures of dinuclear macrocyclic Schiff base copper(I) complexes bearing different bridges. *Polyhedron, 29*(17), 3178-3182.

Kharasch, N. (2013). *Organic sulfur compounds*. UK: Elsevier.

Koca, I., Ozgur, A., Er, M., Gumus, M., Acikalin Coskun, K., & Tutar, Y. (2016). Design and synthesis of pyrimidinyl acyl thioureas as novel Hsp90 inhibitors in invasive ductal breast cancer and its bone metastasis. *European Journal of Medicinal Chemistry, 122*, 280-290.

Koch, K. R. (2001). New chemistry with old ligands: *N*-alkyl- and *N*,*N*-dialkyl-*N*′-acyl(aroyl)thioureas in co-ordination, analytical and process chemistry of the platinum group metals. *Coordination Chemistry Reviews, 216-217*, 473-488.

Kollár, L., & Keglevich, G. (2010). P-Heterocycles as ligands in homogeneous catalytic reactions. *Chemical reviews, 110*(7), 4257-4302.

Kotze, I. A., Smith, V. J., Kangara, E. F., & Koch, K. R. (2017). Rare, hypodentate L-[small kappa]S coordination mode of N,N-dialkyl-N[prime or minute]-aroylthioureas leads to unprecedented mixed-ligand [Pt(phen)(L-[small kappa]S)2] complexes. *New Journal of Chemistry, 41*(24), 14995-15002.

Kumar, R. R., Ramesh, R., & Małecki, J. G. (2017). Versatile coordination ability of thioamide ligand in Ru (ii) complexes: synthesis, computational studies, in vitro anticancer activity and apoptosis induction. *New Journal of Chemistry, 41*(17), 9130-9141.

Levason, W. (1990). Phosphine complexes of transition metals. In F. R. Hartley (Ed.), *Organophosphorus Compounds: Primary, secondary and tertiary phosphines, polyphosphines and heterocyclic organophosphorus (III) compounds* (Vol. 1, pp. 567-641). Federal Republic of Germany: Wiley.

Li, Y., Das, S., Zhou, S., Junge, K., & Beller, M. (2012). General and selective copper-catalyzed reduction of tertiary and secondary phosphine oxides: Convenient synthesis of phosphines. *Journal of the American Chemical Society, 134*(23), 9727-9732.

Liu, X., Manzur, C., Novoa, N., Celedón, S., Carrillo, D., & Hamon, J.-R. (2018). Multidentate unsymmetrically-substituted Schiff bases and their metal complexes: Synthesis, functional materials properties, and applications to catalysis. *Coordination Chemistry Reviews, 357*, 144-172.

Lobana, T. S., Rekha, Sidhu, B. S., Castineiras, A., Bermejo, E., & Nishioka, T. (2005). Syntheses, NMR (^{1}H, ^{31}P) spectroscopy and crystal structures of complexes of copper(I) halides with isatin-3-thiosemicarbazones. *Journal of Coordination Chemistry, 58*(9), 803-809.

Luckay, R. C., Mebrahtu, F., Esterhuysen, C., & Koch, K. R. (2010). Extraction and transport of gold(III) using some acyl(aroyl)thiourea ligands and a crystal structure of one of the complexes. *Inorganic Chemistry Communications, 13*(4), 468-470.

Luther, G. W., & Rickard, D. T. (2005). Metal sulfide cluster complexes and their biogeochemical importance in the environment. *Journal of Nanoparticle Research, 7*(4-5), 389-407.

MacCallum, S. F., Groves, M. J., James, J., Murray, K., Appleyard, V., Prescott, A. R., Drbal, A. A., Nicolaou, A., Cunningham, J., Haydock, S., Ganley, I. G., Westwood, N. J., Coates, P. J., Lain, S., & Tauro, S. (2013). Dysregulation of autophagy in chronic lymphocytic leukemia with the small-molecule Sirtuin inhibitor Tenovin-6. *Scientific Reports, 3*, 1275.

Macrae, C. F., Bruno, I. J., Chisholm, J. A., Edgington, P. R., McCabe, P., Pidcock, E., Rodriguez-Monge, L., Taylor, R., Streek, J. v., & Wood, P. A. (2008). Mercury CSD 2.0–new features for the visualization and investigation of crystal structures. *Journal of Applied Crystallography, 41*(2), 466-470.

Mahmoudi, E., Ng, L. Y., Ba-Abbad, M. M., & Mohammad, A. W. (2015). Novel nanohybrid polysulfone membrane embedded with silver nanoparticles on graphene oxide nanoplates. *Chemical Engineering Journal, 277*, 1-10.

Mahmoudi, G., Castiñeiras, A., Garczarek, P., Bauzá, A., Rheingold, A. L., Kinzhybalo, V., & Frontera, A. (2016). Synthesis, X-ray characterization, DFT calculations and Hirshfeld surface analysis of thiosemicarbazone complexes of Mn^+ ions (n= 2, 3; M= Ni, Cd, Mn, Co and Cu). *CrystEngComm, 18*(6), 1009-1023.

Márquez, H., Plutín, A., Rodríguez, Y., Perez, E., & Loupy, A. (2000). Efficient synthesis of 1-(4′-methylbenzoyl)- 3,3-diethylthiourea under microwave irradiation using potassium fluoride on alumina. *Synthetic Communications, 30*(6), 1067-1073.

Martin, R., & Buchwald, S. L. (2008). Palladium-catalyzed Suzuki−Miyaura cross-coupling reactions employing dialkylbiaryl phosphine ligands. *Accounts of Chemical Research, 41*(11), 1461-1473.

Mertschenk, B., Knott, A., & Bauer, W. (1995). Thiourea and thiourea derivatives *Ullmann's encyclopedia of industrial chemistry* (pp. 1-15). Weinheim, Germany: Wiley-VCH Verlag GmbH & Co. KGaA.

Ming-Yan, Y., Wen, Z., Zhao-Hui, S., Cheng-Xia, T., Jian-Quan, W., & Xing-Hai, L. (2015). Synthesis and biological activity of acylthiourea derivatives contain 1,2,3-thiadiazole and 1,3,4-thiadiazole. *Letters in Drug Design & Discovery, 12*(4), 314-318.

Mohamadou, A., Déchamps-Olivier, I., & Barbier, J.-P. (1994). Synthesis of *N*-morpholine or *N*,*N*-diethyl, *N*′-monosubstituted benzoyl thiourea copper complexes: Characterization and electrochemical investigations. *Polyhedron, 13*(24), 3277-3283.

Mondal, J., Pal, P. K., Mukherjee, A., & Patra, G. K. (2017). Synthesis, structural variation, photophysical, electrochemical and DFT studies of CuX (X=I, Br and Cl) mixed ligand complexes of an azino-pyridyl ligand and triphenylphosphine. *Inorganica Chimica Acta, 466*, 274-284.

Nell, B. P., & Tyler, D. R. (2014). Synthesis, reactivity, and coordination chemistry of secondary phosphines. *Coordination Chemistry Reviews, 279*, 23-42.

Nimthong, R., Pakawatchai, C., Saithong, S., & Charmant, J. P. H. (2008). Iodido(*N*-phenyl-thio-urea)bis-(triphenyl-phosphine)copper(I). *Acta Crystallographica Section E: Structure Reports Online, 64*(7), 977-978.

Noufele, C. N., Pham, C. T., Hagenbach, A., & Abram, U. (2018). Uranyl ccomplexes with aroylbis (*N*, *N*-dialkylthioureas). *Inorganic chemistry, 57*(19), 12255-12269.

Okuniewski, A., Rosiak, D., Chojnacki, J., & Becker, B. (2015). Coordination polymers and molecular structures among complexes of mercury(II) halides with selected 1-benzoylthioureas. *Polyhedron, 90*, 47-57.

Oxford Diffraction, C. P., Oxford Diffr. Ltd., Abingdon, Oxfordshire, England. (2013).

Oyeka, E. E., Asegbeloyin, J. N., Babahan, I., Eboma, B., Okpareke, O., Lane, J., Ibezim, A., Bıyık, H. H., Tőrün, B., & Izuogu, D. C. (2018). Synthesis, crystal structure, computational analysis and biological properties of 1-(4-chlorobenzoyl)-3-[2-(2-{2-[3-(4-chlorobenzoyl)-thioureido]-ethoxy}ethoxy)ethyl]-thiourea and its Ni(II) and Cu(II) complexes. *Journal of Molecular Structure, 1168*, 153-164.

Panicker, C. Y., Varghese, H. T., George, A., & Thomas, P. K. V. (2010). FT-IR, FT-Raman and ab-initio studies of 1,3-diphenyl thiourea. *European Journal of Chemistry, 1*(3), 173-178.

Pavia, D. L., Lampman, G. M., Kriz, G. S., & Vyvyan, J. A. (2008). *Introduction to spectroscopy*. USA: Brooks/Cole.

Pearson, A., O'Mullane, A. P., Bhargava, S. K., & Bansal, V. (2012). Synthesis of CuTCNQ/Au microrods by galvanic replacement of semiconducting phase I CuTCNQ with $KAuBr_4$ in aqueous medium. *Inorganic chemistry, 51*(16), 8791-8801.

Pearson, R. G. (1963). Hard and soft acids and bases. *Journal of the American Chemical Society, 85*(22), 3533-3539.

Plutín, A. M., Alvarez, A., Mocelo, R., Ramos, R., Castellano, E. E., da Silva, M. M., Colina-Vegas, L., Pavan, F. R., & Batista, A. A. (2016). Anti-mycobacterium tuberculosis activity of platinum(II)/*N*,*N*-disubstituted-*N*′-acyl thiourea complexes. *Inorganic Chemistry Communications, 63*, 74-80.

Plutín, A. M., Mocelo, R., Alvarez, A., Ramos, R., Castellano, E. E., Cominetti, M. R., Graminha, A. E., Ferreira, A. G., & Batista, A. A. (2014). On the cytotoxic activity of Pd(II) complexes of *N*,*N*-disubstituted-*N'*-acyl thioureas. *Journal of Inorganic Biochemistry, 134*, 76-82.

Qiu, Q.-M., Liu, M., Li, Z.-F., Jin, Q.-H., Huang, X., Zhang, Z.-W., Zhang, C.-L., & Meng, Q.-X. (2014). Synthesis, structure, terahertz spectroscopy and luminescent properties of copper(I) complexes with mercaptan ligands and triphenylphosphine. *Journal of Molecular Structure, 1062*, 125-132.

Raizada, M., Sama, F., Ashafaq, M., Shahid, M., Ahmad, M., & Siddiqi, Z. A. (2017). New hybrid polyoxovanadate–Cu complex with V··· H interactions and dual aqueous-phase sensing properties for picric acid and Pd^{2+}: X-ray analysis, magnetic and theoretical studies, and mechanistic insights into the hybrid's sensing capabilities. *Journal of Materials Chemistry C, 5*(36), 9315-9330.

Rohini, G., Ramaiah, K., Aneesrahman, K., Aryasenan, M. C., Bhuvanesh, N. S., Reddy, K. L., & Sreekanth, A. (2018). Biological evaluation, DNA/protein-binding aptitude of novel dibenzosuberene appended palladium (II)-thiourea complexes. *Applied Organometallic Chemistry, 32*(12), 4567.

Roy, P., Dhara, K., Manassero, M., & Banerjee, P. (2008). A copper(II) complex with rare µ1,1,1-azide ligand: Active catalyst for heterogeneous olefin epoxidation. *Inorganic Chemistry Communications, 11*(3), 265-269.

Rybak, M. E., Calvey, E. M., & Harnly, J. M. (2004). Quantitative determination of allicin in garlic: Supercritical fluid extraction and standard addition of alliin. *Journal of Agricultural and Food Chemistry, 52*(4), 682-687.

Saeed, A., Khan, M. S., Rafique, H., Shahid, M., & Iqbal, J. (2014). Design, synthesis, molecular docking studies and in vitro screening of ethyl 4-(3-benzoylthioureido) benzoates as urease inhibitors. *Bioorganic Chemistry, 52*, 1-7.

Saeed, A., Khurshid, A., Bolte, M., Fantoni, A. C., & Erben, M. F. (2015). Intra- and intermolecular hydrogen bonding and conformation in 1-acyl thioureas: An experimental and theoretical approach on 1-(2-chlorobenzoyl)thiourea. *Spectrochimica Acta Part A: Molecular and Biomolecular Spectroscopy, 143*, 59-66.

Safin, D. A., Velde, C. M. V., Babashkina, M. G., Robeyns, K., & Filinchuk, Y. (2016). Mononuclear heteroleptic complexes of copper (I) with 5-phenyl-2, 2′-bipyridine and triphenylphosphine: Crystal structures, Hirshfeld surface analysis and luminescence properties. *New Journal of Chemistry, 40*(7), 6156-6163.

Sathishkumar, P. N., Raveendran, N., Bhuvanesh, N. S., & Karvembu, R. (2018). Chemoselective transfer hydrogenation of nitroarenes, ketones and aldehydes using acylthiourea based Ru (II)(*p*-cymene) complexes as precatalysts. *Journal of Organometallic Chemistry, 876*, 57-65.

Schwade, V. D., Kirsten, L., Hagenbach, A., Schulz Lang, E., & Abram, U. (2013). Indium(III), lead(II), gold(I) and copper(II) complexes with isophthaloylbis(thiourea) ligands. *Polyhedron, 55*, 155-161.

Selvakumaran, N., Ng, S. W., Tiekink, E. R. T., & Karvembu, R. (2011). Versatile coordination behavior of *N*,*N*-di(alkyl/aryl)-*N*′-benzoylthiourea ligands: Synthesis, crystal structure and cytotoxicity of palladium(II) complexes. *Inorganica Chimica Acta, 376*(1), 278-284.

Selvakumaran, N., Pratheepkumar, A., Ng, S. W., Tiekink, E. R. T., & Karvembu, R. (2013). Synthesis, structural characterization and cytotoxicity of nickel(II) complexes containing 3,3-dialkyl/aryl-1-benzoylthiourea ligands. *Inorganica Chimica Acta, 404*, 82-87.

Seth, S. K. (2018). The importance of CH center dot center dot center dot X (X= O, pi) interaction of a new mixed ligand Cu (II) coordination polymer: Structure, Hirshfeld surface and theoretical studies. *CRYSTALS, 8*(12).

Seth, S. K., Saha, I., Estarellas, C., Frontera, A., Kar, T., & Mukhopadhyay, S. (2011). Supramolecular self-assembly of M-IDA complexes involving lone-pair··· π interactions: crystal structures, hirshfeld surface analysis, and DFT calculations [H2IDA= iminodiacetic acid, M= Cu (II), Ni (II)]. *Crystal Growth & Design, 11*(7), 3250-3265.

Shakhatreh, S., Lalia-Kantouri, M., Gdaniec, M., & Akrivos, P. D. (2012). Study of copper(I) heteroleptic compounds with 1-phenyl-1, 4-dihydro-tetrazole-5-thione and triphenylphosphine. *Journal of Coordination Chemistry, 65*(2), 251-261.

Sheldrick, G. M. (2015). Crystal structure refinement with SHELXL. *Acta Crystallographica Section C: Structural Chemistry, 71*(1), 3-8.

Shen, X., Shi, X., Kang, B., Liu, Y., Tong, Y., Jiang, H., & Chen, K. (1998). Syntheses, crystal structures and properties of Zn(II) and Cd(II) complexes derived from *N*-(*o*-nitrophenyl)-*N*′-(methoxycarbonyl) thiourea(H^2omt) and 2,2′-bipyridine(bpy) or *o*-phenanthroline(phen). *Polyhedron, 17*(23), 4049-4058.

Sim, J.-H., Jamaludin, N. S., Khoo, C.-H., Cheah, Y.-K., Halim, S. N. B. A., Seng, H.-L., & Tiekink, E. R. (2014). In vitro antibacterial and time-kill evaluation of phosphanegold (I) dithiocarbamates, R_3 PAu [S_2 CN (iPr) CH_2 CH_2 OH] for R= Ph, Cy and Et, against a broad range of gram-positive and gram-negative bacteria. *Gold Bulletin, 47*(4), 225-236.

Singh, D. P., Pratap, S., Pandey, S. K., Butcher, R. J., & Marverti, G. (2015). *N*-(naphthyl)-*N'*-(methoxy carbonyl)thiocarbamide and its Cu(I) complex: synthesis, spectroscopic, X-ray, DFT and in vitro cytotoxicity study. *Journal of Coordination Chemistry, 68*(2), 261-276.

Spackman, M. A., & Jayatilaka, D. (2009). Hirshfeld surface analysis. *CrystEngComm, 11*(1), 19-32.

Spackman, M. A., & McKinnon, J. J. (2002). Fingerprinting intermolecular interactions in molecular crystals. *CrystEngComm, 4*(66), 378-392.

Spek, A. L. (2009). Structure validation in chemical crystallography. *Acta Crystallographica Section D: Biological Crystallography, 65*(2), 148-155.

Sugimoto, S., Ohtsu, H., & Tsuge, K. (2018). Luminescent mixed-ligand iodido copper(I) coordination polymers having antenna effect. *Journal of Photochemistry and Photobiology A: Chemistry, 353*, 602-611.

Sumrra, S. H., Hanif, M., Chohan, Z. H., Akram, M. S., Akhtar, J., & Al-Shehri, S. M. (2016). Metal based drugs: design, synthesis and in-vitro antimicrobial screening of Co(II), Ni(II), Cu(II) and Zn(II) complexes with some new carboxamide derived compounds: crystal structures of N-[ethyl(propan-2-yl)carbamothioyl]thiophene-2-carboxamide and its copper(II) complex. *Journal of Enzyme Inhibition and Medicinal Chemistry, 31*(4), 590-598.

Swor, C. D., & Tyler, D. R. (2011). Synthesis and coordination chemistry of macrocyclic phosphine ligands. *Coordination Chemistry Reviews, 255*(23), 2860-2881.

Tadjarodi, A., Adhami, F., Hanifehpour, Y., Yazdi, M., Moghaddamfard, Z., & Kickelbick, G. (2007). Structural characterization of a copper(II) complex containing oxidative cyclization of N-2-(4-picolyl)-N′-(4-methoxyphenyl)thiourea, new ligands of 4-picolylthiourea derivatives and the precursor molecular structure of oxidative cyclization of N-(2-pyridyl)-N′-(4-methoxyphenyl)thiourea. *Polyhedron, 26*(15), 4609-4618.

Turner, M., McKinnon, J., Wolff, S., Grimwood, D., Spackman, P., Jayatilaka, D., & Spackman, M. (2017). *CrystalExplorer17*. Australia: University of Western Australia.

Veidis, M. V., Schreiber, G. H., Gough, T. E., & Palenik, G. J. (1969). Jahn-Teller distortions in octahedral copper(II) complexes. *Journal of the American Chemical Society, 91*(7), 1859-1860.

Vijayan, P., Viswanathamurthi, P., Sugumar, P., Ponnuswamy, M. N., Malecki, J. G., Velmurugan, K., Nandhakumar, R., Balakumaran, M. D., & Kalaichelvan, P. T. (2017). Solvent-assisted formation of ruthenium (II)/copper (I) complexes containing thiourea derivatives: Synthesis, crystal structure, density functional theory, enzyme mimetics and in vitro biological perspectives. *Applied Organometallic Chemistry, 31*(7), 3652.

Walia, S., Kaur, S., Kaur, J., Sandhu, A. K., Lobana, T. S., Hundal, G., & Jasinski, J. P. (2015). Synthesis, spectroscopy, and structures of mono- and dinuclear copper(I) halide complexes with 1,3-imidazolidine-2-thiones. *Zeitschrift für anorganische und allgemeine Chemie, 641*(10), 1728-1736.

Wang, D., Wu, S.-Y., Li, H.-P., Yang, Y., & Roesky, H. W. (2017). Synthesis and characterization of copper complexes with the *N*-(2,6-diisopropylphenyl)-*N*′-acylthiourea ligands. *European Journal of Inorganic Chemistry, 2017*(10), 1406-1413.

Wang, Z. Y., Ban, S. R., Yang, M. C., & Li, Q. S. (2016). Highly enantioselective Michael addition of cyclohexanone to nitroolefins catalyzed by pyrrolidine-based bifunctional benzoylthiourea in water. *Chirality, 28*(11), 721-727.

Wauters, I., Debrouwer, W., & Stevens, C. V. (2014). Preparation of phosphines through C–P bond formation. *Beilstein Journal of Organic Chemistry, 10*, 1064.

Wei, J.-J., Xiao, J.-J., Yu, J.-W., Yi, X.-Y., Liu, S., & Liu, G.-Y. (2017). Synthesis and structural characterization of silver(I) and gold(I) complexes of *N*,*N*′-diisobutyloxycarbonyl-*N*″,*N*‴-(1,3-propylene)-bisthiourea. *Polyhedron, 137*, 176-181.

Woldu, M. G., & Dillen, J. (2008). A quantum mechanical study of the stability and structural properties of substituted acylthiourea compounds. *Theoretical Chemistry Accounts, 121*(1-2), 71-82.

Wolff, S., Grimwood, D., McKinnon, J., Turner, M., Jayatilaka, D., & Spackman, M. (2012). Crystal explorer: The University of Western Australia Perth, Australia.

Wu, S. Y., Zhao, X. Y., Li, H. P., Yang, Y., & Roesky, H. W. (2015). Synthesis and characterization of *N*, *N*-di-substituted acylthiourea copper (II) complexes. *Zeitschrift für anorganische und allgemeine Chemie, 641*(5), 883-889.

Xu, Y., Mao, S., Shen, K., Shi, X., Wu, H., & Tang, X. (2018). Different structures of two Cu(I) complexes constructed by bridging 2,2-(1,4-butanediyl)bis-1,3-benzoxazole ligand: Syntheses, structures and properties. *Inorganica Chimica Acta, 471*, 17-22.

Yang, W., Liu, H., Li, M., Wang, F., Zhou, W., & Fan, J. (2012). Synthesis, structures and antibacterial activities of benzoylthiourea derivatives and their complexes with cobalt. *Journal of Inorganic Biochemistry, 116*, 97-105.

Yang, W., Zhou, W., & Zhang, Z. (2007). Structural and spectroscopic study on *N*-2-fluorobenzoyl-*N′*-4-methoxyphenylthiourea. *Journal of Molecular Structure, 828*(1), 46-53.

Yaseen, S., Rauf, M. K., Zaib, S., Badshah, A., Tahir, M. N., Ali, M. I., Imtiaz ud, D., Shahid, M., & Iqbal, J. (2016). Synthesis, characterization and urease inhibition, in vitro anticancer and antileishmanial studies of Co(III) complexes with *N,N,N′*-trisubstituted acylthioureas. *Inorganica Chimica Acta, 443*, 69-77.

Yuan, H., He, M., Cheng, F., Bai, R., da Silva, S. R., Aguiar, R. C., & Gao, S. J. (2017). Tenovin-6 inhibits proliferation and survival of diffuse large B-cell lymphoma cells by blocking autophagy. *Oncotarget, 8*(9), 14912-14924.

Yun, T., Qin, T., Liu, Y., & Lai, L. (2016). Identification of acylthiourea derivatives as potent Plk1 PBD inhibitors. *European Journal of Medicinal Chemistry, 124*, 229-236.

Yusof, M. S. M., Jusoh, R. t. H., Khairul, W. M., & Yamin, B. M. (2010). Synthesis and characterisation a series of *N*-(3,4-dichlorophenyl)-*N′*-(2,3 and 4-methylbenzoyl)thiourea derivatives. *Journal of Molecular Structure, 975*(1), 280-284.

LIST OF PUBLICATION

a) Zubir, M. Z. M., Jamaludin, N. S., & Halim, S. N. A. (2019). Hirshfeld surface analysis of some new heteroleptic copper (I) complexes. *Journal of Molecular Structure*, *1193*, 141-150